# UNIVERSITÀ DEGLI STUDI DI GENOVA

**Scuola di Scienze Mediche e Farmaceutiche**
**CORSO DI LAUREA IN MEDICINA E CHIRURGIA**

**Tesi di Laurea**
Dipartimento di neuroscienze, riabilitazione, oftalmologia, genetica e scienze materno-infantili-DINOGMI

# "Dermal and Subepidermal biopsy as a window to a deeper understanding of SFN"


**Relatore**
Prof. Angelo Schenone
Prof. Dott. Ssa Claudia Sommer

**Candidata**
Silvia Busi

**Correlatrice**
Dott. Ssa Sara Massucco


*Anno Accademico 2023/2024*

# *Contents*

# *Abstract*

**INTRODUCTION:** Small fiber neuropathy (SFN) is characterized by selective impairment of myelinated Aδ and unmyelinated C nerve fibers. Skin biopsy is the gold standard in the diagnosis of SFN. Often, patients with SFN or other types of neuropathies complain of itching or pain, but the pathomecanisms of these two symptoms are still not completely known.

**AIM OF THE STUDY:** Compare neurovascular structures in sub-epidermis and dermis between subjects affected by peripheral neuropathy (PN) with/without pain and/or itch and healthy controls (HC), to detect any differences in neurovascular contacts, which may give information regarding the pathophysiology of these symptoms.

**MATERIALS AND METHODS:** We enrolled 25 HC and 79 PN patients, divided into 4 groups according to the symptoms. The skin samples, taken from the thigh, were stained with double immunofluorescence (PGP9.5 and CD31). The images acquired with the microscope Leica DMi8 "Thunder" were analyzed with the software Fiji, using the "Dermal Layer Analysis" tool.

**RESULTS:** Comparing the groups of patients with PN complaining of itch and/or pain with HC, significant differences emerged between HC and patients with PN and itch. Subjects with itch had significantly lower values of (a) vessel area($p=0.046$) and density($p=0.051$), (b) small fiber number($p=0.011$), area($p=0.007$), and density($p=0.002$), (c) vascular contact number ($p=0.015$), area($p=0.002$), and density($p=0.002$) in the sub-epidermis. Moreover, they showed lower values of d) small fiber number($p=0.021$), area($p=0.018$), and density($p=0.008$), and (e) vascular contact number($p=0.012$) and area($p=0.023$) in the dermis. Similar differences were also found between patients with PN and itch vs patients with PN and pain.

**CONCLUSION:** Patients with NP and itch showed the greatest impairment in subepidermal and dermal neurovascular structures, suggesting that itching is more correlated with an impairment of the contacts between vessels and small nerve fibers in the skin, than pain.

# 1. INTRODUCTION

## 1.1 Small Fiber Neuropathy

### *1.1.1 Definition and Anatomy*

Small fiber Neuropathy (SFN) is a heterogeneous group of diseases of the Peripheral Nervous System (PNS), characterized by selective or predominant impairment of small myelinated Aδ and unmyelinated C fibers.[1,2]

Peripheral nerve fibers can be classified according to the "Erlanger Gasser" system, which takes into account physical characteristics and signal conduction properties. According to that classification system, nerve fibers are grouped based on the presence of myelin sheath, diameter, and conduction velocity *(Figure 1)*.

**Erlanger /Gasser classification of nerve fibers**

| Fiber types | Function | Avg. fiber diameters (µm) | Avg. cond. Velocity (m/s) |
|---|---|---|---|
| Aα | Primary muscle spindle afferents, motor to skeletal muscle | 15 | 100 (70-120) |
| Aβ | Cutaneous touch and pressure afferents | 8 | 50 (30-70) |
| Aγ | motor to muscle spindle | 5 | 20 (15-30) |
| Aδ | Cutaneous temperature and pain afferents | <3 | 15 (12-30) |
| B | Sympathetic preganglionic | 3 | 7 (3-15) |
| C | Cutaneous pain afferents sympathetic postganglionic | 1 | 1 (02-2) |

*Figure 1. PNS' nerve fibers according to Erlanger and Gasser classification.*

Image taken from internet at the link: "https://goo.gl/images/F7y61c"

Small fibers (Aδ and C) represent approximately 80-90% of peripheral nerves and are mainly involved in thermal and pain sensitivity, as well as in the regulation of certain autonomic functions. Clinically, SFN is characterized by the development of sensory (mainly thermal and painful) and autonomic disturbances that negatively impact the patient's life.[1]

Aδ fibers are myelinated, have a small diameter (1–6 μm), and are primarily afferent. They convey rapid pain ("first pain") described as a prick or an electric shock. [1]

C fibers are afferent too but are unmyelinated and have a smaller diameter (0.3-1.5 μm). They convey slow, dull, persistent pain ("second pain"), which is less easily localized. These fibers originate from multimodal receptors and are effectively activated by thermal, mechanical, and inflammatory chemical stimuli.[1]

Small fibers conduct both somatic sensory and preganglionic autonomic stimuli. They play a fundamental role in regulating certain autonomic functions, in particular they innervate sweat glands (sudomotor function), hair follicles (pilomotor function), and skin vessels (vasomotor function). [1]

In SFN, selective involvement of Aδ or C fibers or involvement of both fiber types can occur. Small fiber impairment is frequently present in large fiber neuropathies, with an unequal damage distribution among the different types of nerve fibers. Small fibers may be predominantly or exclusively damaged compared to large fibers in certain polyneuropathies. Notably, SFN may represent the initial stage of sensory or sensorimotor peripheral polyneuropathy, with subsequent involvement of large fibers.[1]

A milestone in the SFN’s study and definition has been skin biopsy, which has allowed for reliable quantification of intraepidermal nerve fiber density (IENFD).

### *1.1.2 Epidemiology*

The correct prevalence of SFN in the general population is still unknown.

The current available epidemiological data on SFN mainly come from one epidemiological study conducted in the southern part of the Netherlands that reported a prevalence of 53 cases per 100.000 and an annual incidence of 12 cases per 100.000. [2]

Moreover, comparing incidence and prevalence between men and women and between old and young people, the study reported that incidence and prevalence are higher in men and elderly patients. [3]

Another interesting study carried out in Olmested, Minnesota, and nearby countries between January 1998 and December 2017 reported a mean SFN incidence of 1.3 per 100,000 inhabitants/year and a prevalence of 13.3 per 100,000 inhabitants. It was noted an upward trend incidence during the study period, probably due to increased awareness, not to test availability. Additionally, the authors reported a median age at onset of 54 years, with a range between 14 and 83 years, and a female prevalence (67%). [4]

The incidence of SFN in the study conducted in Minnesota was much lower compared to the one reported in the study performed in the Netherlands, probably because of the different methodologies used.

Nowadays, the incidence of SFN is probably underestimated. New epidemiological studies will be able to provide further information only if shared diagnostic criteria will be convincingly adopted. [5]

### *1.1.3 Etiology*

The etiology of SFN can be identified in about two-thirds of the cases, while the remaining third is idiopathic.[1] The definition of SFN etiology is often challenging, also because of the fragmentary news regarding the association between SFN and systemic diseases. Notably, some associations are supported by strong evidence, while for others the association is reported in small case series or as anecdotal cases.[2]

According to the etiology, SFN can be divided into Primary and Secondary.[1]

SFNs are defined as "*Primary"* when a genetic cause is recognized. Inherited neuropathies are a rare heterogeneous group of progressive disorders with an involvement of either motor, sensory, and/or autonomic nerves.[6]

Hereditary SFN cover a broad spectrum of clinical presentations going from multisystem diseases and predominantly large fiber polyneuropathies with an additional impairment of small fibers, to channelopathies, caused by mutation of distinct genes with exclusive damage of Aδ- and C-fibers.[7] Among the gene mutation, several studies identified a mutation in genes codifying for voltage-gated sodium channels. Voltage-gated sodium channels play a fundamental role in regulating the excitability of nociceptive primary afferent neurons. In particular, three voltage-gated sodium channels, NaV1.7, NaV1.8, and NaV1.9, codified by the genes *SCN9A*, *SCN10A*, and *SCN11A*, are mostly expressed in peripheral nervus system, hence any modification in their expression can lead to neuronal disorders.[8] Gain-of-function *SCN9A* variants have been described in three human painful conditions: inherited erythromelalgia (IEM), paroxysmal extreme pain disorder (PEPD), and SFN. Conversely, the loss of function of *SCN9A* is associated with pain intensity (CIP), due to elevated levels of intracellular calcium that can contribute to the degeneration of small nerve fibers. [8] In addition to sodium channel dysfunction, mutations in the *COL6A5* gene coding for a collagen protein can also lead to a peculiar phenotype of familial and sporadic SFN characterized by neuropathic itch.[9] Other genetic conditions associated with SFN include the presymptomatic stage of familial amyloidosis, caused by *TTR* gene mutations. The symptomatic stage is then typically characterized by a mixed neuropathy with the involvement of both small and large fibers. Another rare genetic disease characterized by SFN is Fabry disease. In this context, genetic analysis is not recommended in isolated SFN but should be performed in the presence of other clinical features of the disease. Moreover, SFN has been reported in patients with Gaucher disease as a possible explanation for the neuropathic origin of chronic pain. At last, small fiber impairment correlated to widespread pain has also been described in fibromyalgia and Ehlers-Danlos syndrome.[2]

*Secondary* SFNs can be caused by metabolic disorders, infections, vaccinations, immune-mediated or neoplastic/paraneoplastic disorders.[1] Among acquired conditions, diabetes and impaired glucose tolerance (IGT) are the main causes. Notably, diabetes alone is liable for about 20% of all SFN, and considering prediabetes conditions characterized by impaired oral glucose tolerance test (OGTT), the frequency rises to 56%.[5] In diabetic patients, rapid glycemic control may cause an acute somatic and autonomic treatment-induced neuropathy, named as “insulinic neuropathy”, and the severity of the clinical picture correlates with the magnitude of glycated hemoglobin (HbA1c) reduction.[5] Since HbA1c is considered an important predictor of diabetic neuropathy, it should be tested routinely.[2] Recent studies have demonstrated a direct correlation between triglyceride levels (dyslipidemia) and impairment of SFN function, suggesting a possible role of hyperlipidemia or other metabolic syndrome components in the pathogenesis of SFN.[2,5] Other metabolic conditions that can be related to SFN are hypovitaminosis (B1, B6, B12), renal, hepatic, and thyroid dysfunction.[7] Regarding infections, a strong association between SFN and HIV infection has been described, while the association with hepatitis C is weaker, based only on anecdotal reports.[5] Recent studies have reported autonomic symptoms such as tachycardia, frequent urination, dry eyes, dry mouth, and digestive or visual disturbances in post-COVID (COronaVIrus Disease 19) conditions and ME/CFS (Myalgic Encephalomyelitis/Chronic Fatigue Syndrome) patients. In these cases, impairment of small nerve fibers with non-length-dependent distribution (NLD-SFN) has been described. Furthermore, small fiber impairment may be caused by a systemic inflammatory state.[10] Among immune-mediated disorders, small fibers are involved in Sjogren’s syndrome, celiac disease, and sarcoidosis.[5] Cases of SFN have also been reported after exposure to neurotoxic drugs (such as antibiotics, heavy metals, chemotherapy, and alcohol).[5] The pathophysiology underlying secondary SFN is still incompletely understood.[7] In diabetes and glucose intolerance oxidative stress by increased flux of polyol regulated by aldose reductase, macro- and microangiopathy, glycosylation, and deposition of glycosylated products can lead to a chronic inflammatory state that can cause small fiber impairment.[7] In SFN associated with alcoholism, small nerve fiber impairment can be caused by nutritional deficiency for thiamine (vitamin B1), cobalamin (vitamin B12), and pyridoxine (vitamin B6), which are fundamental for

peripheral myelin development, but it may also be caused by direct toxic effect of alcohol or its metabolites on peripheral nerves.[7] In immune-mediated disorders, different studies have reported high levels of autoantibodies and pro-inflammatory cytokines.[7]

In some neurodegenerative disorders such as Parkinson's disease (PD) or amyotrophic lateral sclerosis, small nerve fibers are also involved, possibly due to dopaminergic drugs, vitamin deficiency, or deposition of α-synuclein in the nerve.[7]

The main causes of SFN are listened in *Table 1*.

| ***Primary (genetic)*** |
|---|
| - AAAS, ABCA1 (Tangier disease), ARL6IP1, ATL1, ATL3, CLTCL1, DNMT1, DST, FAM134B, FLVCR1, FXN, GMPPA, IKBKAP, KIF1A, LRRK2, NAGLU, NF1 (neurofibromatosis), NGF, NTRK1, PRDM12, RAB7A, SCN9A (erythromelalgia, corneal neuralgia), SCN10A, SCN11A, SNCA (alpha-synuclein), SPTLC1, TRPA1, VGSC, WNK1, COL7A1 (epidermolysis bullosa), Ross Syndrome.<br>- GLA (Fabry disease)<br>- TTR (transthyretin-related amyloidosis)<br>- SPTLC2 (Hereditary sensory autonomic neuropathy type 1)<br>- ATP7B (Wilson disease) |
| ***Secondary*** |
| *- Metabolic*<br>• Glucose metabolism-related (diabetes, impaired glucose tolerance)<br>• Hypothyroidism<br>• Hyperlipidemia<br>• Chronic kidney disease<br>• Vitamin B12 deficiency |
| *- Infectious*<br>• Hepatitis-C virus<br>• HIV<br>• Borreliosis, Lyme<br>• Leprosy<br>• SARS-CoV-2 |

| |
|---|
| - *Vaccination*<br>• Rabies, varicella, human papillomavirus, Lyme, SARS-CoV-2 |
| - *Toxic*<br>• Multiple chemical sensitivity syndrome, alcohol, heavy metals, chemotherapeutics (e.g., bortezomib), N-hexane, pyridoxine, nitrofurantoin, metronidazole, remdesivir, immune checkpoint inhibitors |
| - *Immune-mediated*<br>• Sjögren syndrome<br>• Sarcoidosis<br>• Monoclonal gammopathy<br>• Mixed connective tissue disease<br>• Celiac disease<br>• Systemic vasculitis<br>• Lupus erythematosus<br>• Behçet disease<br>• Familial Mediterranean fever<br>• Antibodies against TS-HDS and FGFR3<br>• GBS, CIDP<br>• SARS-CoV-2<br>• Inflammatory bowel disease |
| - *Neoplastic/paraneoplastic*<br>• Lymphoblastic leukemia<br>• Keloids<br>• Paraneoplastic syndromes |
| - *Various*<br>• Parkinson's disease<br>• Pure autonomic failure (deposition of alpha-synuclein)<br>• Critical illness |

*Table 1: Etiology of small fiber neuropathy.*
Table taken from the paper "Small fiber neuropathy" written by Josef Finsterer and Fulvio A. Scorza, modified.

Note: Abbreviations: IVIG= intravenous immunoglobulins; LTX= liver transplantation; NTX=kidney transplantation; PE=plasma exchange; SCT=stem cell
Transplantation; CoV-2 = severe acute respiratory syndrome coronavirus 2; TS-HDS = trisulfated heparin disaccharide; FGFR3= fibroblast growth factor receptor 3; GBS = Guillain-Barré syndrome; CIDP = chronic inflammatory demyelinating polyradiculoneuropathy.

### *1.1.4 Clinical Presentation*

The clinical presentation of SFN is characterized by the presence of negative or positive sensory phenomena, and by autonomic dysfunction [11], related to the Aδ and C-fiber degeneration and consequent conduction impairment. [2]

Neuropathic pain often prevails in the clinical picture. It has been described by patients as burning, shooting, stabbing, stitching, stinging, electric shock, compression sensing, or painful cold.[1] Even though the patients often complain of spontaneous pain, sometimes it can be triggered by stimuli that usually should not cause pain[1], such as thermal or mechanical stimuli: this phenomenon is called allodynia. Some patients even report that their feet have become so exquisitely tender that they cannot bear the touch of bed sheets on them, so they are forced to sleep with their feet uncovered.[12]. Furthermore, examination often reveals hyperalgesia, described as an increased perception of pain[1,12]. Few patients do not complain about pain but experience a feeling of tension and swelling in their feet (even though the feet seem normal).[12]

Although neuropathic pain mostly dominates the clinical picture, another common symptom of SFN is itch.[13] Pain and itch are transmitted by the same peripheral nerve fibers (unmyelinated slow-conducting C fibers), and for this reason, itch often matches neuropathic pain[14]; only 8% of patients exclusively complain of itch without the presence of pain.[13]

Regarding sensory symptoms, the patient could suffer from paresthesia or numbness, and also from thermo-algesic hypoesthesia, since small fibers are involved in thermal conduction[1]. The vibratory sensation is generally preserved, but sometimes an isolated abolition of pallesthesia at the level of the hallux may be present.[1]

Approximately half of the patients with SFN suffer from autonomic symptoms.[3]

Patients can complain of dry eyes and/or mouth, a phenomenon known as sicca syndrome, due to the impaired innervation of lachrymal and salivary glands. Sweat glands can also be impaired, with sudomotor dysfunction and impaired thermoregulation. The cardiovascular system can be also corrupt leading to orthostatic dizziness, palpitations, heart rate variability (as in the case of POTS, postural tachycardia syndrome), or hot flashes.[1,2] Additionally, the impairment of the autonomic innervation in the gastroenteric, urinary, and reproductive systems can lead to constipation and/or diarrhea, chronic intestinal pseudo-obstruction, gastropathy, bladder incontinence, dysuria, or sexual dysfunction.[15] The visual manifestations of SFN consist of impaired accommodation with photophobia, and poor near vision that causes difficulty in reading; the ophthalmological examination may show a tonically dilated pupil named Adie's pupil.[15] During the physical examination, skin changes are sometimes reported; the skin over the affected area may appear atrophic, dry, changed from the usual color, swollen and additionally there could be a reduction in hair/nail growth with hair loss, as the result of sudomotor and vasomotor abnormalities *(Figure 2)*.[1,12]

**Symptoms suggesting small fiber neuropathy (SFN).**

| |
|---|
| *Sensory symptoms* |
| Pain (burning sensations, tingling, painful cold sensation, shooting pain, pins and needles…) |
| Allodynia in response to rubbing |
| Hypoesthesia to heat, cold, and pinprick |
| Hyperalgesia |
| *Symptoms of dysautonomia* |
| Dyshidrosis (hypo/anhidrosis, hyperhidrosis) |
| Impairments in vasomotricity or thermoregulation (hot flashes, erythermalgia) |
| Gastrointestinal symptoms (gastroparesis, diarrhea, constipation, intestinal pseudoobstruction) |
| Disorders of micturition (urinary incontinence or retention), erectile dysfunction |
| Ocular or oral sicca syndrome |
| Visual impairments: disorders of accommodation with blurred vision, photophobia, impaired near vision, tonically dilated Adie's pupil by ophthalmological examination |
| Orthostatic hypotension |
| Cardiac arrhythmias: premature atrial or ventricular beats, sinus bradycardia or tachycardia |

*Figure 2: Summary table with sensory and autonomic symptoms suggesting SFN.*

Image taken from the paper "Small fiber neuropathy: Diagnosis, causes, and treatment" by Damien Sène

Around 40% of SFN patients have also experienced restless leg syndrome at least once.[2]

It is important to underline that symptoms are usually worse at night, causing insomnia and fatigue during the day.[1,12]

Additionally, some symptoms are specific to certain forms of SFN, e.g., oxaliplatin-induced neuropathy is triggered by cold, instead erythromelalgia's symptoms are exacerbated by heating and relieved by cold.[2]

SFN's symptoms and signs, according to their body distribution, can identify different clinical presentation patterns: length-dependent polyneuropathy, non-length-dependent neuropathy, and asymmetric mono/multiplex neuropathy *(Figure 3).*

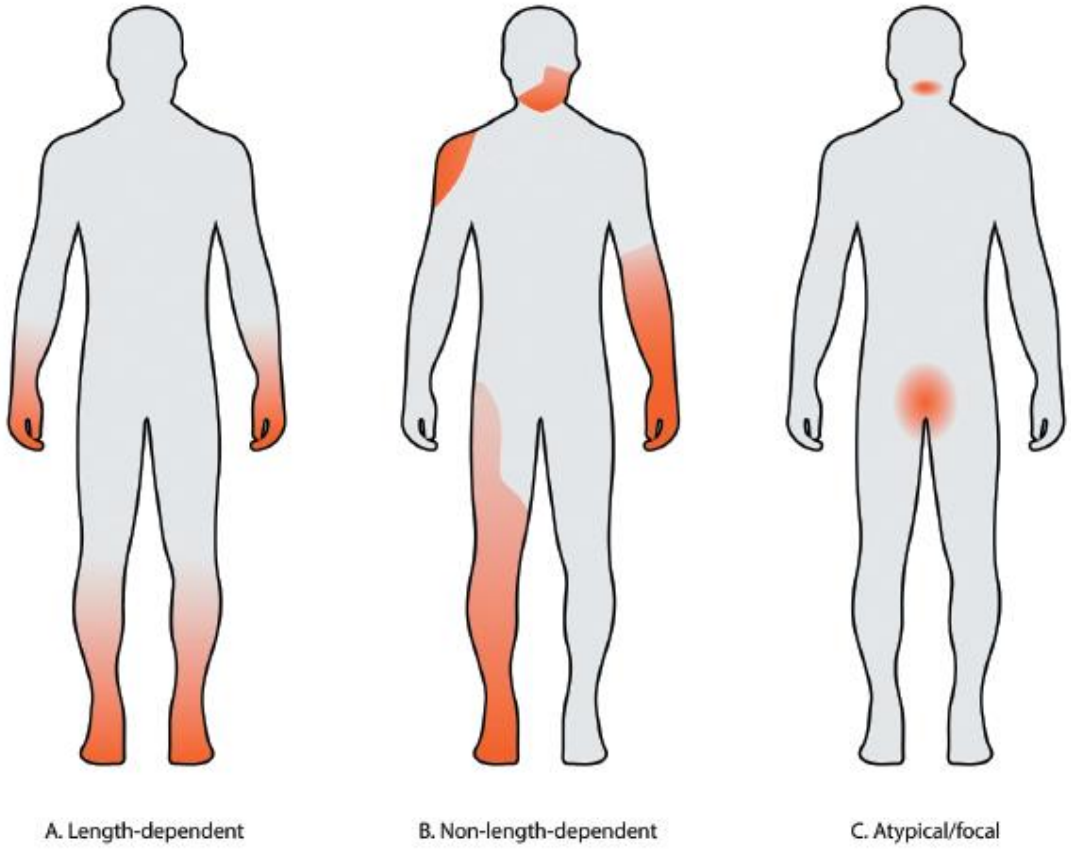


*Figure 3: Clinical presentation patterns of SFN*

Image taken from the paper "Clinical diagnosis and management of small fiber neuropathy: an update on best practice", by Devigili et. al. [2]

-*Length-dependent SFN*: patients typically complain of spontaneous burning pain starting at distal limb extremities and gradually ascending proximally, involving upper limbs with a similar distal-to-proximal evolution. This pattern is mostly seen

in patients with metabolic causes, such as diabetes, reduced glucose tolerance, or after neurotoxic exposures. [2]

-*Non-length-dependent SFN*: it is characterized by a proximal, diffuse, or mottled distribution of symptoms in different body districts, with involvement of upper limbs that can be previous or simultaneous to lower limbs. This pattern is predominantly seen in immune-mediated (e.g., Sjogren's syndrome) and paraneoplastic disorders. [2] The topographic pattern of NLD-SFN is probably a ganglionopathy with a prevalent involvement of the small neurons of the dorsal root ganglia (DRG).[1] Diagnosis is more challenging than Length-dependent SFN because of the atypical clinical presentation. For this reason, probably this SFN phenotype is still under-recognized. Nowadays NLS-SFN represents about one-fifth of total SFN patients, involving mostly women, and with an earlier onset.[16] It is possible to recognize different combinations of topographic patterns, categorized as patchy, asymmetrical, upper limb predominant, proximally predominant, and diffuse *(Figure 4)*. [16]

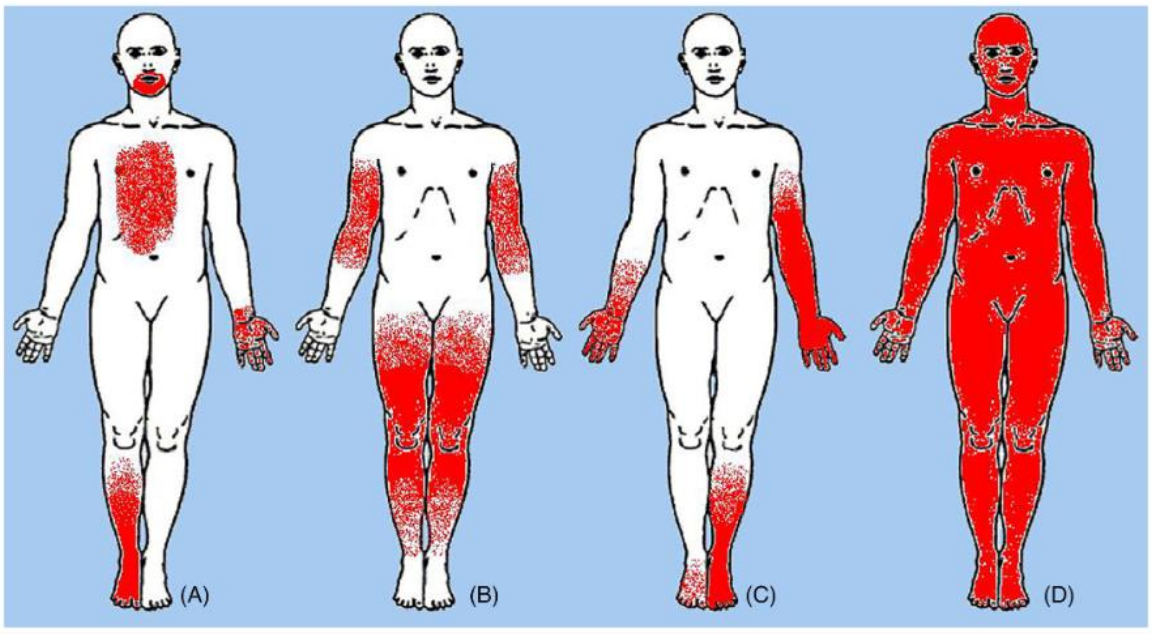


*Figure 4: Topographic patterns of sensory symptoms in NDL-SFN.* A) Patchy, B) Proximally predominant I, C) Asymmetric, upper limb predominant, D) diffuse

Image taken from the paper "non-length-dependent small fiber neuropathy: Not a matter of stockings and gloves" by Franco Gemignani et. al. [16]

- *Asymmetrical mono/multiplex neuropathy*: in this pattern, clinical manifestations are due to the involvement of single or multiple sensory peripheral nerve fibers. Examples are burning mouth syndrome, notalgia and meralgia paraesthetica, vulvodynia, and Wartemberg neuropathy. [2]

In conclusion, SFN leads to an important reduction in life quality, mainly due to pain and autonomic symptoms.[8]

As shown in *Figure 5*, in 2018 Levine divided SFN into 4 different groups, according to the presence of sodium channel impairment (= SFFCD), classic neuropathic symptoms such as burning, stabbing pain (=SFMPN), widespread pain (=SFMWP), and autonomic symptoms such as irritable bowel syndrome or vomit (=SFMAD).

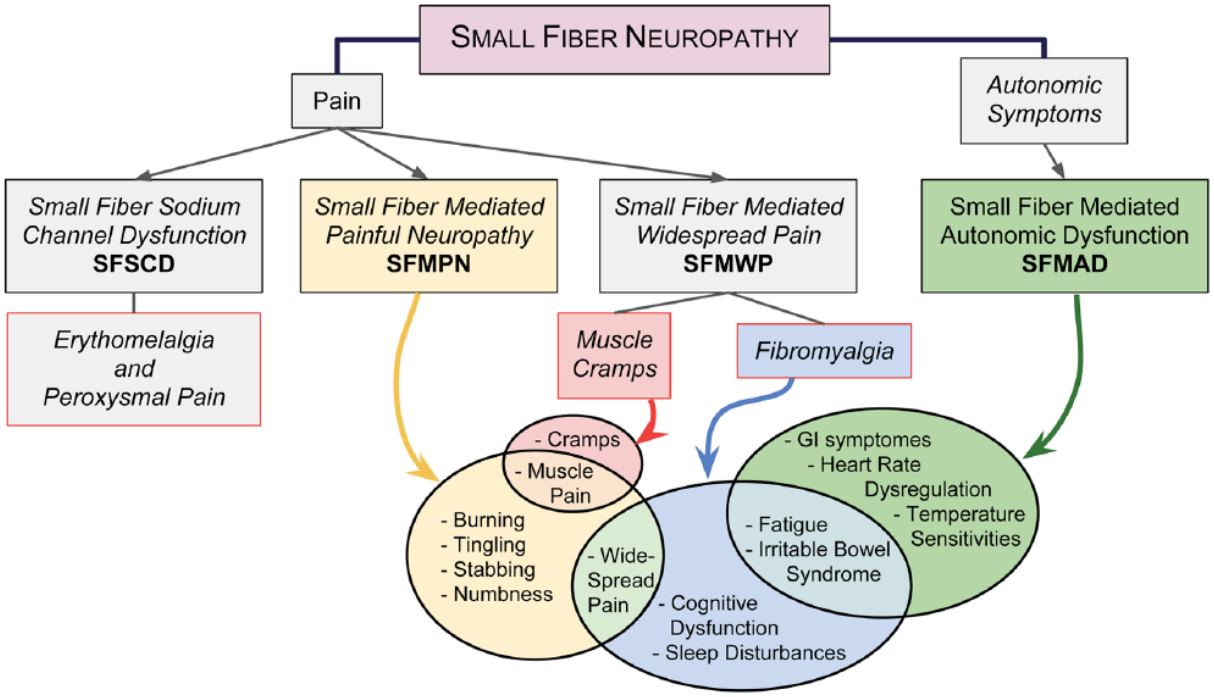


*Figure 5: Small fiber neuropathy symptom clusters and neuropathy classifications.*
Image taken from the paper "Small Fiber Neuropathy: Disease Classification Beyond Pain and Burning", written by T.D.Levine et. al.

### *1.1.4.1 Pruritus*

One possible symptom of SFN is itch. When assessing a patient reporting a chronic itch with the skin seeming normal, SFN should be considered a potential

pathophysiologic mechanism underlying the itch.[13] Itch occurs in a limited percentage of patients affected by small-fiber neuropathy (SFN), and its pathogenesis is still largely unknown.[17]

Itch is a common experience of cutaneous discomfort with the urgent need to scratch for immediate relief, that has different causes including allergies, insect bites, or a healing wound. Itch can complicate the course of a wide range of systemic illnesses (e.g., atopic dermatitis, psoriasis…). Itch can also occur in peripheral and central nervous system diseases such as post-herpetic neuralgia, neuropathies, and inflammatory or vascular lesions of the thalamus. Moreover, itch can be a side effect of drugs like opioids and chloroquine. Some patients complain of chronic itch of unknown etiology, which can be related to psychological distress, especially in the elderly.[9]

Itch is defined as neuropathic itch when it occurs in patients with neurological diseases involving the somatosensory pathway, as in post-herpetic neuralgia (PHN), multiple sclerosis, or peripheral neuropathies.[17] Neuropathic pruritus (NP) represents approximately 8% to 19% of chronic pruritic dermatoses and includes a wide variety of neurologic diseases. NP is caused by neuronal damage, that leads to dysregulation of the somatosensory nervous system. Regarding clinical presentation, core findings of NP include the presence of normal skin or skin with only secondary changes or signs of excoriation, which helps as an initial differentiator from primary inflammatory dermatoses. Itch has typically a localized distribution and can also coexist with alloknesis and hyperkinesis due to central sensitization, in which limited nerve damage leads to heightened neurotransmitter release and hyperexcitable spinal neurons. NP can be associated with sensory complaints symptoms, such as burning, paresthesia, tingling, and stinging perceptions. [18]

Different models of coding to characterize the relationship between itch and pain have been proposed. Itch and pain are both related to specific sensory neurons with distinct pathways that respond only to the corresponding stimuli.[18] In particular, some studies have demonstrated that cowhage-induced itch is mediated by both C and Aδ fibers; indeed, when itch is triggered by histamine, it is mediated only by C fibers.[17] Despite itch neurons being molecularly distinct from

their pain-sensing counterparts, neuropathic itch shares common mechanisms with neuropathic pain.[19]

Pruriceptive neurons are a subset of nociceptive neurons whose afferents can elicit itch also in response to pain-inducing chemical, mechanical, and heat stimuli. When C-fibers are activated by noxious heat and capsaicin, pain sensation is induced, instead when C-fibers are activated by histamine, itch sensation is elicited. When both Aδ and C fibers are exposed to non-histaminergic pruritic agents, such as cowhage spicules, histamine-independent itch is induced. Itch induced by pruritic agents such as histamine or cowhage spicule is usually followed by slighter and shorter-lasting pricking and burning sensations. Nowadays, it is uncertain if the itch mediator function is specific, because neurons responsive to pruritic agents can also be activated by painful stimuli. However, a transgenic mouse expressing the transient receptor potential vanilloid type 1 (TRPV1) exclusively in a subset of neurons sensitive to histamine has recently allowed the demonstration that capsaicin can evoke itch-related behavior instead of painful sensation, suggesting a specific via. [17]

Several studies reported that the most common trigger factors are warmth and calmness, indeed the application of emollients and cold water alleviates the itch.[13]

Regarding scratching, most patients reported only scratching when they experienced itch, but others admitted scratching also when they did not perceive itch, as an automatic behavior. Scratching is thus considered both a trigger for the itch and an alleviating factor. In some patients, scratch lesions were reported, with no difference recorded between males and females. Age and itch intensity assessed with the NRS (average intensity in the 24 hours of the day) and the VAS (average in the 24 hours) did not differ between patients with no, some, or multiple scratch lesions. [13]

A study published in 2014 demonstrated, for the first time, that neuropathic itch can be related to a gene variant, encoding for a sodium channel subunit. This gene is involved in the generation of nociception. Further channels are probably involved in other itch phenotypes. Most recently, the target screening of genes encoding for Nav1.7 and Nav1.8 subunits of sodium channels has led to the identification of novel mutations in SFN patients. Nav1.7 is encoded by the *SCN9A*

gene, and it is broadly expressed in dorsal root ganglions (DRG) and sympathetic ganglion neurons. Gain-of-function mutations recognized in SFN have been found to cause changes of the biophysical properties of the channel and to alter the excitability of small DRG neurons and the superior cervical ganglion neurons. These findings indicate that sodium channel-related painful SFN represents a novel and distinct nosologic condition occurring either in sporadic or, more rarely, in familial cases. Patients with the I739V variant in the *SCN9A* gene are characterized by paroxysmal neuropathic itch attacks, mainly triggered by warmth and spicy food, associated with transient burning pain. Autonomic disturbances are reduced to episodic flushing without evidence of cardiovascular or cholinergic sudomotor dysautonomia. Skin biopsy demonstrated a significant decrease in IENF density at the distal leg. The neuropathic nature of itch was suggested by its overlap with impaired superficial sensation (e.g., hypoesthesia and hypoalgesia) in the same body area, and by the fact that all of the patients under examination showed a good response to pregabalin, a first-line drug for neuropathic pain, in terms of both itch intensity and attack frequency. [17]

The presence of chronic itch (≥6 weeks), the beginning of the itch on normal-appearing skin, and the decreased number of intraepidermal nerves, assessed by IENFD, constitute mandatory criteria for diagnosing SFN associated with chronic generalized itch. Facultative criteria include the presence of a daily, moderate to severe itch, pruralgia (e.g., additional painful sensations such as burning, tingling, or a sensation like needle pricks) next to the presence of itch, the occurrence of itch in attacks, alleviation of itch with cold/ice application or emollients and worsening with warmth. These criteria should help physicians to identify patients with chronic itch caused by small fiber impairment.[13]

Itch intensity, the amount of scratch lesions, and the humanistic burden (ItchyQol, HADS) are not increased in patients with highly reduced IENFD. Thus, this parameter does not reflect disease severity, which seems to be independent of the magnitude of the IENFD reduction.[13]

Moreover, some studies have shown that women with chronic pruritus suffer more frequently from psychosomatic disorders and report more often a worsening of the pruritus in correlation to emotional and psychosomatic factors compared to men.[13]

#### *1.1.4.2 Pain*

Neuropathic pain has been defined as pain that arises as a direct consequence of a lesion or disease affecting the somatosensory system, including small nerve fibers.[20]

Chronic pain often follows from direct neural injury (i.e., neuropathic) and often persists after the resolution of transient noxious conditions. In the case of chronic pain, the peripheral and central mechanisms of nociception and the cortical mechanisms of pain perception are dissociated, such that the presence/absence of one does not inherently preclude the presence/absence of the other.[20,21]

Pain is multidimensional: pain not only reflects an anatomic lesion or a deficit alongside the nervous system network but is also seen as an unpleasant sensory and emotional experience.[21]

Pain is assumed to be a static assessment parameter. However, different pain conditions show distinctive pain patterns with fluctuations throughout the circadian cycle. Biopsychological, environmental, and genetic factors seem to play a role in the chronobiology of pain. Recently, circadian rhythms in neuropathic pain in diabetic neuropathy and postherpetic neuralgia have been demonstrated. [20]

Regarding neuropathic pain, there are two main unresolved issues: not all individuals with neuropathy develop pain and it is not possible to predict who is more or less susceptible to pain among those with similar risk exposure. Recent studies have suggested that certain polymorphisms act to facilitate or increase pain or modulate the response to analgesics. In particular, in the last couple of years, the role of voltage-gated sodium channel mutations in the pathophysiology of pain in subjects with SFN has become clearer.[22]

Sodium channels, which are integral membrane proteins, play a critical role in the generation and conduction of action potentials and are determinant for the electrical signaling of most excitable cells. In myelinated axons, sodium channels are mostly restricted to the nodes of Ranvier where they are present in high density, while in nonmyelinated C-fibers, they are distributed in low density along the entire length of the axon. Nine isoforms of sodium channel α-subunit have

been recognized (Nav1.1–Nav1.9), each with a main distribution in the central and peripheral nervous system. Notably, three of these sodium channels (Nav1.7, encoded by the *SCN9A* gene; Nav1.8, encoded by the *SCN10A* gene; Nav1.9, encoded by the *SCN11A* gene) are involved in the generation and conduction of action potentials throughout the nociceptive pathway and seem to be a possible cause of painful neuropathies. Loss-of-function and gain-of-function mutations in the *SCN9A* gene encoding for Nav1.7 could explain, respectively, the absence of pain in congenital insensitivity to pain syndrome and the excruciating pain of primary erythromelalgia (PE) and paroxysmal extreme pain disorder (PEPD). Recently, a correlation between mutations in sodium channels and SFN has been found, leading to a distinct condition presenting with intense burning in the feet.[22]

### *1.1.5 Diagnostic Criteria*

In the last years, different diagnostic approaches have been proposed, and the main two are the “Besta criteria”, published in 2008, and the “NEURODIAB criteria”, published in 2010 (*Figure 6)*.[2]

Table 3. Diagnostic criteria for small fiber neuropathy.

| SFN CRITERIA 2008 [42] | |
|---|---|
| Presence of at least two of the following: | **Absence of the following:** |
| Clinical signs of small fiber neuropathy, including pinprick and thermal sensory loss or reduction and/or the presence of positive signs (allodynia and hyperalgesia) | Reduced vibratory sensation<br>Loss of deep tendon reflexes<br>Altered sensory nerve conduction |
| Abnormal thermal threshold assessed at the foot by QST | |
| Reduced IENFD at the distal leg | |

| NEURODIAB CRITERIA [43] | |
|---|---|
| Possible | Length-dependent symptoms and/or clinical signs of small-fiber damage |
| Probable | Length-dependent symptoms, clinical signs of small-fiber damage, and normal sural NCS |
| Definite | Length-dependent symptoms, clinical signs of small-fiber damage, normal sural NCS, and reduced IENFD at the ankle and/or abnormal QST thermal thresholds at the foot |

*Figure 6: Diagnostic criteria for small fiber neuropathy*

Image taken from the paper “Clinical diagnosis and management of small fiber neuropathy: an update on best practice” by Grazia Devigili, Daniele Cazzato & Giuseppe Lauria.

*Besta criteria* are based on the combination of abnormal findings in at least two out of three assessments including:

1) clinical signs of SFN (e.g., reduced pinprick and thermal sensation, allodynia, and/or hyperalgesia),

2) abnormal foot thermal threshold assessed by quantitative sensory test (QST),
3) reduced IENFD at the distal leg.

Exclusion criteria are clinical signs of large sensory fiber impairment, such as reduced vibratory sensation, reduced deep tendon reflexes, and/or electrophysiological evidence of sensory nerve involvement. Hence, the limit of the Besta criteria is to exclude patients with mixed small and large fiber neuropathy, considering only pure SFN.[2]

*NEURODIAB criteria* were included in the updated guidelines for the diagnosis of diabetic neuropathy by the Diabetic Neuropathy Study Group of the European Association for the Study of Diabetes. These criteria adopted a probabilistic approach for assessing length-dependent SFN, basing the diagnosis of SFN on:

1) presence of symptoms and signs of SFN,
2) normal sural nerve conduction study (NCS),
3) a confirmatory test including skin biopsy or QST.

It is a three-step grading diagnostic system ranging from *possible* to *probable* or *definite*, relating to abnormalities identified at different assessments.[2]

- Possible: presence of symptoms and/or signs of SNF, such as decreased sensation, or positive sensory symptoms, with a length-dependent distribution, thus predominantly in the toes, feet, or legs;
- Probable: presence of symptoms and signs of SNF and normal sural nerve conduction study;
- Definite: presence of symptoms and clinical signs of small fiber impairment, normal sural nerve conduction study, and abnormal foot QST thresholds and/or decreased IENFD at the lower leg. [23]

This definition only includes length-dependent symptoms, thus not considering non-length-dependent patterns. Furthermore, according to this diagnostic approach, only patients with pure or isolated impairment of the Aδ- and C-fibers are considered for the diagnosis of SFN, excluding subjects with clinical and NCS findings of large sensory fiber dysfunction that can have a mixed (small and large fiber) sensory neuropathy. [8]

Some recent studies compared the diagnostic power of the two diagnostic approaches described above, showing a strict agreement between them.[2]

The presence of at least two clinical signs increased the reliability of the diagnosis of SFN. Notably, the combination of clinical signs and abnormal QST and/or IENFD findings has higher diagnostic power than the combination of abnormal QST and IENFD findings with no clinical signs. There are patients with symptoms but no clinical signs who reported complete recovery after a mean of 18-month follow-up and did not have abnormal skin biopsy or QST findings. So, symptoms alone should not be considered reliable for diagnosing SFN and must be appropriately evaluated in the clinical context. [2]

Despite the IENFD measurement being the most accurate test to confirm SFN diagnosis, its clinical utility is restricted due to the price, limited availability in centers, and impracticality of performing serial studies to determine disease course and response to treatment. For these reasons, IENFD is not commonly used in routine clinical practice. [24] Uniform criteria are essential to ensure a certain, valid, and standard diagnosis. For this reason, in 2017, Blackmore and colleagues developed diagnostic criteria that do not require IENFD.

*Blackmore criteria* propose the following probabilistic approach for diagnosing SFN, in the presence of appropriate neuropathic symptoms:

- Definite SFN, abnormal neurological examination (impaired pain/thermal sensation), and any two of QSART or QST or HRV;
- Probable SFN, abnormal neurological examination, and either QSART or QST or HRV;
- Possible SFN, abnormal neurological exam or QSART, or QST.

Although this classification is based on symptomatic presentations, being an effective and practical method for the screening of SFN patients in practice, when available, further investigations with skin biopsy may help to further clarify this observation. [24]

Studies investigated in a large cohort of patients the weight of clinical (symptoms and signs), psychophysical (QST), and structural (IENFD) components,

confirming the significantly higher diagnostic accuracy of skin biopsy compared with QST (sensitivity 94.3%, specificity 91.9%). [2]

In the absence of an easily available diagnostic test, definitive diagnosis of SFN remains challenging both within the routine clinical setting and for clinical trials. The diagnosis of SFN is tentative because it is based on the patients' symptoms and subjective responses on the bedside neurological exam. [24]

## 1.2 Diagnostic tools

### *1.2.1* Clinical and Neurological Examination

The first step of clinical examination should be a careful inspection to check for any visible signs of potential peripheral autonomic dysfunction, such as discoloration, dryness of the skin, or dystrophic changes. Additionally, heart rate variability, blood pressure in clinostatism and orthostatism, and pupil motility should be assessed.[2]

Secondary, superficial and proprioceptive sensations must be examined to identify negative sensory signs (such as sensory loss) and positive sensory signs (such as allodynia, paresthesia, and restless leg syndrome).[25] In particular, a comparison between affected and non-affected areas is needed to detect the neuropathy distribution. Cutaneous sensory dysfunction is tested by applying various tactile stimuli on the skin and asking the patient to keep his eyes closed. The inability of the patient to detect hand touch is a sign of tactile hypoesthesia, instead, the excessive reply to a cotton bud or a stick is an expression of allodynia. On the other hand, the outbreak of prickling with needle touch is a manifestation of hyperalgesia. ,[2] It is important to underline that the presence of allodynia and hyperalgesia could hide sensory loss.[26] Thermal sensation is assessed using tubes filled with cold and warm water while proprioceptive vibratory sensation is tested using the 128 Hz graduated tuning fork. [2]

The quality and intensity of pain should also be investigated using scales, such as the VAS (visual analogue scale) or NRS (numeric rating scale).

Furthermore, additional exams to recognize the etiology should be performed (e.g., OGTT or HbA1 for diabetes or impaired glucose intolerance).[25]

### 1.2.2 *Quantitative Sensory Testing (QST)*

QST is a non-invasive psychophysical examination based on measurements of responses to graded sensory stimuli (e.g., mechanical or thermal).[2] This test is considered an expansion of routinary clinical examination, and it is used to determine the functional impairment of small nerve fibers by measuring warmth, cooling, and thermal pain thresholds. QST can evaluate both gain and loss of sensory function related to the clinical aspect of neuropathic pain.[5]

The current QST battery was described for the first time in the German Research Network on Neuropathic Pain (DFNS) and it has been employed worldwide since 2002.[27]

The test should be conducted by trained investigators, and precise oral instructions should be given to the patients. A total of 13 parameters are typically evaluated, providing an overview of the complete sensory profile within about 1 hour. [27]

Different protocols of QST are available; two methods broadly used to detect thermal and thermal pain thresholds are the method of limits and the method of levels.

In the *method of limits,* the stimulus starts on a neutral level and its intensity gradually increases or decreases until it is stopped. Patients are required to press a button twice, first when they detect a change in the stimulus intensity, and then when the stimulus turns into painful. [2,27]

Instead, in the *method of levels,* there is a forced choice algorithm after a pre-defined stimulus. Thus, there are two buttons, one for “yes” and the other for “no”. This method does not require a time-dependent reaction, hence it allows to reduce bias correlated to cognitive and behavioral variables, showing a better diagnostic efficacy for diagnosing SFN, especially when it is performed bilaterally. [2,27]

Thermal threshold testing (TTT) is sufficient to assess the integrity of thinly myelinated A-delta fibers and unmyelinated C-fibers. A thermode starting from a baseline temperature of 32°C and then gradually increasing or decreasing by 1°C/sec is typically used. The unit automatically stops measurements when it reaches the temperature of 0° C or 50° C and returns to the starting temperature

of 32 °C to avoid skin irritation. Usually, the thermal threshold is above 41°C and below 25°C, while the painful thermal threshold is above 45°C and below 5°C.[27]

To assess the mechanical pain threshold, needle stimulators (pinprick) are used. The needle stimulator consists of blunt needles contained in steel tubes in which there are different weights responsible for the different weight force applied on the skin. The pinpricks are applied perpendicularly to the skin in five test series of increasing and decreasing stimulus intensity with a skin contact time of about 1–2 seconds. To determine the mechanical pain sensitivity of the skin a set made up of needle stimulators, a Q-tip, a soft brush, and a cotton pad (non-painful stimuli) is used. These stimulators are applied in a balanced order in a skin area of 2 cm for about 2 seconds. The stimuli are applied in five pseudo-randomized sequences over the tested area, each characterized by three light touch stimuli and seven needle stimuli, so, in the end, this testing procedure is composed of 50 stimuli. The stimuli intensity is rated on a scale from 0 to 100 (0 = no pain; 100 = worst pain imaginable). In the end, the mechanical pain sensitivity is calculated as the mean of all the individual numerical values of the thresholds.[27]

The vibration threshold is evaluated by applying over a bony prominence a Rydel–Seiffer tuning fork at a vibration frequency of 64-128 Hz, with an 8/8 scale. This type of threshold is the only test in the entire QST method.[27]

Lastly, the pressure pain threshold is assessed using a pressure characterized by a blunt rubber contact surface with which a pressure of 0–2000 kPa can be applied. After three repeated measurements, the pressure pain threshold is calculated as an arithmetic mean.[27]

QST has the limit of suffering from the variability of instruments and methodological approaches for location, stimulus application, and sensation qualities examined. The tested area of the body has a significant impact on the measured threshold.[27] Moreover, the algorithms used must be adjusted for the anatomical site, age, and sex. This test requires an active collaboration of the patient, and the patient's mood or cognitive settings could decrease the reliability, hence the results should be interpreted considering the clinical context. Another important limit of QST is the incapacity to discriminate between central and peripheral impairment of the somatosensory system. [2,5]

### *1.2.3 Corneal Confocal Microscopy (CCM)*

The ocular surface is fully innervated with sensory nerves, in particular the cornea which is a clear dome-like tissue forming the frontmost part of the eye.[28]

Corneal Confocal Microscopy (CCM) is a non-invasive and repeatable method that examines the cornea microstructures. This diagnostic tool, using a light ray focused on the corneal layer, allows in vivo visualization of unmyelinated C fibers originating from the ophthalmic division of the trigeminal nerve.[2]

Four parameters can be calculated by the software program CCMetrics*: corneal nerve fiber density* (CNFD), *corneal nerve branch density* (CNBD*), corneal nerve fiber length* (CNFL), and *corneal nerve fiber tortuosity* (CNFT). [8]

Most of the studies have been conducted in diabetic polyneuropathy with a reported sensitivity of 91% and specificity of 93%. In particular, an association between corneal fiber degeneration and the severity of diabetic polyneuropathy has been shown.[2] Moreover, by the use of CCM, decreased density or alterations in corneal nerve fibers have been reported in patients with Sjögren's syndrome and, more recently, in those with HIV infection, amyloidosis, Fabry's disease, or sarcoidosis.[15]

The diagnostic utility of this tool has been proved by several studies conducted on small cohorts of patients with length-dependent and non-length-dependent SFN, in which a reduction of corneal nerve fiber density was observed.[2] Some studies suggest that values should be adjusted to the corneal area to obtain more objective and standard measurements.[5]

Since CCM is still available in a few centers, its diagnostic use in clinical practice remains confined.[2]

### *1.2.4 Conventional Nerve Conduction Study (NCS)*

NCS should be performed as part of the first-line diagnostic work-up to explore the involvement of large sensory and motor nerve fibers. In pure SFN, NCS is expected to be normal. The sensory nerve action potential amplitude and conduction velocity of the sural nerve should be examined.[2] The evaluation of

terminal distal branches such as medial dorsal cutaneous nerve and dorsal sural nerves may improve the diagnostic sensitivity of NCS.[29]

### *1.2.5 Microneurography*

Microneurography is a neurophysiological technique that records the activity of single C-nociceptors, thermoreceptors, mechanoreceptors, and sympathetic fibers from peripheral nerves in awake subjects.[2]

A needle electrode is inserted percutaneously in the direction of a nerve in a limb or the face, freely able to float in the skin. All adjustments of electrode position are done by hand, thanks to the fact that movements of the electrode tip, inserted depth in the skin, are much smaller than movements at the surface. No anesthetic is required, and subjects are alert during the experiment and can cooperate while nerve signals are being recorded.[28] Searching for neural activity can be aided by electrical stimulation down the electrode to assess its position in relation to the nerve and target fascicle. [2]

This technique provided data regarding the physiological activity of C fiber, helping to clarify pathophysiological correlates of clinical phenomena in painful syndromes such as spontaneous activity, sensitization, and hyperexcitability.[30] This technique relies on the fact that unmyelinated nerve fibers exhibit a post-activation transmission delay in the wake of preceding impulses.[28] Microneurography is important to detect abnormal C-nociceptor activity in SFN and other conditions characterized by peripheral neuropathic pain.[2] Furthermore, it allows for investigating the effect of drugs on blocking the abnormal ongoing activity of C-nociceptors.[2]

The use of microneurography in disorders affecting the peripheral nervous system is increased, but its application in clinical practice, however, remains partly limited due to the technical challenges, the amount of time that is required to perform the exam, the fact that collaboration of the patient is needed, and the small number of nerve fibers that can be studied.[2,8]

### *1.2.6 Pain-Related Evoked Potentials (PREPs)*

Pain-related evoked potentials (PREPs) can be used to study the conduction properties of small nerve fibers with an approach not dependent on patients' cooperation and attention. [8]

PREPs can be recorded from the scalp by applying on the skin painful stimuli, obtained by rapid skin heating. Skin heating is generated either by radiant heat (laser-evoked potentials, LEPs) or contact heat rated up to 70° C/s (contact heat-evoked potentials, CHEPs). Both LEPs and CHEPs are based on selective activation of Aδ- and C-fibers.[2,8] Recently, cool-evoked potentials have also been introduced as a technique to study the Aδ fiber-free nerve endings and spinothalamic pathway, but their diagnostic value in SFN is still to be examined. [31]

One limit of PREPs is that, like QST, they are not able to discriminate between a central or peripheral involvement of the somatosensory system. For this reason, PREP findings should be interpreted in the clinical context.

PREPs can be missing, and several studies found that missing PREPs indicate advanced small nerve fiber damage. That is supported by studies that showed that the proximal-to-distal gradient of PREP loss is in line with the clinical and pathophysiological considerations of distally pronounced fiber damage. Furthermore, missing PREPs were three times more frequent in patients with no recordable sural nerve SNAP than in those with preserved sural nerve SNAP. PREPs were also frequently missing in patients with loss of distal epidermal innervation.[32]

*Laser-evoked potentials (LEPs)*

LEPs are a validated technique to investigate the neural bases of nociception. [8]

Low-intensity pulses directed to the skin evoke pinprick sensations and brain potentials (LEPs), caused by the activation of type II AMH mechanothermal nociceptors, from which the afferent signal is conducted along small-myelinated Aδ-fibers to spinothalamic neurons and brain. [33]

Although several types of laser stimulators are now available, a $CO_2$ laser is frequently used. Its advantage is to have a wavelength (10.6 mm) that closely matches the thermophysical properties of the skin. This allows for a negligible skin reflectance and a fully absorption within the most superficial skin layers. [34]

The main LEP signal that is usually measured in a clinical setting is a widespread negative–positive complex (N2–P2). This complex is mostly generated by the anterior cingulate gyrus, with a plausible contribution from the bilateral insular regions. The N2–P2 complex is preceded by an earlier, far smaller negative component (N1) which is lateralized, bilateral, and probably generated by the secondary somatosensory cortex. [35]

Skin denervation induced by topical capsaicin results in decreased LEP amplitude at the vertex, which correlates with the IENFD. Moreover, LEP amplitudes correlate with the intensity of perceived pain, and negatively with age. LEP amplitude is also modulated by opioids and pain expectation.[8]

LEPs have a diagnostic sensitivity of 78% and a specificity of 81%, using skin biopsy as a reference. However, LEP amplitude shows a high inter-individual variability. Vertex LEPs do not reflect a nociceptive-specific neural activity because they can be elicited also by non-nociceptive somatosensory stimuli and their amplitude is mainly due to the stimulus saliency rather than its intensity. [2]

LEPs have been recognized by the European Federation of Neurological Societies as the most reliable laboratory tool for assessing pain pathways. Although several studies reported normal values of LEPs, they have been collected only in a small sample of normal subjects, with a narrow age range. Moreover, the effects of important clinical variables, such as body height, age, and gender have not been studied.[35]

*Contact heat-evoked potentials, CHEPs*

Contact heat-evoked potential is a non-invasive technique for investigating the electrophysiology of thermal and nociceptive pathways.[36]

The diameter of the circular thermode is 27 mm, the heating rate is 70˚C/s, and the cooling rate is 40˚C/s. Cooling begins immediately after the thermode reaches its target stimulus temperature, based on default algorithms. During the procedure, the patients sit on chairs with their eyes closed and muscles relaxed to reduce artifacts, in a semi-dark temperature-controlled room (25˚C). The heat stimulus is typically applied to the hairy skin area of the lateral leg, and the skin area is divided into 6 adjacent non-overlapping districts. The thermode is moved clockwise or counterclockwise across these sites, with a heat pulse delivered from 32˚C to 51˚C. The interstimulus interval is randomly set to approximately 20 to 22 seconds. At the start of the CHEP recording, several heat stimuli are delivered to the subjects to avoid startle responses. During the study, subjects are asked to pay consistent attention to the stimuli and to verbally rate the intensity of their pain 3 seconds after each stimulus using a scale (0-10), in which “0” corresponds to no sensation, “4” corresponds to their pain threshold, and “10” corresponds to maximal pain.[36]

CHEPs are used to investigate SFN, showing a good correlation between CHEP amplitudes and the IENFD. In particular, patients with sensory neuropathies and decreased IENFD have lower amplitude CHEPs. These potential values must be adjusted according to age and gender.[2] Even though, CHEPs can be absent also in healthy individuals. [37]

CHEPs have a diagnostic sensitivity of 81.3% and 73.8% for diabetic neuropathy and small-fiber neuropathy respectively. Reference values for CHEPs have recently been proposed by Granovsky et al. Their study might represent the foundations of applying CHEPs as a physio-logical measure of small nerve fibers. However, the reported normative values are valid only when the same equipment, setup, and stimulation parameters are used.[36]

*Surface concentric electrode stimulation*

The skin of the dorsum of the right forearm is stimulated, using a planar surface concentric electrode. This electrode is an assembly of a central metal cathode (Ø: 0.5 mm), isolation inserts (Ø: 5 mm), and an external anode ring (Ø: 6 mm), providing a stimulation area of 19.6 $mm^2$. Each stimulus typically consists of a train

of three consecutive shocks at 300 Hz subjectively felt as a single pulse. Individual perception can be determined by two series of ascending and descending stimuli, with 0.2 mA increments. Low-intensity stimulation, slightly above the pinprick detection threshold, is usually used. Nociceptive specificity is probably lost when performing high-intensity stimulation.

### *1.2.7 Autonomic Function Tests*

Changes in peripheral autonomic nervous system function may be an early manifestation of SFN, therefore nowadays several diagnostic tools can be used to investigate sudomotor, vasomotor, and cardiovascular functions.[38]

#### 1.2.7.1 *Sudomotor Function Tests*

Sudomotor nerves are unmyelinated or thin myelinated fibers, with mainly cholinergic neurotransmission.[2] The principal neurotransmitter is acetylcholine, although other neurotransmitters are involved, such as vasoactive intestinal peptide (VIP), calcitonin gene-related polypeptide (CGRP), ATP, and substance P. Moreover, adrenergic transmission mediated by epinephrine and norepinephrine is also involved, as it has been shown by immunohistochemical studies.[39,40]

Dysfunction of the sudomotor system can lead to an increase or decrease in sweat production, causing disturbances in thermoregulation. Human thermoregulation is a complex and tightly controlled homeostatic system, in which central and peripheral thermoreceptors are involved. They send information to the central thermoregulatory center located in the hypothalamus. The ability to regulate body temperature via sweating is unique to humans and primates and is mediated through eccrine sweat glands.[41]

Nowadays several standardized techniques are used to quantify sweating and the innervation of sweat glands. Among those, the thermoregulatory sweat test (TST), iontophoretic stimulation with acetylcholine or pilocarpine, dynamic sweat test (DST), and quantitative sudomotor axon reflex test (QSART) are the most employed in the clinical practice. Each test has benefits and drawbacks.[2,41]

The *thermoregulatory sweat test (TST)* is used to evaluate the integrity of central and peripheral sympathetic sudomotor pathways.[41] It consists of increasing the ambient room temperature to raise blood and skin temperature. The amount of sweat production is therefore detected with an indicator dye.[2] The room temperature is adjusted to 45–50 °C with a relative humidity of 35–40%. The subject lays supine on a table, fully covered with an indicator that changes color according to a pH-reaction activated by sweat. The skin temperature needs to be kept between 38.5 and 39.5 °C by overhead infrared heaters, and the heating time should not surpass 70 minutes to avoid hyperthermia and hydromeiosis, which consists of sweating reduction in response to elevated temperature and high levels of skin moisture. Maximal sweating is achieved within 30–65 minutes. In the end, a sweat density map is generated based on digital photographs taken during the test execution. Sweating is typically symmetric, but different in quantity. In SFNs, asymmetric sweat patterns and anhidrotic areas (focal, segmental, regional, length-dependent) may be observed. The severity of the autonomic failure is given by the level of TST%, which is the measured area of anhidrosis divided by the area of the anatomic figure, multiplied by 100. The limits of this test are that it is time-consuming, requires special equipment and preparation, and therefore is only performed in highly specialized centers, thus reducing its clinical applicability.[41]

*Quantitative sudomotor axon reflex test (QSART)* is a sensitive and reproducible technique used to evaluate the postganglionic sympathetic cholinergic sudomotor function by measuring the axon-reflex mediated sweat response over time.[8,41] Sweat glands are stimulated by a cholinergic agent and the sweat production is detected as increased humidity through a hygrometer.[42] Specifically, stimulation and recording are performed using a multi-compartmental sweat capsule, located in standard testing sites, such as the forearm, proximal leg, distal leg, and dorsum of the foot. Each sweat cell is made up of three concentric compartments: the outer one is filled with 10% acetylcholine, the middle one is used as an air spacer, and the inner one is used for humidity recording. Normally, the sweat output starts with a delay of 1–2 minutes, then the sweat output increases for up to 5 minutes after stimulation until it reaches the inflection point and subsequently decreases slowly. Sweat response could be absent, decreased, or increased. Increased sweat production is often a sign of axonal excitability, which is seen in conditions

such as diabetic neuropathy, reflex sympathetic dystrophy, and other small fiber neuropathies. Instead, in diabetic neuropathy, especially in the early stages, a length-dependent pattern of sweat reduction can be seen.[41]

QSART helps to evaluate sudomotor nerve fiber damage also in SFN, with a sensitivity of about 50%.[2] The disadvantages of this technique are that QSART measures only the postganglionic sudomotor response, so it is unable to detect preganglionic lesions, it is time-consuming, requires special equipment, and is not broadly available. [41]

*Quantitative direct and indirect axon reflex test (QDIRT)* is a technique that also allows the evaluation of the postganglionic sympathetic cholinergic sudomotor function by measuring the direct and axon-reflex-mediated sweat response. Sweat glands are stimulated by acetylcholine iontophoresis and sweat produced is shown via an activator dye, through digital photographs caught over time.[43] Sweat droplets are quantified by number, size, and percent area over the area of interest, making a distinction between direct and indirect sweat production. The advantages of this test are that it is simple, inexpensive, quick (15 minutes are required to complete the entire test), and can be used also in centers without sophisticated autonomic laboratories.[41]

The *silicone impression method* is used to evaluate the postganglionic sympathetic cholinergic sudomotor function by measuring the direct and axon-reflex mediated sweat response at specific time points. Sweat glands are stimulated by iontophoresis of acetylcholine, pilocarpine, or methacholine.[44] A thin layer of modulable material is then applied to the skin. The formation of sweat droplets, due to the activation of sweat glands, displaces the silicone material during polymerization resulting in permanent impressions that can be quantified by various methods. Droplet number, size, and distribution are reported, and the volume of sweat production can be estimated by assuming the droplets form a hemisphere. Even though the silicone impression method is probably one of the easiest methods to conduct, artifacts because of hairs, dirt, skin surface texture, air bubbles, or contact with certain types of gloves can influence the results.[8,41]

The *sympathetic skin response (SSR)* measures a multi-synaptic reflex depending on the integrity of both the central and peripheral nervous systems.[8] It is a

measure of electrodermal activity and, even though it does not represent a proper “sweat” test, SSR provides a surrogate measure of sympathetic cholinergic sudomotor function. Perturbation of the autonomic nervous system caused by changes in skin potential can be seen in response to rapid inspiration, electrical stimulation, or also emotions. The sources of the skin potential are presumed to be the sweat glands and the epidermis. Recording electrodes are placed on the dorsal and ventral surface of the hand, medial forearm, proximal leg, distal leg, or proximal foot, and the presence or absence, as well as amplitude and latency of SSRs, are reported. The main advantage of this technique is that it is extremely easy to perform, but it cannot localize the lesion site and is afflicted by high variability within and between subjects. In particular, SSR reliability declines with age, as the responses are absent in many subjects over 50 years old. Moreover, patients with a congenital absence of sweat glands (ectodermal anhidrotic dysplasia) can still have a response. [2,41]

The *Neuropad test* allows the detection of sweat production via the color change of a cobalt II compound applied on the skin in a bandage.[45] Moderate sensitivity and specificity (68% and 49%, respectively) have been reported, and the role of this test for the diagnosis of SFN has still to be established. [8]

The *Electrochemical skin conductance (ESC*), known also as *Sudoscan*, is a recent, simple, quick, painless, and non-invasive technique that measures C-fiber postganglionic sympathetic nerve function in sweat glands. The areas of interest are the palms of the hands and soles of the feet, characterized by a high density of these glands. The Sudoscan measures the electrochemical skin conductance. This test is based on an electrochemical reaction between the chloride ions in sweat and stainless steel-based plate electrodes, on which the subject's hands and feet are placed. A low-voltage current (<4 V) is applied through the electrodes and attracts chloride ions from the sweat glands. The measurement of conductance for the hands and feet is generated from the derivative current associated with the applied voltage.[46] Most of the studies conducted till now have been performed in diabetic neuropathy, demonstrating a decrease in electrochemical skin conductance and a correlation with small-fiber dysfunction and neuropathic symptoms.[8] ESC showed very good sensitivity (65%–78 %) and

specificity (80%–92 %), and recent studies have demonstrated its role also in Fabry disease, Sjögren's syndrome, and chemotherapy-induced SFN.[15]

The *stimulated skin wrinkling (SSW)* is a test that helps to study the sympathetic function by detecting changes in dermal arteriovenous vasoconstriction of the digits.[8] In clinical practice, SSW is usually performed in the hands and graded using a standardized 5-point scale.[47,48] Foot skin wrinkling is hardly ever performed, due to the reduced wrinkling formation. Reduced SSW was found in patients with diabetic neuropathy and idiopathic SFN, but the value of SSW as a diagnostic tool is limited.[8]

#### 1.2.7.2 *Sympathetic Noradrenergic Tests*

*Quantitative pilomotor axon-reflex test (QPART)* is an axon-reflex test, activated by the noradrenergic sympathetic nerves. Iontophoresis with phenylephrine leads to local direct and indirect piloerection. The line connecting the most peripheral edges of erected hairs is the outline of the total area. The indirect area is calculated by subtracting the area of phenylephrine application from the outline area. This technique allows the creation of a topographic map using silicone impressions. The reliability of this test to diagnose SFN is still not clear, due to the limited literature available.[49,50]

*MIBG/SPECT* is an imaging technique that assesses the cardiac sympathetic function and can be used to determine SFN. The radioactive molecule I-meta-iodobenzylguadine (MIBG) is visualized through single-photon emission computed tomography (SPECT). I-MIBG acts as a substrate for norepinephrine, marking post-ganglionic sympathetic noradrenergic innervation. Both impaired uptake of I-MIGB or accelerated washout after 3–5 hours represent signs of autonomic or cardiac disorders. For quantifying the sympathetic innervation, the heart-to-mediastinal uptake ratio (H/M ratio) and washout ratio (WR) are used. Some studies showed a high correlation between the H/M ratio and IENFD in Parkinson's Disease, but the same result was not demonstrated in diabetes. [51]

#### 1.2.7.3 *Microvascular Reactivity Tests*

The microvascular vasomotor reactivity is mediated by autonomic small nerve fibers. Several tests can be used to assess the neural microvascular control. They are all based on axon-reflex detection that can be evoked by different stimuli such as pharmacological, electrical, or mechanical stimuli. The axon reflex generated in cutaneous nerve fibers induces the release of vasoactive substances, which cause a vasodilatory response into a skin area close to the one previously stimulated.

The vasodilatory response is recorded by using a laser Doppler flowmetry or laser speckle contrast imaging. Vasogenic and neurogenic responses can be distinguished temporally and topographically. Patients with SFN showed reduced or absent skin flare areas.[2]

#### *1.2.7.4 Cardiovascular Autonomic Tests*

Cardiovascular autonomic tests (CATs) include a standardized battery of provoked tests that allow the investigation of both the parasympathetic and sympathetic branches of the Autonomic nervous system (SNA).[2]

These well-established batteries of tests help to identify the presence of cardiovascular autonomic neuropathy (CAN) in diabetes, an important traditional risk factor for cardiovascular events and sudden death. In the context of SFN, cardiovascular autonomic dysfunction represents an independent measure of SFN, with no correlation with sensory clinical signs, IENF density, or QST.[2]

CAN is divided into three categories:

1) possible or early CAN if confirmed with one abnormal cardiovagal test;
2) definite CAN with at least two abnormal cardiovagal tests;
3) severe CAN with orthostatic hypotension in addition to definite CAN.[51]

The most widely Cardiovascular autonomic tests used are 1) heart rate (HR) response to a Valsalva maneuver, 2) HR response to postural change, 3) HR response to deep breathing, 4) blood pressure (BP) response to a Valsalva maneuver, 5) BP response to postural change, and 6) BP response to sustained

handgrip. This battery of tests assesses both the parasympathetic and sympathetic adrenergic function.[51]

*Heart Rate Response to a Valsalva Maneuver.* The Valsalva maneuver is a voluntary forced expiratory effort against closed airways, that causes increased thoracic pressure and consequently decreased preload, provoking a complex autonomic reflex to compensate for the reduction of arterial pressure. Heart activity is measured with an electrocardiogram (ECG) and RR intervals are used to assess HR variability. The maneuver is organized into 5 different phases:

- phase (0) deep inspiration,
- phase (I) onset of strain,
- phase (II) continued strain,
- phase (III) release,
- phase (IV) recovery.

The Valsalva ratio is calculated by dividing the shortest RR interval of phase II by the longest interval of phase IV. In Individuals who suffer from SFN, an absence of the bradycardia reflex during phase IV is observed, with a decreased Valsalva ratio.[51]

*HR Response to Postural Change.* Postural changes, such as switching from a supine to an upright position, cause movement of blood volume from the central to the peripheral compartment, such as legs, buttocks, pelvis, and splanchnic circulation. This orthostatic stress evokes a sequence of compensatory cardiovascular responses to maintain homeostasis.[51,52] The homeostasis is maintained by the sympathetic system, parasympathetic system, and baroreflex altogether.[51] Active standing causes an abrupt increase in heart rate in the first 3 seconds, followed by a more gradual increase of the HR during approximately 12 seconds after standing. Approximately 30 seconds are needed to heart rate and blood pressure to return to baseline. [52] The “30:15” ratio assesses the HR physiological response to postural change, by calculating the ratio of the HR increase after approximately 15 seconds from postural change by the relative bradycardia that occurs after approximately 30 seconds. In healthy individuals, HR usually increases by 10 beats/minute, whereas in subjects affected by SFN with autonomic failure, bradycardia is missing.[51]

*HR Response to Deep Breathing.* Respiratory-mediated heart rate variability is an index of cardiac parasympathetic function. The heart rate variability is predominantly mediated by the vagus nerve, whose function might be impaired in SFN. HR can be confounded by respiratory frequency, tidal volume, age, hypocapnia, and increased sympathetic flow. The respiratory-mediated heart rate variability is called “Respiratory sinus arrhythmia” and is dependent on both the frequency and depth of respiration. HR typically increases during inspiration and decreases with expiration. The tests to assess heart rate variability with deep breathing are usually performed in the supine position, where vagal tone is greatest, and commonly 6-10 respiratory cycles (gradual deep inspiration and expiration) per minute are performed. [52] To measure the HR variability, the amplitude of individual heartbeats is measured by ECG. The mean square successive difference, mean circular resultant, standard deviation of the RR interval, and expiratory-inspiratory ratio can be used as additional measures.[51] HR value should be adjusted to age, as several studies showed a relationship between age and HR variability, with a decline of 3–5 beats per minute per decade in healthy subjects. [52]

*Blood Pressure Response to a Valsalva Maneuver.* During the Valsalva maneuver, increased HR occurs in response to decreased BP, and for detecting the hemodynamic response to the Valsalva maneuver, direct measures can be made with a non-invasive beat-to-beat blood pressure monitor. There are no well-established normative values for this test. Patients with autonomic dysfunction show absent overshoot in BP and bradycardia reflex.[51,52]

*BP Response to Postural Change.* The blood pressure response to postural change (active standing or passive tilting) assesses the sympathetic nervous system function. Standing or tilting from the supine position causes a redistribution of blood volume, with a greater accumulation of blood in the sub-diaphragmatic venous system, which consequently results in a decreased stroke volume. The compensatory mechanism consists of tachycardia and vasoconstriction of the vessels in splanchnic, musculocutaneous, and renal vascular districts. In healthy individuals, BP increases by approximately 10 mmHg, and 1-2 minutes after the postural change, BP starts to decrease. In patients with severe autonomic dysfunction, blood pressure and heart rate abnormalities can be noticed until 5–10

minutes after the postural change, but early or mild adrenergic failure may need a longer period of standing or duration of tilt to be seen. BP response can be evaluated using the head-up tilt test, which helps to eliminate the active leg muscle contraction that occurs during standing and allows to obtain more sensitive results.[51,52]

*BP Response to Sustained Handgrip.* Sustained muscle contraction results in a reflex rise in BP. During the test, the subject is required to hold a dynamometer for 3–5 min, and BP is measured every minute. The difference between diastolic BP before contraction and then before handgrip release is used as a measure of BP response. No rise in BP is seen in patients with autonomic dysfunction. The sensitivity and specificity of this technique are low, due to confounders, such as poor standardization of muscle effort, reduced muscle afferent activity in trained muscles, and decreased muscle chemoreceptor afferent activity.[51]

- *Cold Pressor and Mental Stress Test.* The cold pressor test consists of immersing one hand in iced water with a subsequent increase in BP. This reflex is due to increased muscle sympathetic nerve activity and venous plasma norepinephrine. The mental stress test consists of tasks such as subtracting seven series from 100 or applying the Stroop color word-naming test. Mental stress also leads to a BP increase. In sympathetic dysfunction, BP increase is lowered or absent. The limits of this technique are that the sensitivity and specificity are low and inter-subject variability is high. [51]

The tests mentioned above are part of the Ewing battery of tests, except for the “Cold Pressor and Mental Stress Test”.

#### 1.2.7.5 *Pupillometry*

Pupillometry is the study of changes in pupil diameter as a window of cognitive arousal.[53] Sympathetic and parasympathetic autonomic nerve fibers mediate the pupil light reflex, which consists of changes in pupil radius in response to environmental light. More precisely, the parasympathetic system mediates the dilation of the pupil (mydriasis), while the sympathetic system mediates the constriction of the pupil (miosis). Changes in pupil diameter related to arousal or

cognitive states do not exceed 0.5 mm, while changes correlated to switching from light to dark can result in an increase from 1.5 to 9 mm. The pupil size can be used as an indicator for several autonomic neuropathies. [51]

#### *1.2.7.6 Bladder Function Tests*

Bladder function, compared to other visceral organs' functions, is under voluntary control, so depends on learned behavior. Voluntary control is possible due to autonomic and somatic efferent innervation.[54] The bladder neck and urethra are innervated by Aδ and C-fibers; Aδ fibers are involved in normal micturition, while C fibers are responsive to pathologic or noxious stimuli, such as chemical irritation or cooling.[55,56] In SFN, bladder dysfunction may develop. Therefore, several tests to detect bladder function can be accomplished.[51]

*Cystometry, uroflowmetry*. Cystometry primally assesses the passive filling component of the bladder. Notably, sensation, capacity, and involuntary detrusor activity are evaluated. Sterile water or normal saline is generally used to fill the empty bladder.[57] While increasing the volume, the bladder can maintain approximately the same compliance (P ves). The patient marks the 3 phases of filling: 1) first sensation of filling, 2) first desire to void, and 3) strong desire to void. Any bladder contraction during the filling phase is considered abnormal. In normal conditions, all three phases will be noticed, indeed one or more phases could be missing in the case of autonomic dysfunction.[51]

*Sphincter electromyography urethral pressure profilometry*. Bladder pressure is measured via the urethral catheter (P ves) and abdominal pressure is measured with an intrarectal catheter (Pabd). The difference between P ves and P abd represents the detrusor or bladder pressure (P det). [51]

*Uroflowmetry* is the analysis of the flow pattern during micturition, the voided volume, and the residual volume. This technique uses a uroflowmeter to measure the urinary stream in milliliters per second (mL/s). Instead, the residual volume is measured with an Ultrasound (US) scan.[58] In normal subjects the flow pattern is continuous with good flow velocity, while a decreased flow velocity with increased duration of micturition is a sign of obstruction, and intermitted flow can be

suggestive of impaired bladder contractility, obstruction, or voiding with abdominal straining. Normally, discomfort occurs at a filling volume of around 300–500 mL. Patient with a neurogenic bladder can miss the first sensation of filling at around 100–200 mL, and their capacity can be increased to 2L. [51]

S*phincter electromyography (EMG).* This technique uses an electrode placed in or near the sphincter muscle. Voiding starts with the relaxation of the sphincter, and normally no muscular activity is recorded, while constant activity is measured after voiding. EMG shows a slowly increasing activity until the command to void. Several supra sacral spinal cord pathologies may cause detrusor external sphincter dyssynergia (DESD), which can result in huge EMG changes such as detrusor contraction against a relatively closed sphincter. This will result in high pressures and may eventually cause impaired bladder compliance. [51]

*Urethral pressure profilometry.* A catheter with a pressure sensor is inserted in the urethra. During the sensor withdrawal, a pressure profile along the length of the urethra is drawn.[51]

### *1.2.8 Questionnaires*

Several questionnaires are available for the screening of neuropathic pain symptoms.

For a clearer overview of questionnaires, they can be categorized into:

- screening questionnaires,
- assessment questionnaires,
- specific small fiber questionnaires,
- pain intensity questionnaires.

Screening questionnaires are helpful for the identification of neuropathic pain, which especially relates to patients with complex medical conditions (e.g., spinal cord injury). Instead, assessment questionnaires are helpful for the quantification of neuropathic symptoms. Some questionnaires belong to two categories at the same time, due to multiple types of questions.

The most suitable questionnaire is chosen based on the patient population and their symptoms.

For SFN questionnaires, a distinction can be made between autonomic symptoms (survey of autonomic symptoms (SAS), autonomic symptom profile (ASP)), validation based on Chemotherapy Induced Polyneuropathy (CIPN) (Total Neuropathy Scale (TNS)), validation based on diabetes (modified Toronto Clinical Neuropathy Score (mTCNS), Utah Early Neuropathy Scale (UENS)), pure SFN with the focus on frequency of symptoms (SFN-Symptom Inventory Questionnaire (SFN-SIQ)), isolated SFN with the focus on activity and participation restrictions due to SFN (SFN-RODS) and isolated SFN validated in sarcoidosis patients with the focus on both frequency and intensity of symptoms (Small Fiber Neuropathy Screening List (SFNSL)). [51]

#### *1.2.8.1 Overall disability sum score (ODSS)*

This overall disability sum score (ODSS) is part of the Guy's neurological disability scale.[59] ODSS consist of an arm and leg disability scale with a total score ranging from 0 (no signs of disability) to 12 (most severe disability score) (*Figure 7*). [59,60] The ODSS is based on a good arms and legs functional examination, descripted in a checklist form suitable for interviewing patients. Daily arm activities, such as dressing the upper part of the body, doing and undoing buttons and zips, washing and brushing hair, using a knife and fork, and turning a key in a lock can be scored as not *affected*, *affected but not prevented*, or *prevented*. These results are translated into an arm grade based on a score range from 0 (normal arm abilities) to 5 (severe symptoms and signs in both arms preventing all purposeful movements). On the other hand, the leg scale analyzed problems of walking, and taking into account the use of a device. Also for the leg the results are translated into a leg grade with a score range from 0 (walking is not affected) to 7 (restricted to wheelchair or bed most of the day, preventing all purposeful movements of the legs). [61]

| Arm disability scale – function checklist | Not affected | Affected but not prevented | Prevented |
|---|---|---|---|
| Dressing upper part of body (excluding buttons/zips) | O | O | O |
| Washing and brushing hair | O | O | O |
| Turning a key in a lock | O | O | O |
| Using knife and fork (/spoon—applicable if the patient never uses knife and fork) | O | O | O |
| Doing/undoing buttons and zips | O | O | O |

**Arm grade**

0 = Normal
1 = Minor symptoms or signs in one or both arms but not affecting any of the functions listed
2 = Moderate symptoms or signs in one or both arms affecting but not preventing any of the functions listed
3 = Severe symptoms or signs in one or both arms preventing at least one but not all functions listed
4 = Severe symptoms or signs in both arms preventing all functions listed but some purposeful movements still possible
5 = Severe symptoms and signs in both arms preventing all purposeful movements

| Leg disability scale – function checklist | No | Yes | Not applicable |
|---|---|---|---|
| Do you have any problem with your walking? | O | O | O |
| Do you use a walking aid? | O | O | O |
| How do you usually get around for about 10 metres? | | | |
| Without aid | O | O | O |
| With one stick or crutch or holding to someone's arm | O | O | O |
| With two sticks or crutches or one stick or crutch and holding to someone's arm | O | O | O |
| With a wheelchair | O | O | O |
| If you use a wheelchair, can you stand and walk a few steps with help? | O | O | O |
| If you are restricted to bed most of the time, are you able to make some purposeful movements? | O | O | O |

**Leg grade**

0 = Walking is not affected
1 = Walking is affected but does not look abnormal
2 = Walks independently but gait looks abnormal
3 = Usually uses unilateral support to walk 10 metres (25 feet) (stick, single crutch, one arm)
4 = Usually uses bilateral support to walk 10 metres (25 feet) (sticks, crutches, two arms)
5 = Usually uses wheelchair to travel 10 metres (25 feet)
6 = Restricted to wheelchair, unable to stand and walk few steps with help but able to make some purposeful leg movements
7 = Restricted to wheelchair or bed most of the day, preventing all purposeful movements of the legs (eg, unable to reposition legs in bed)

Overall disability sum score = arm disability scale (range 0–5) + leg disability scale (range 0–7); overall range: 0 (no signs of disability) to 12 (maximum disability).
For the arm disability scale: allocate one arm grade only by completing the function checklist. Indicate whether each function is "affected," "affected but not prevented," or "prevented."
For the leg disability scale: Allocate one leg grade only by completing the functional questions.

*Figure 7: Description of overall disability sum score (ODSS).*
Description of the questionaries used for assessing the arm and leg disability scales.

Image taken from the paper Clinimetric evaluation of a new overall disability scale in immune mediated polyneuropathies by M. I S J Merkies et. al.

### *1.2.8.2 mTCNs questionary*

The Toronto Clinical Neuropathy Score (TCNS) consists of a brief, easily semi-structured clinical interview and examination (*Figure 8*). The TCNS was elaborated to detect early diabetic sensorimotor neuropathy (DSP), emphasizing sensory symptoms and deficits, first manifestation of DSP.[62] The TCNS is reliable scale for the diagnosis and staging of DSP; it has been validated against sural nerve morphology and electrophysiology, with a significant negative correlation with sural nerve fiber density.[63] Currently, the TCNS has been shown to be a valid and reliable scale in a wide spectrum of PNPs, so it could be useful in clinical practice and research.[62]

| Symptom scores | Sensory test scores | Reflex scores |
|---|---|---|
| Foot pain | Pinprick | Knee reflexes |
| Numbness | Temperature | Ankle reflexes |
| Tingling | Light touch | |
| Weakness | Vibration | |
| Ataxia | Position sense | |
| Upper limb symptoms | | |
| Symptom scores graded as | Sensory test scores graded as | Reflexes graded as |
| 0 = absent | 0 = normal | 0 = normal |
| 1 = present | 1 = abnormal | 1 = reduced |
| | | 2 = absent |

Maximum TCNS is 19 points.
Symptoms and signs (sensory tests) are considered present if because of diabetic sensorimotor polyneuropathy (DSP) in the opinion of the investigator. Details of the TCNS have been published previously [9].

*Figure 8: Descriptive table of the original Toronto Clinical Neuropathy Score (TCNS)*

Image taken from the paper Reliability and validity of the modified Toronto Clinical Neuropathy Score in diabetic sensorimotor polyneuropathy by V. Bril et. al.

The modified Toronto Clinical Neuropathy Score (mTCNS), derived from the TCNS, includes a scale of simple sensory tests and does not consider reflex testing, that are variable among subjects. The mTCNS is a combination of two sub-scores: a symptom score and a sensory test score. The symptom of neuropathy considered are six: pain, numbness, tingling, weakness in the feet, similar symptoms in the upper limbs, and unsteadiness while walking (ataxia). The value of each symptom analyzed ranges from 0 (not present) to 3 (interferes with the sense of well-being and activities). A value of 1 indicates that the symptom is present but does not interfere with the sense of well-being or activities, and a value of 2 indicates that the symptom is present and interferes with the sense of well-being but not with activities. Adding all the values together the total score is ranged from 0 to a maximum of 180. Regarding sensory test, pinprick sensation, temperature discrimination, proprioception, light touch, and vibration are assessed in the lower extremities. Each sensory test ranges from 0 (normal) to 3 (impaired to proximal to the ankle level); a value of 1 for a sensory test indicates impairment only at the toes, and a value of 2 indicates impairment up to the ankle. The total value of all sensory tests ranges from 0 to 15 (*Figure 9*). The mTCNS is part of the routine PNP assessment. In particular, the mTCNS is a validated scale for DSP and correlates with severity of the disease. It is based on a simplified neurological examination assessing peripheral sensory perception and the presence of neuropathy symptoms.[62]

Comparing to the TCNS the mTCNS is more reliable and sensitive to early detection of DSP.[62] However, both scales are valid instruments to detect the presence and stage severity of DSP and can be used both in the clinic and in clinical research trials.[64]

| Symptom scores | Sensory test scores |
|---|---|
| Foot pain | Pinprick |
| Numbness | Temperature |
| Tingling | Light touch |
| Weakness | Vibration |
| Ataxia | Position Sense |
| Upper limb symptoms | |
| Symptom scores graded as | Sensory test scores graded as |
| 0 = absent | 0 = normal |
| 1 = present but no interference with sense of well-being or activities of daily living | 1 = reduced at the toes only |
| 2 = present, interferes with sense of well-being but not with activities of daily living | 2 = reduced to a level above the toes, but only up to the ankles |
| 3 = present and interferes with both sense of well-being and activities of daily living (both) | 3 = reduced to a level above the ankles and/or absent at the toes |

Maximum mTCNS is 33.
Symptoms and signs (sensory tests) are considered present if as a result of diabetic sensorimotor polyneuropathy (DSP) in the opinion of the investigator.

*Figure 9: Descriptive table of the modified Toronto Clinical Neuropathy Score (mTCNS)*

Image taken from the paper Reliability and validity of the modified Toronto Clinical Neuropathy Score in diabetic sensorimotor polyneuropathy by V. Bril et. al.

### *1.2.9 Functional magnetic resonance imaging (fMRI)*

Pain perception is modulated by the Central nervous system (CNS). Several studies comparing brain functionality in subjects with SFN and healthy controls detected a volume reduction in pain-processing regions (anterior cingulate cortex). Studies showed a correlation between the degree of volume reduction and the degree of IENFD. Moreover, a significant reduction in functional connectivity from the bilateral anterior cingulate cortices (ACCs) to the limbic areas (the parahippocampal gyrus and the posterior cingulate cortex), pain-processing area (the insula), and visuospatial areas (the cuneus) was observed. The entity of reduction in functional connectivity was linearly correlated with the severity of intraepidermal nerve fiber depletion. [51,65]

### *1.2.10 Peripheral Nerve Ultrasound*

Another test that can be used to detect small fiber impairment is Peripheral Nerve US.[66] US sural nerve measurements may highlight structural changes in subjects with SFN in comparison with healthy controls. Instead, no structural changes have been observed during superficial peroneal measurements.

Cross-sectional area was increased in SFNs, while thickness-to-width ratio did not differ between healthy controls and patients affected by SFN. The pathophysiology of increased cross-sectional area is still unknown, but there are several theories, such as loss or injury of distal small fibers or impaired sodium channel function causing an impaired axoplasmic flow.[51]

## 1.3 Skin biopsy

Skin biopsy, a technique available for about 20 years, can provide a reliable quantification of somatic and autonomic small nerve fibers. The quantification of IENFD (intra-epidermal nerve fiber density) can be considered the “gold standard” for the diagnosis of SFN when associated with clinical signs and other tests, although a true gold standard for the diagnosis of SFN is still missing.[2,8]

Nerve fibers in the human epidermis were described for the first time in 1868 by Paul Langerhans, but it was possible to stain and visualize them only after the development of an antibody directed against the pan-neuronal marker protein gene product 9.5 (PGP 9.5).[67]

Nerve fibers derived from neurons in the dorsal root ganglia as well as the sympathetic and parasympathetic ganglia terminate in the skin, innervating the epidermis as “free nerve endings”.[68] The majority of skin nerve fibers are unmyelinated C-fibers, but there are also thinly myelinated Aδ-fibers, which lose the Schwann cell ensheathment at the level of the dermal-epidermal junction. The intra-epidermal nerve fibers (IENF) derive from the subepidermal nerve plexus, which consists of nerve fiber bundles oriented horizontally just below the epidermis. From the subepidermal nerve plexus, the IENFs proceed through the

epidermal basement membrane, ascending vertically between the keratinocytes.[8,68] Glabrous skin, but also blood vessels, arrector pilorum muscles (in hairy skin), and sweat glands are richly innervated.[68]

Several techniques for tissue processing and nerve fiber assessment are nowadays available, including techniques for staining, quantification of the intraepidermal and subepidermal nerve fibers, and different antibodies to distinguish different subtypes of nerve fibers.[67]

### *1.3.1 Execution*

Skin biopsy is a sterile, minimally invasive technique, performed under local anesthesia (lidocaine), with a disposable punch. A 3-mm-diameter punch is commonly used with no need for sutures, and healing generally occurs within 1 week, barely leaving a visible scar. A disposable punch with a diameter of 6 mm can be also used; in the cylindric skin sample, both the epidermis and derma with sweat glands and hair follicles are included.[67]

No side effects or complaints are usually reported after the execution of the biopsy, but informed consent is required, and information on the risk of bleeding, infection, and delayed healing must be provided to the patients.[67]

Contraindications to the execution are local infections, severe wound healing deficits, and bleeding disorders (e.g., anticoagulation). [68]

Skin biopsy can be performed at any site of the body (e.g., face, trunk, or fingers), but for diagnostic purposes is typically performed at a distal site on the leg (10 cm above the lateral malleolus) and a proximal site on the thigh (20 cm below the iliac spine). Taking skin samples both at a proximal and distal site allows the detection of a length-dependent SFN. [67] Moreover, in severe SFN, the distal site may be completely denervated, and any abnormalities (e.g., axon swellings or prolonged Ranvier nodes) may only be seen in the proximal sample.[68]

Around 50 vertical sections of 50 µm are obtained from each skin biopsy. The first and last few sections should not be considered for nerve examination because of the possible presence of artifacts.[69]

Punch biopsy produces a cylindric sample of skin that includes the epidermis and the superficial (subpapillary and reticular) dermis. [67]

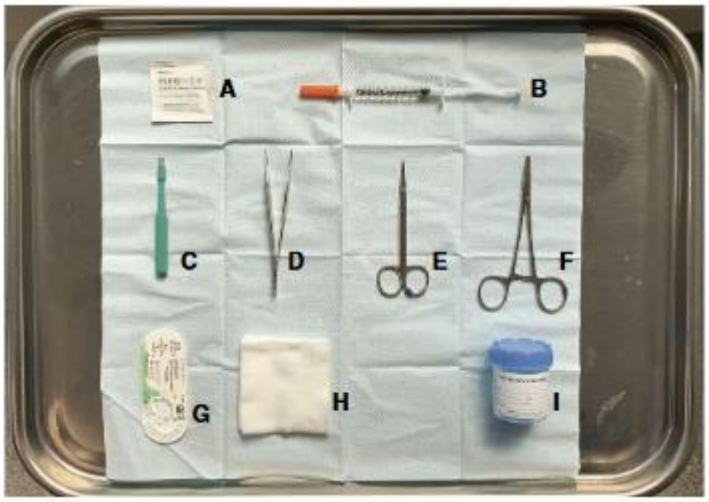


*Figure 10: Set up for a punch biopsy.* A) Isopropyl alcohol wipe, B) local anesthetic, C) punch biopsy, D) forceps, E) scissors, F) needle holder, G) suture material (generally not necessary), H) gauze, I) specimen jar. In this picture, strip patches, which are necessary to close the wound, are missing.

Image taken from the paper "How to perform a skin biopsy", written by Kirsty JL Wark, Saxon D Smith, and Deshan F Sebaratnam.

### *1.3.2 Immunostaining*

The two widely used immunostaining methods are the *Bright-field immunohistochemistry (BFI)* and *indirect immunofluorescence with or without confocal microscopy*.

The most used marker for nerve fibers is the antibody to PGP 9.5 (protein gene product 9.5), which is broadly distributed in the peripheral nervous system and is a non-specific pan-axonal marker. PGP 9.5 is a form of ubiquitin carboxyl-terminal hydrolase (a cytosolic enzyme that removes ubiquitin) found mostly in neurons which accompanies the slow component of axonal transport (*Figure 11*).[67]

To preserve PGP 9.5 immunoreactivity, fixation is necessary. In the absence of fixation, PGP 9.5 immunoreactivity is lost, and it will not be possible to detect nerve fibers. On the other hand, over fixation is also a problem as it may also lead to loss of immunoreactivity. Several fixation protocols have been established. A standard protocol involves fixation overnight in fresh 4% paraformaldehyde or 2%

paraformaldehyde-lysine periodate (2% PLP), or Zamboni's fixative (2% paraformaldehyde and picric acid), followed by cryoprotection in 10% sucrose (or in glycerol) overnight, washing and keeping in buffer at 4°C until use.[68]

Other antibodies can be used to investigate unmyelinated and myelinated cutaneous nerve fibers, such as antibodies against specific components of the cytoskeleton (e.g., microtubules and neurofilaments) and specific components of myelin (e.g., myelin basic protein, peripheral myelin protein 22, and myelin-associated glycoprotein).[67] However, they have not gained widespread use in the clinical routine.[68]

Through immunostaining, different structures included in the thickness of skin samples can be marked, such as nerve fibers, sweat glands, blood vessels, and resident or infiltrating cells. Autonomic fibers innervating sweat glands and blood vessels can be highlighted with antibodies against neuropeptides (e.g., vasointestinal peptide, substance P, or calcitonin-gene-related peptide), whereas the dermis–epidermis junction and blood vessels can be marked by antibodies against collagen IV.[67]

Using double immunofluorescence multiple structures can be marked simultaneously (e.g., double IF for PGP9.5 and CD31 allows to highlight the neurovascular structures).

The confocal laser microscopy leads to obtaining a remarkable three-dimensional reconstruction of the section and allows the quantification of the IENFD through computerized image analysis. This technique is particularly useful in the study of cutaneous receptors, sweat glands, and blood vessels, even though it is complex and time-consuming. [67]

Another technique to obtain skin samples is the *Blister technique*. This skin biopsy method is less invasive than punch biopsy, and it is also used to investigate epidermal innervation. In the blister technique, a suction capsule that separates the epidermis from the dermis at the junction level is used. There is no need for local anesthesia, no risk of bleeding, and the area of the epidermis investigated is bigger than the surface of the 3-mm-diameter sections obtained from punch biopsy. Indeed, the disadvantage of this technique is that it does not provide information on the innervation of the dermis or the morphology of intraepidermal nerve fibers. This technique was developed at the University of Minnesota. [67,69]

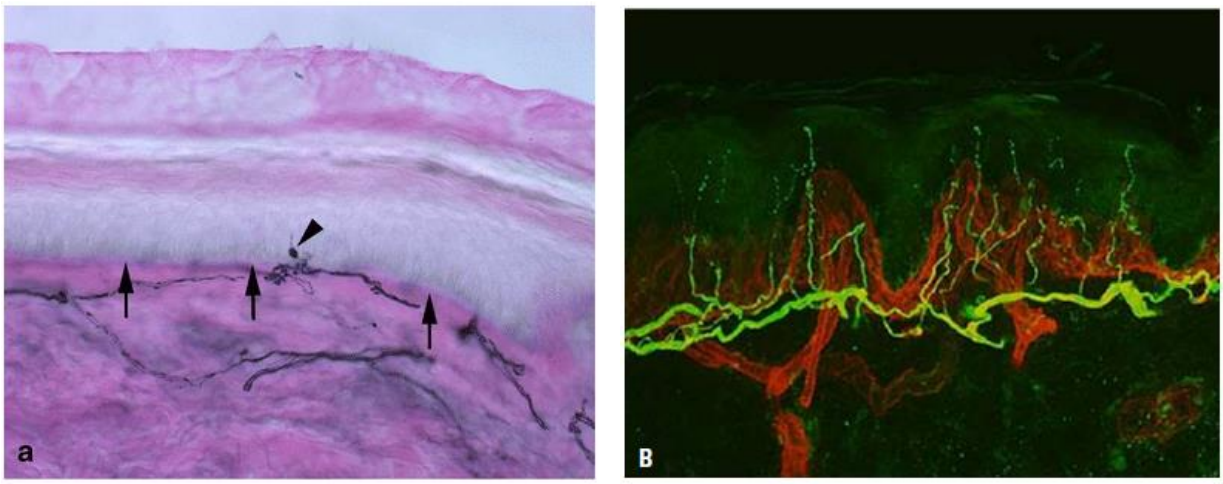


*Figure 11: Dermal and intraepidermal nerve fibers stained with anti-PGP 9.5 antibodies.*

A) Bright-field microscopy; B) Confocal microscopy (indirect immunofluorescence), blood vessels are red, indeed small fibers are green.

Image taken from the paper: A) Utility of Skin Biopsy to Evaluate Peripheral Neuropathy by Arthur P. Hays; B) Skin biopsy: an emerging method for small nerve fiber evaluation by Eun Hee Sohn et. al.[70]

### *1.3.3 Microscopy, Quantification of IENFD*

A minimum of three sections should be analyzed. Sections are observed using a light or fluorescence microscope, according to the staining method previously used. It is important to measure the epidermal length for the following IENF quantification, and this can be done by digitalization of the images. IENFD can also be calculated by using a microscope intraocular lens ruler or by dividing the number of counted fibers by 3, but only if the biopsy was done with a 3-mm punch. This last method has shown comparable values to the data obtained by using

software. However, it cannot be used if sections are divided to be processed in different ways for several analyses, for example, for histology and gene expression. For this reason, this quantification method is not widely used. [68]

By convention, only the number of nerve fibers crossing the dermis–epidermis junction is quantified, counting them at high magnification (i.e., 40x objective), while secondary branching and fragments are excluded from quantification. The linear density of intraepidermal nerve fibers per millimeter (IENF/mm) is calculated by measuring the length of the surface of each section using software.[8,67] Till now, no study provided information on the rules for counting IENF fragments*(Figure 12)*.[69]

Intra- and interobserver variability, and interlaboratory agreement on IENF counts have been evaluated. [69]

The quantification of sudomotor nerve fibers is challenging due to the complex three-dimensional structure of the sweat glands. Several methods have been proposed, but none has been standardized. [69]

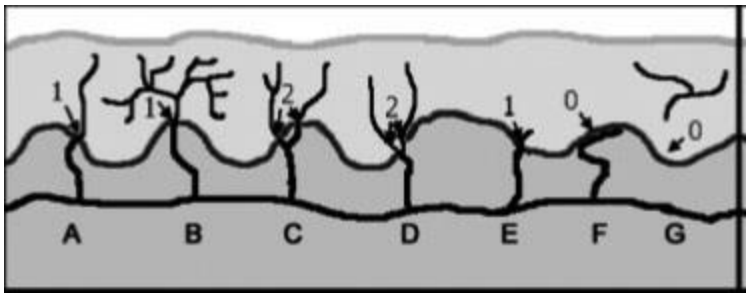


*Figure 12: Intraepidermal nerve fiber counting rule.* Diagram of skin innervations, in which: nerves are colored black, basement membrane dark grey, dermis medium grey, and epidermis light grey. Only nerve fibers crossing the basement membrane are counted as one nerve fiber. Indeed, nerve fibers that branch after crossing the basement membrane or which reside only in the epidermis should be excluded. The epidermal nerve fiber branches before crossing the basement membrane should be counted.

Image taken from the paper Skin biopsy: an emerging method for small nerve fiber evaluation by Eun Hee Sohn et. al. (Originally adapted from Lauria et al.)[70]

### *1.3.4 Normative values of intraepidermal nerve fiber density*

Both bright-field immunohistochemistry and indirect immunofluorescence have provided standard values of IENFD in the legs. The bright-field microscopy is a reliable method, which significantly correlated with stereological techniques of skin-nerve morphometry and with the quantification of nerve fibers per area. Using indirect immunofluorescence rather than bright-field microscopy, the density of intraepidermal nerve fibers at the distal leg is higher (33·0 nerves per millimeter vs 7·4 nerves per millimeter). Nowadays, normative reference values are available for bright-field immunohistochemistry and indirect immunofluorescence (PROVITERA ET AL.), but not yet for the blister technique.[68,69]

Values obtained must be compared with age and gender-matched normative values. Aging is correlated with a decreasing IENFD in the distal leg.[67] Moreover, IENFD at the distal leg may be lower in men than in women, while weight and height do not have any significant impact on IENFD. [69]

The IENFD cutoffs of 7.63/mm and 8.8/mm at the distal leg were associated with a specificity of 90% and 79.6% and a sensitivity of 82.8% and 77.2%, respectively.[69]

### *1.3.5 Findings in patients with neuropathies*

Skin biopsy can help in the early diagnosis of SFN and is easier than a sural nerve biopsy. Comparative studies show that IENFD can be significantly reduced despite normal morphometry of small nerve fibers on the ultrastructural examination. In about 25% of people with symptoms suggestive of neuropathy, skin biopsy was the only technique to detect SFN.

Skin biopsy can help to detect both the degeneration in somatic nerves and subclinical autonomic impairment in people with painful neuropathies. This is extremely important because of the potentially life-threatening events caused by dysautonomia.[67]

Skin biopsy is also helpful for detecting the primary site of nerve pathology. In length-dependent axonal polyneuropathies (e.g., diabetic neuropathy), a reduction in the IENFD at the distal leg rather than at the proximal site is typical, reflecting the dying-back degenerative process. On the other hand, in sensory

neuronopathies (e.g., Sjögren's syndrome), a degeneration of dorsal root ganglia neurons occurs, with a major IEFND decrease at the proximal site, reflecting the pattern of non-length-dependent skin denervation. [67]

The assessment of morphological changes, such as increased density of large or diffuse axonal swellings, in skin nerve fibers might be an early sign of peripheral neuropathies. However, axonal swellings also occur in many healthy people, so their relevance should be evaluated in the context of other morphological and clinical findings. In patients reporting symptoms, the swellings are commonly associated with degenerative changes in nerve bundles, seen as a weaker signal and fragmented appearance of the nerve fibers after immunostaining with PGP 9.5.[67]

IENFD has been reported to be reduced also in other painful conditions, such as Guillain-Barré syndrome, meralgia paresthestica, notalgia, Ehlers-Danlos syndrome, and fibromyalgia and in nonpainful disorders, such as Parkinson's disease and related disorders, amyotrophic lateral sclerosis, critical illness, and peripheral arterial disease. [8]

Several studies over the years have shown a good sensitivity and specificity of IENFD for the diagnosis and follow-up of SFN, if compared to integrated clinical judgment. However, a reduction in IENFD does not automatically provide a diagnosis of SFN, because for example gain-of-function neuropathies may not be detected by IENFD quantification. [68]

There are only limited data on the relation between IENFD and pain in SFN. In several studies, the number of PGP 9.5 immunoreactive IENFs was not associated with measures of pain.[68]

## 1.4 Blood vessel in the skin

The epidermis has an avascular circulation, while the other layers of the skin are crossed by different types of hematic vessels: arteries, capillaries, and veins.[71]

The skin contains a highly specialized vascular network, organized into two plexuses within the dermis that run parallel to the surface of the skin, located in the

superficial and deep layers, respectively.[72] The majority of vessels consists of high-resistance terminal arterioles, papillary loops (capillaries), and post-capillary venules and they are located in the superficial papillary dermis, 1–2 mm below the epidermal surface. In particular, the papillary loops are responsible of heat exchange with the environment, because of they are located close to the dermal–epidermal junction where there is both a high thermal gradient (due to the large surface area) and high blood flow. Indeed, the second vascular plexus is located at the dermal–subdermal junction, where the vessels have greater diameter than those of the upper plexus. From this lower plexus, ascending arterioles connect hair follicles, and sweat glands to the upper plexus. In the glabrous (non-hairy) skin of the palms, lips and plantar aspect of the feet, arteriovenous anastomoses (AVAs) bypass the resistance vessels, directly connecting the arterioles and venules. Compared to papillary loops AVAs are considered less efficient for thermoregulation, because they have a smaller surface area and lie deeper in the dermis.[73]

The regulation of blood flow through anastomosis is governed principally by the nervous system, in response to reflex activation by temperature receptors or by higher centers of the central nervous system, in fact the thick muscular walls of the vessel are richly supplied with nerve fibers. Stimulation of sympathetic nerve fibers to skin blood vessels (arteries, veins, and arterioles) induces vasoconstriction, and severance of the sympathetic nerves induces vasodilation. Parasympathetic vasodilator nerve fibers do not innervate the cutaneous blood vessels. However, stimulation of the sweat glands, which are innervated by cholinergic fibers of the sympathetic nervous system, dilates the resistance vessels in the skin. [74]

Despite the known major role of skin blood vessel innervation in blood flow control, little information on the co-innervation of blood vessels by sensory and autonomic fibers and the relationships of these fibers to one another is available. Vasodilation appears to result from sensory and parasympathetic fiber activation, instead there is evidence that vasoconstriction is controlled only by sympathetic fibers.  effect that appears to be mediated by means of α-adrenergic receptors. [75]

The possibility of a nerve-muscle relationship between the sympathetic nerve fibers and vascular smooth muscle was demonstrated. The existence of such a

relationship is supported by the evidence that it has been demonstrated a decline with age in the number of adrenergic nerve endings as visualized by fluorescence, parallel to a reduced innervation with age. Moreover a direct trophic influence of the SNS has been documented on the cultured vascular smooth muscle cells, and it was observed that these explant cell maintain their differentiated characteristics longer in the presence of the sympathetic ganglion extracts than in their absence.[76]

## 2. AIM OF THE STUDY

The study aimed to aimed to clarify the pathomechanisms underlying specific symptoms, like itch and pain, in patients with small fiber neuropathy and/or polyneuropathy of different types, by studying in great details the morphology and morphometry of skin samples obtained through a conventional skin biopsy, focusing on neurovascular structures. To this purpose, we compare neurovascular structures in sub-epidermal and dermal layers between (a) patients with small fiber neuropathy and/or polyneuropathy associated with itch, (b) subjects with small fiber neuropathy and/or polyneuropathy associated with pain, (c) patients with small fiber neuropathy and/or polyneuropathy associated with both pain and itch, (d) patients with small fiber neuropathy and/or polyneuropathy without these symptoms, and (e) healthy individuals.

To achieve the main aim of this study, we evaluated the occurrence of any differences among the various groups regarding the number and area of vascular structures, small nerve fibers, and neurovascular contacts at different layers of the skin (dermis, sub-epidermis, and epidermis). That comparison was performed for both the distal leg and proximal thigh, to allow also for the assessment of any length-dependent changes.

To obtain more information regarding the pathomechansims of itch and pain in SFN and in other types of neuropathies, we also correlated these differences with the severity of neuropathy and the symptoms reported by the patient.

# 3. MATERIALS AND METHODS

## *3.1 Data Source*

We analyzed the skin samples taken from the proximal thigh of the patients using a disposable 6-mm diameter punch.

We enrolled 25 healthy subjects and 79 patients with small fiber neuropathy and/or polyneuropathy of various aetiologias.

The 79 samples taken from patients affected by neuropathy were divided into four groups; the classification was based on symptomatology, notably on the presence or absence of pruritus and/or pain.

Considering the total of 104 samples, the following groups were obtained:

- *GROUP 1*: 11 patients diagnosed with peripheral neuropathy complaining of pruritus;

- GROUP 2: 25 patients diagnosed with peripheral neuropathy complaining of pain;

- GROUP 3: 31 patients diagnosed with peripheral neuropathy with both pruritus and pain;

- GROUP 4: 12 patients diagnosed with peripheral neuropathy presenting neither pain nor pruritus;

- GROUP 5: 25 healthy control individuals, without any symptoms or signs compatible with peripheral neuropathy.

The initial phases of cryostat sectioning, image acquisition under the microscope, and analysis with the Fiji software were performed blindly. Notably, the operator was informed of the various group membership of the skin samples only after the image analysis.

Regarding groups 1, 2, 3, and 4, the main inclusion criterion was a diagnosis of polyneuropathy of any kind, including small fiber neuropathy. Most of the patients enrolled, indeed, received a small fiber neuropathy diagnosis, confirmed by referring to the diagnostic criteria of Devigili et al. (2008)[2], that are based on clinical aspects, alteration of quantitative sensory tests, and reduction of IENFD. Both patients with isolated small fiber neuropathy and patients with the involvement of large fibers and therefore a diagnosis of sensory or any type of sensorimotor polyneuropathy were included.

Regarding the symptoms, we investigated not only the presence/absence of pain and/or pruritus, but also their intensity, using the numerical rating scale (NRS: 0-10, where 0 corresponds to the absence of the symptom and 10 to the maximum intensity of the symptom).

Then, the patients underwent a neurological evaluation with careful exploration of symptoms and signs, sensory and motor nerve conduction studies, quantitative sensory testing (QST), and skin biopsy with a 6-mm-diameter punch.

Patients with acute skin infections, other causes of chronic itching (e.g., dermatological, systemic, iatrogenic), secondary causes of pain (e.g., traumatic event, joint pathology), major psychiatric disorders, and patients unable to understand and consent, or incapable of signing an informed consent form were excluded. Oral anticoagulant therapy did not represent an exclusion criterion since punch skin biopsy represents a minimally invasive method that does not require any suture and is associated with a low risk of bleeding.

## *3.2 Sample collection from the proximal thigh and storage at -20°C.*

Using a disposable 6-mm-diameter punch, after local anesthesia with lidocaine, 2 skin biopsies were performed on each patient at two sites:

- Distal: 10 cm proximal to the lateral malleolus
- Proximal: 20 cm distal to the iliac spine

The 2 skin biopsies were taken on the same side of the body where nerve conduction tests and quantitative sensory tests had previously been performed.

Each skin sample was then divided into two equal parts of 3 mm each, intended for distinct uses:

- One part was used for evaluating the IENFD. This is the crucial analysis for the diagnosis of SFN (Devigili criteria).[2]
- The other part was used to assess any inflammatory changes or anomalies in the tissue.

Subsequently, the skin samples underwent cryopreservation:

- Immersion in Optimal Cutting Temperature (OCT) cryopreservation solution.
- Placement inside a refrigerator at -20°C.

The OCT solution is a water-soluble glycol resin that serves as an ideal embedding medium for sectioning samples on a cryostat at temperatures of -10°C and below.

Maintaining the sample at low temperatures is necessary to ensure the solid state of OCT and, consequently, is crucial for preserving the tissue's genetic integrity.

*3.3 Cutting at the cryostat (20 µm)*

The Leica CM3050 S cryostat-microtome available at the University of Würzburg was used to cut the skin samples *(Figure 13).* Starting from frozen samples, the cryostat-microtome allows cutting thin sections that can be subsequently analyzed under an optical microscope.

This instrument consists of:

- A cryostatic chamber (cryochamber) made of stainless steel which, through a compression cooling system, maintains low temperatures for the entire cutting process.
- A microtome, located inside the cryochamber, which, with a mechanism controllable from the outside via a knob, cuts the sample into sections with a thickness in the order of microns.


*Figure 13; Cryostat*. Photo of the cryostat showing: the console (which allows setting adjustments), the cryochamber, and, at the center, the microtome. It is also possible to notice the presence of tools such as brushes and tweezers, very useful during cutting to facilitate the orientation and adhesion of the sections on the slide.

The instrument was set to a temperature of -20°C for the procedure, and the thickness of the sections was set to 20µm. To facilitate cutting, the instrument allows for adjusting the orientation and advancement of the samples. The precise sample orientation system with reference position allows X/Y adjustment up to 8°, while the horizontal advancement system allows advancement up to 25 mm.

Once cut, the sections were placed on a SuperFrost® Plus slide, equipped with a positive charge that allows them to remain attached to the slide during subsequent immunofluorescence staining steps. For each skin sample, 3 sections were obtained, and they adhered to the same slide and were positioned along the longitudinal axis, as equidistant from each other as possible. To distinguish them during subsequent image analysis phases, they were identified with a letter assigned based on their position relative to the slide's identification label:

- "m" (medial), for those placed near the label;
- "c" (central), for those placed in the center;
- "l" (lateral), for those placed farthest from the label.

For slide identification, the following information was reported on the label:

- The identification code of the skin biopsy;
- The current date;
- The initials of the operator.

The sections, once adhered to the slide, were viewed in real-time under an optical microscope to assess the appropriateness of the cutting: in the presence of ruptures (holes or missing parts) or curling, it was necessary to repeat the cutting. The higher the quality of the cutting on the cryostat and the fewer artifacts present, the better and cleaner the image analysis under the Thunder microscope was.

Once the suitability of all sections was assessed, all the slides were placed in a plastic slide holder box; it was needed to wait for approximately 30 minutes before storing them in a refrigerator to allow proper section-slide adhesion. Store all the sections in a refrigerator is necessary to ensure proper preservation of the sections while waiting to proceed with immunofluorescence staining.

## *3.4 Double Immunofluorescence Staining (PGP9.5 and CD31)*

The protocol of the University of Würzburg was used for staining biopsy sections in double immunofluorescence (PGP9.5 and CD31). Specifically, the following antibodies were used:

- *Primary Antibodies:*
    - Protein Gene Product 9.5 - PGP9.5 (188): rabbit primary antibody "anti-human"; 1:1000 dilution; Zymoted 516-3344.
    - CD31- PECAM1 (180): mouse primary antibody "anti-human"; 1:500 dilution; BD Biosciences 550389 *(Figure 14)*.
- *Secondary Antibodies*:
    - Cy™ AffiniPure: Rabbit anti-IgG monkey secondary antibody (H+L); (H1); 1:100 dilution; Jackson ImmunoResearch 711-165-152.
    - Alexa Fluor 488: Mouse anti-IgG monkey secondary antibody (H+L) (Z3); 1:100 dilution; Jackson ImmunoResearch 715-545-150.

As specified in the protocol, the staining process took two days.

The steps performed during the first day were as follows:

- Unfreezing and drying of slides for 30 minutes (exposure to air at room temperature).

- Labeling each slide with the current date, the operator's initials, and the abbreviation of the primary antibodies used.

- Preparation of a humid chamber by placing bloating filter paper previously moistened with distilled water in a plastic container.

- Delimitation of each section on the slide using the "PAP pen". This step aims to contain the antibody or its reactive counterpart on the sample, preventing its dispersion during various stages of staining.

- Adding to each section 50 µL (1 drop) of 10% BSA/PBS solution (BSA = Bovine Serum Albumin; PBS = phosphate-buffered saline) and letting slides in the humid chamber for 30 minutes. The 10% BSA/PBS solution is important to ensure the best binding of primary antibodies to the specific target.

- Preparation of the primary antibody solution using 1% BSA/PBS and 0.3% Triton X-100. For 10 mL of solution: 9 mL PBS + 1 mL 10% BSA/PBS + 30 µL Triton X-100. For 500 µl of primary antibody solution: 1 µl CD31 (1:500) + 0.5 µl PGP9.5 (1:1000) + 498 µl 1% BSA/PBS with 0.3% Triton X-100.

- After 30 minutes, the humid chamber was opened, and the solution was removed from each section by "tapping" the edge of the slides, one by one, on a hard surface, also using filter paper to remove any remaining residue, taking care not to touch the section.

- Primary antibodies were then added to each section, and the sections, placed horizontally in the humid chamber, were left to incubate overnight in a refrigerator at 4°C, in the dark.


*Figure 14: Primary Antibodies*. Photo of the primary antibodies PGP9.5 (188) and CD31 (180) used during the first day of the staining protocol.

The steps performed during the second day were as follows:

- The slides were rinsed four times in PBS solution (each wash lasted at least 30 seconds). A good washing is essential to ensure that only antibodies bound to their target remain on the section, avoiding nonspecific staining arising from the background.

- The secondary antibody solution was prepared using 1% BSA/PBS. For 10 mL of solution: 9 mL PBS + 1 mL 10% BSA/PBS. For 1000 µl of secondary antibody solution: 20 µl AF488 (Z3, mouse, 1:100) + 20 µl Cy3 (H1, rabbit, 1:100) + 960 µl 1% BSA/PBS.

- After applying the secondary antibodies (pre-diluted 1:2), the slides were incubated in the humid chamber for 2 hours at room temperature.

- The slides were then rinsed four times in PBS solution (each wash lasted at least 30 seconds).

- The slides with sections over were covered using Vectashield with DAPI (4',6-diamidino-2-phenylindole, hydrochloride anti-fading solution), and a coverslip was placed on each slide, finally sealing the edges with an appropriate solution.

- The slides were then left to air dry at room temperature for at least 30 minutes; then the slide holder was placed inside a refrigerator at 4°C to ensure proper preservation of the stained sections.

## *3.5 Leica Thunder Microscope, Image Acquisition*

The microscope model used for the analysis of sections stained with double immunofluorescence is the Leica DMi8 "Thunder" *(Figure 15)*

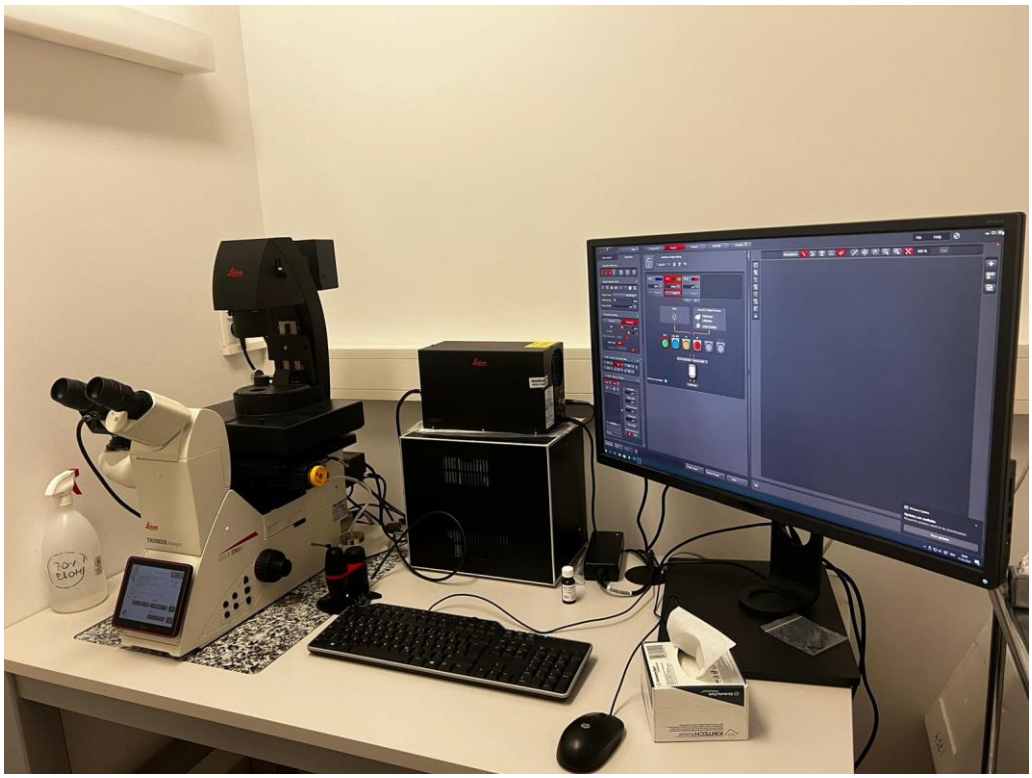

*Figure 15: Microscope and Image Acquisition*. On the left, you can see the Leica DMi8 Thunder microscope; on the right, there is the monitor through which the images are displayed.

The Leica DMi8 microscope is an inverted microscope model that uses Thunder technology.

In the inverted microscope model, light illuminates from above, while the objectives and turret are positioned below the stage where the sample to analyze is placed.

Thunder is an opto-digital technology that employs Computational Clearing for generating high-resolution and high-contrast images (an example is shown in *Figure 16*). Computational Clearing efficiently removes signal components from out-of-focus planes (blur), all performed in real time. Thanks to this technology, achieving imaging sharpness with 3D samples is as easy as working with widefield fluorescence microscopes.

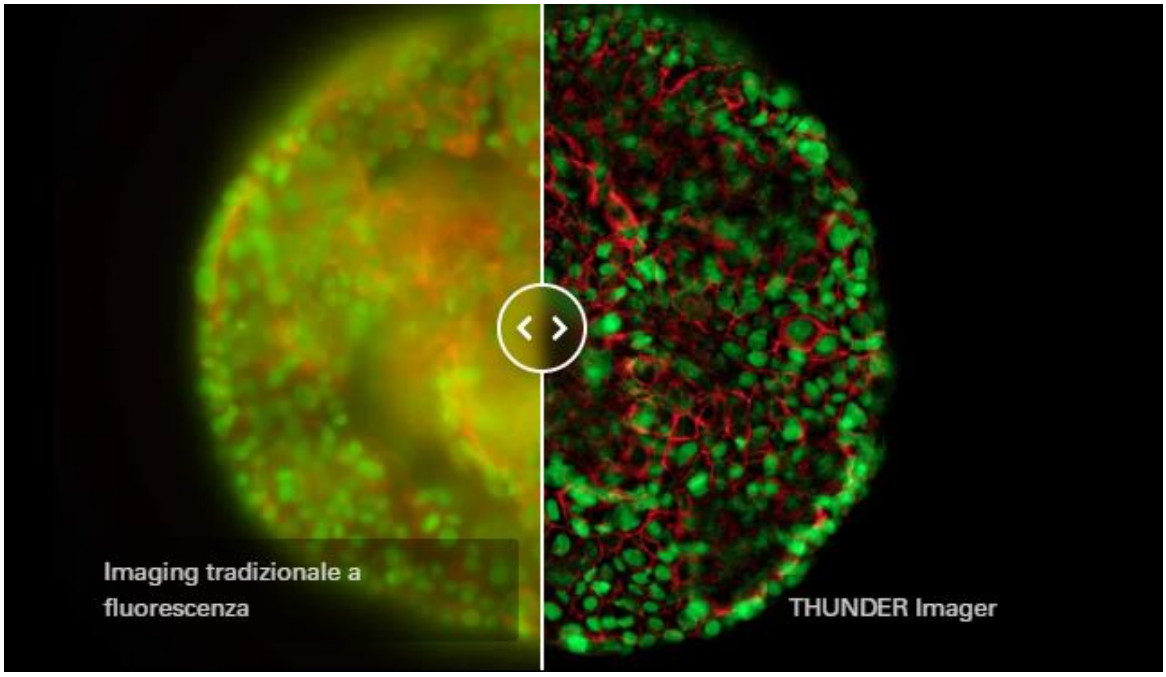


*Figure 16: Example of an image acquired with the Thunder Imaging System*. This photograph was taken from the Thunder Imaging System presentation brochure, and the cell in question is a HeLa cell labeled with AF568 phalloidin (actin) and YOYO 1 iodide (nucleus). In this sample image, you can see the improvement in image quality with the Thunder option.

The acquisition of 3D images is ensured by selecting the "Z-stack" function. Z-stacking is a digital image processing method that combines multiple images taken

at different focal distances to provide an image characterized by a greater depth of field than that of the individual source images.

The Leica DMi8 microscope utilizes:

- Objectives: 5x, 10x, 20x, 40x, 63x;
- Monochrome camera with a 4MP CMOS sensor (pixel size 6.5 µm x 6.5 µm);
- LED fluorescence light source with a spectrum shown in *Figure 17.*

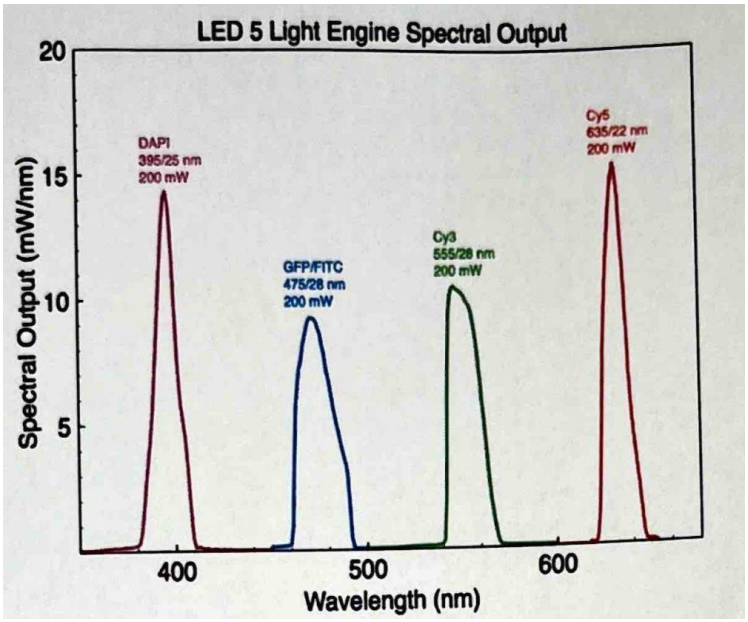


*Figure 17: LED fluorescent light spectrum*

There is a choice regarding:

- Type of lens used;
- Thickness of the section to be analyzed ("Z-Position [µm]");
- Number of sections into which the selected thickness will be divided ("Number of Steps").

For the study we conducted, the following settings were established (*Figure 18)*:

- Magnification: 10x;
- Sample thickness: 5 µm;

- Number of sections acquired per sample: 15.

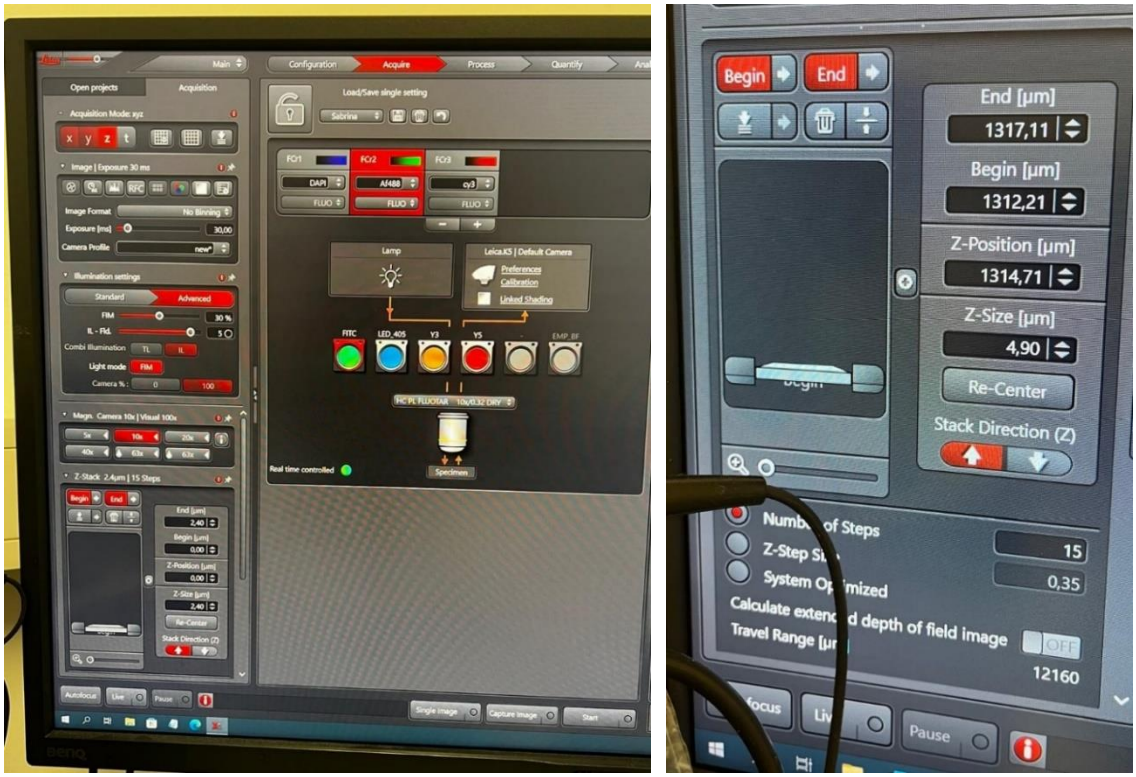


*Figure 18: Settings used for image acquisition*. The image on the left shows the settings used with the three channels (FCr1, FCr2, FCr3), necessary to highlight the different structures that were analyzed in the image. In the image on the right, more detailed settings of the "Z-Stacking."

## *3.6 Software Fiji*

Once the digital images in raw format were acquired at the microscope, their computer analysis was carried out using the Fiji software (logo shown in *Figure 19).*

*Figure 19: Logo of the Fiji software*

The Fiji software ("Fiji is just ImageJ") is a free program that allows the processing and analysis of digital images; it utilizes a basic package of tools and various plug-ins that enable the user to manage the analysis according to their needs.

More specifically, the Fiji tool used in this study is the "Dermal Layer Analysis," a plug-in created specifically last year (October-November 2022) by Dr. Jan Brocher, programmer, and founder of Bio Voxxel, in collaboration with Alessandro Gualco, a former student at the University of Genoa who participated in the project.

Once the program is opened and the "Dermal Layer Analysis" option is selected in the "AG Sommer" command, the interface shown in *Figure 20* appears.

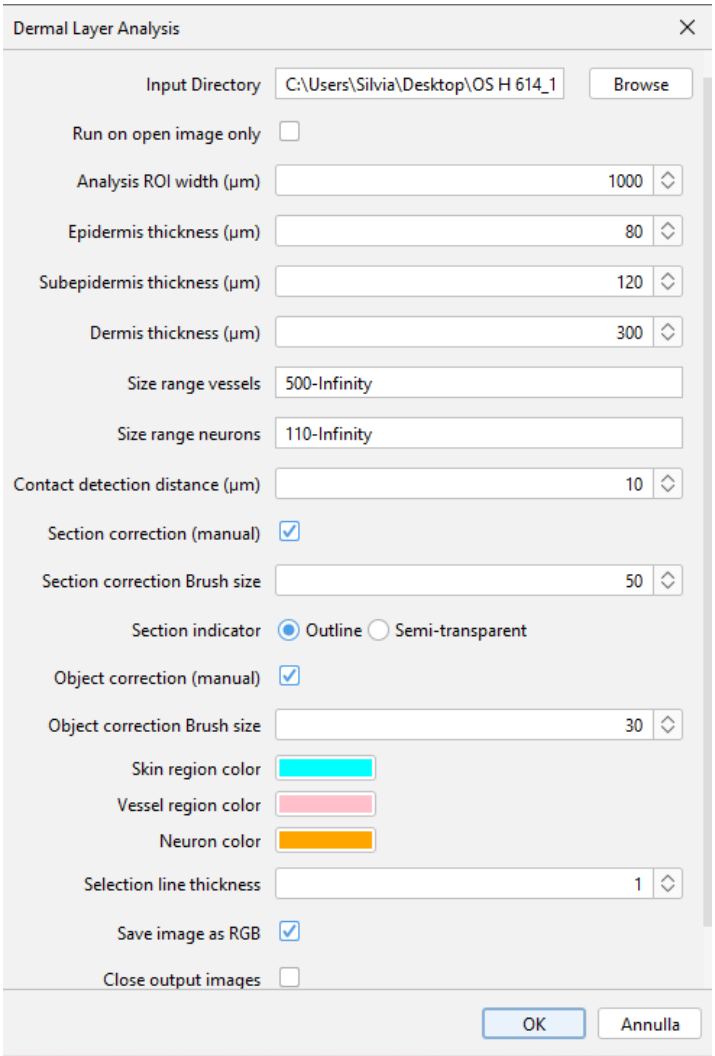


*Figure 20: Opening interface page*

As illustrated in Figure 20, after selecting the "Dermal Layer Analysis" option, it is possible to establish the main parameters required by the software to analyze the image:

- *Input directory*: Selects the folder where the images acquired at the microscope that have to be analyzed are stored. Once the image analysis is complete, the corresponding data will be automatically saved in the same folder in both TIF image format and TSV file format.

- *Run on open image only*: If checked, the software will only analyze the selected image without proceeding autonomously with the analysis of subsequent images in the previously selected folder.

- *Analysis ROI width (µm):* Allows the establishment of the length of the Region of Interest (ROI).

- *Epidermidis thickness (µm):* Establishes the depth of the epidermal space within the ROI.

- *Sub-epidermis thickness (µm):* Establishes the depth of the subepidermal space within the ROI.

- *Dermis thickness (µm):* Establishes the depth of the dermal space within the ROI.

- *Size range vessels*: Selects the pixel range within which the software considers specific vessel structures (CD31-AF488 antibody staining). This command allows the elimination of nonspecific structures from the background that may complicate the image analysis.

- *Size range neurons*: Selects the pixel range within which the software considers specific nerve fiber structures (PGP9.5-Cy3 antibody staining). The concept is the same as the previous command.

- *Contact distance*: Establishes the maximum distance between a vessel and a small nerve fiber that defines a neurovascular contact. In practice, an

"onion shape" will be drawn around each vessel, with a vessel-nerve fiber distance equal to that set in the "contact distance."

- *Section correction (manual):* If checked, allows manual correction of the detected section.

- *Section correction Brush size*: Establishes the size, in µm, of the brush used for manual corrections. This parameter can also be modified during the current image analysis. By doing so, different brush sizes can be chosen for different structures, correlating with their varying sizes.

- *Section indicator*: Allows the selection of one of two layouts indicating the region of interest. One layout involves a yellow line tracing the border of the area of interest, while the other involves a semi-transparent mask.

- *Object correction Brush size:* Establishes the size, in µm, of the brush used for manual corrections. This parameter can also be modified during the current image analysis. By doing so, different brush sizes can be chosen for different structures, correlating with their varying sizes.

- *Skin/Vessel/Neuron color*: Allows the selection of the color of the lines delineating the different structures.

- *Selection line thickness*: Establishes the thickness of the lines delineating the structures identified either autonomously by the system or manually by the operator.

- *Save images RGB*: If checked, automatically saves a summary image of the just-completed analysis in RGB.

- *Close output images/tables*: If checked, automatically closes the windows belonging to the original file that are redundant for analysis purposes and may therefore cause confusion during analysis.

Once the aforementioned parameters are set and the image is loaded, the analysis proceeds as follows:

1. Highlight the area of interest by manually drawing a quadrangular figure in a yellowish color above it. The length and depth dimensions of the ROI are established beforehand by setting them in the initial window under the entries: "Analysis ROI width" (1000 μm), "Epidermis thickness" (80 μm), "Subepidermis thickness (120 μm), "Dermis thickness (300 μm).
   In this phase, specifically, the operator only controls the orientation of the box, which should be positioned as perpendicularly as possible to the orientation of the skin section, as shown in *Figure 21.*

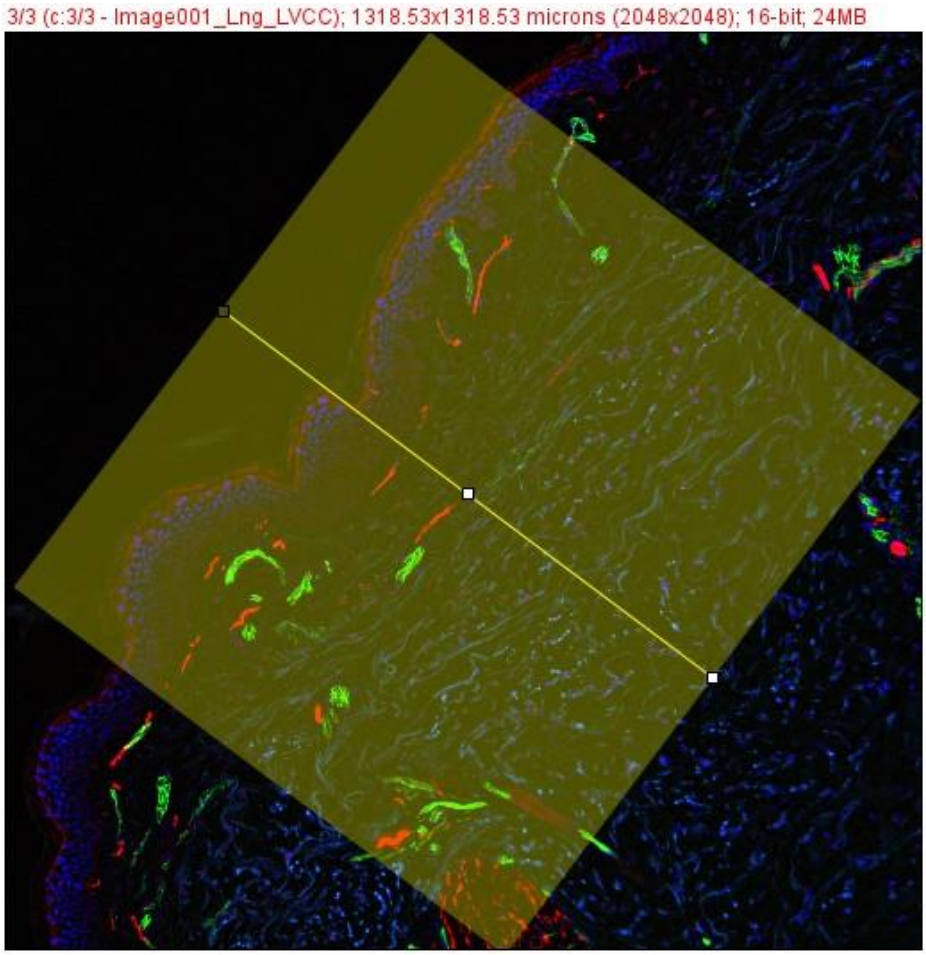


*Figure 21: Example image of the yellow box manually drawn on the ROI.*

2. Proceed with the manual correction of the margins of the epidermis (upper margin of the section) identified by the software with a yellow line. A brush whose size is pre-set at 100 μm was used for the correction. This step is of fundamental importance for the correct identification of the skin layers in the subsequent phase. To make the method as standardized as possible

among the various operators, it was chosen to follow as a guideline for the brush not the line related to the outer keratin layer, but the line of the dermal-epidermal junction *(Figure 22)*.

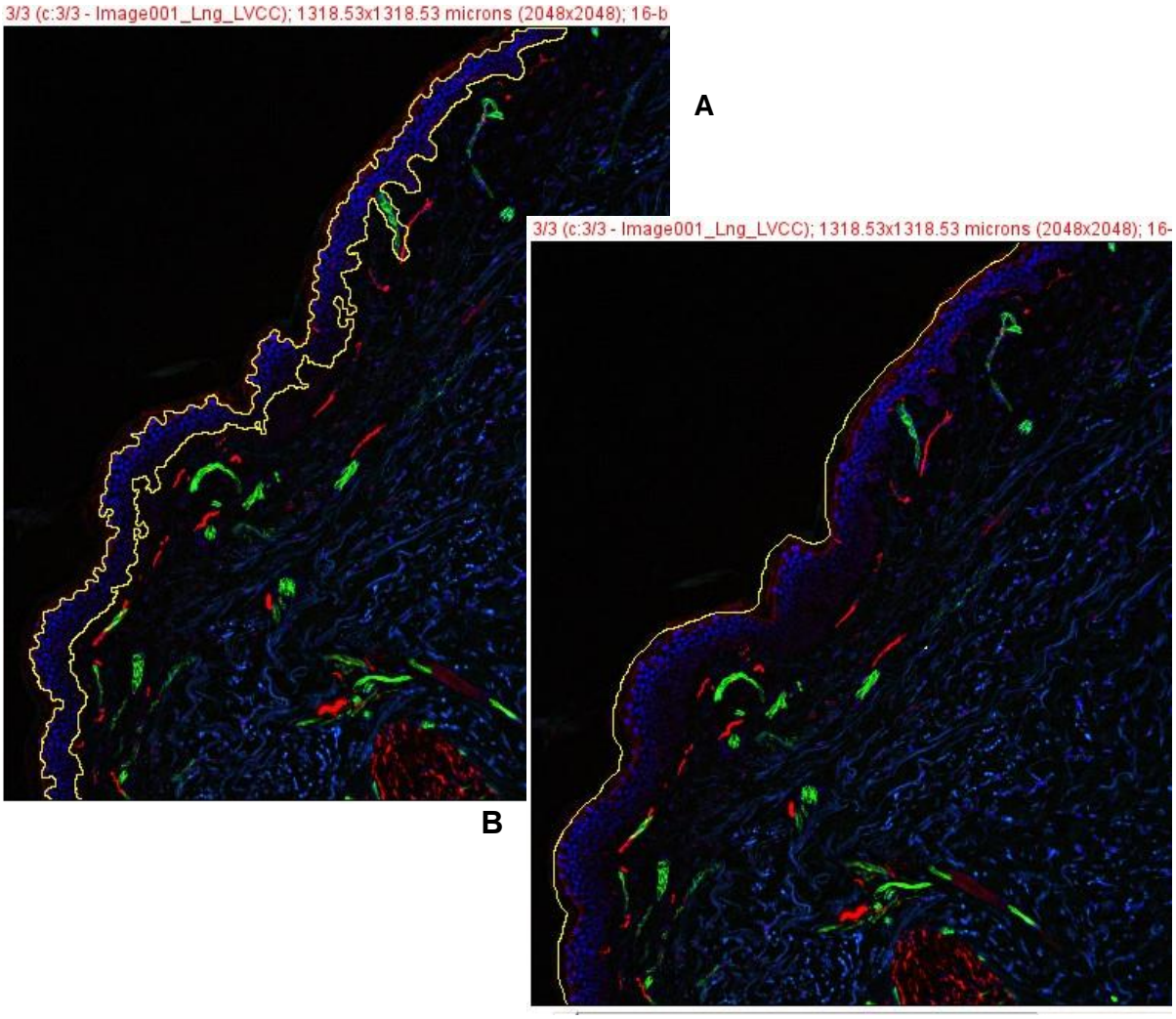


*Figure 22 correction of the upper margin of the section: A) incorrect delineation line of the epidermis; B) epidermis line after the manual correction process*.

3. The software identifies and circumscribes with a blue line the various layers of the ROI: epidermis, sub-epidermis, dermis, and subcutaneous layer (*Figure 23*). The orientation corresponds to that of the box manually delimited in step 1, while the dimensions (length, depth) are equal to those established in the initial window. The operator in this phase can modify in real time the dimensions related to the depth of the substrates of the ROI, a very important aspect since the thickness of the epidermal layer can vary from patient to patient due to the physiological irregularities of the skin.

Therefore, manual correction is necessary on a case-by-case basis. In collaboration with other colleagues who worked on the project, it was decided, starting from the basic values chosen in the initial interface, to modify only the thickness of the epidermis (generally from 80 to 70/60 µm), leaving unchanged the depth of the other layers.

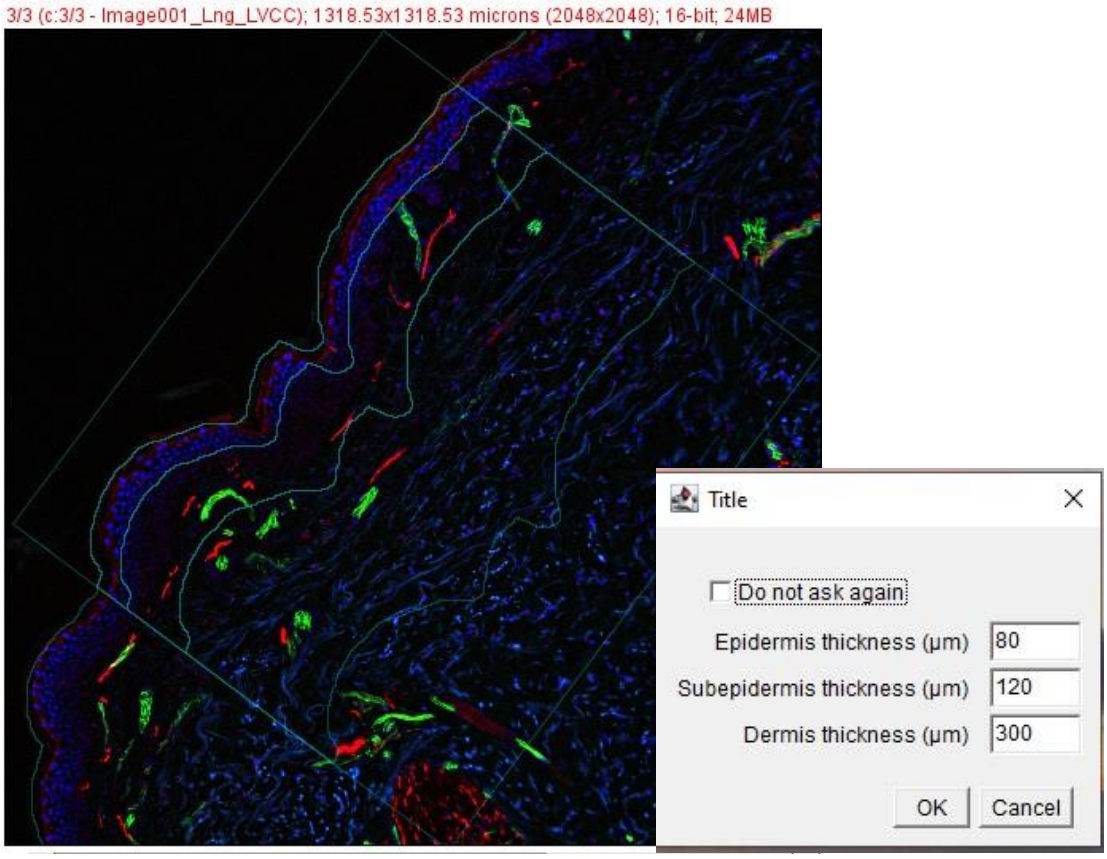


*Figure 23: Delimitation of skin layers*. In the image, the lines that identify the different layers of the skin within the ROI can be appreciated. The table on the right shows the thickness of the different skin layers.

4. In a few seconds, the software autonomously identifies vascular structures, colored in green. In most cases, in this phase, the operator has the assignment to manually modify what has been wrongly identified by the software, using a brush with a fixed size of 15 µm. Erroneous structures highlighted as vessels will thus be erased, while vessels that have not been correctly recognized by the software will be delineated. This mechanical correction is a consequence of the fact that the area of such unrecognized

structures falls outside the range indicated in the initial window under the heading 'Size range vessels'.

In this phase, two additional windows are presented (shown in *Figure 24*):

- 'ROI manager' which allows choosing which region of interest to display.
- 'Channels' which allows selecting which channel(s) to highlight.
  - Channel 1 = blue (DAPI);
  - Channel 2 = red (PGP9.5);
  - Channel 3 = green (CD31).

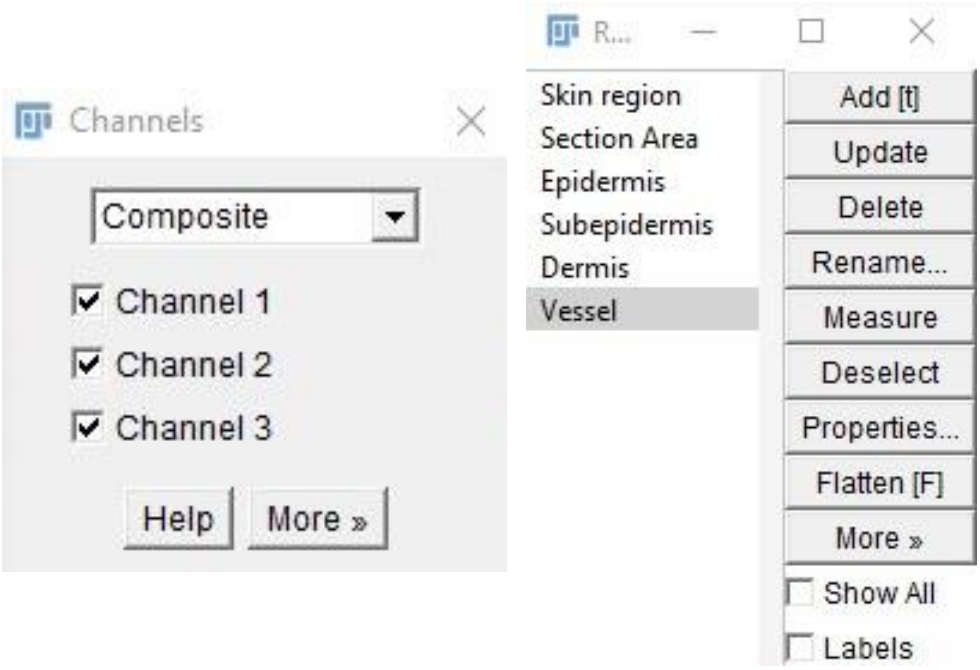


*Figure 24:* 'Channels' (left) and 'ROI manager' (right) windows of Fiji software.

An example of the changes made with manual correction is illustrated in Figure 25.

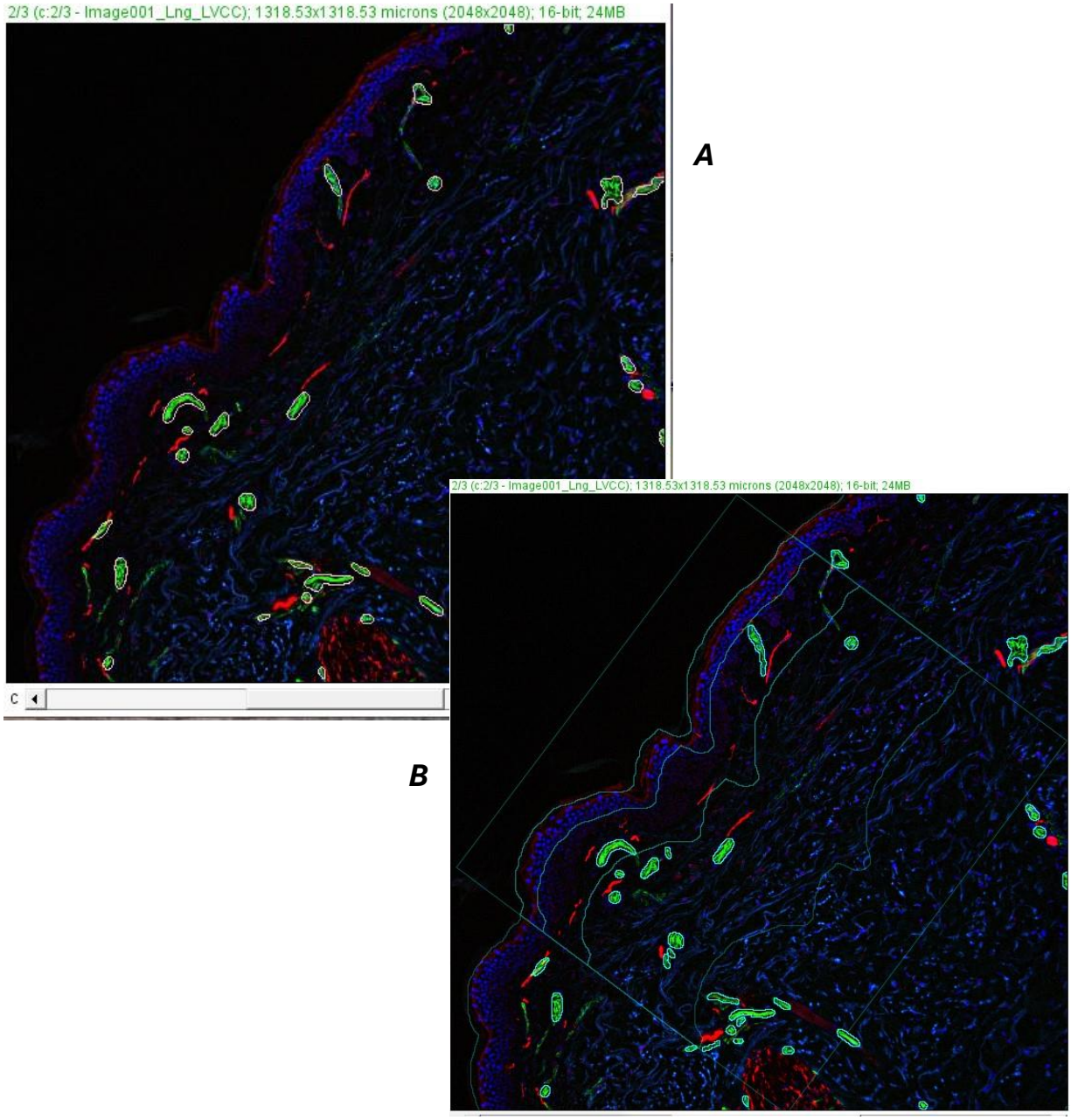


*Figure 25: Vessel*: A) Vessels automatically identified by the software (green structures, delineated by blue line); B) Identification of all vessels after manual correction.

5. In a few seconds, the software autonomously identifies the structures of small fibers, colored red (*Figure 26*); then, the same procedure listed in point 4 is repeated for this channel but using a brush with a fixed size of 5 µm.

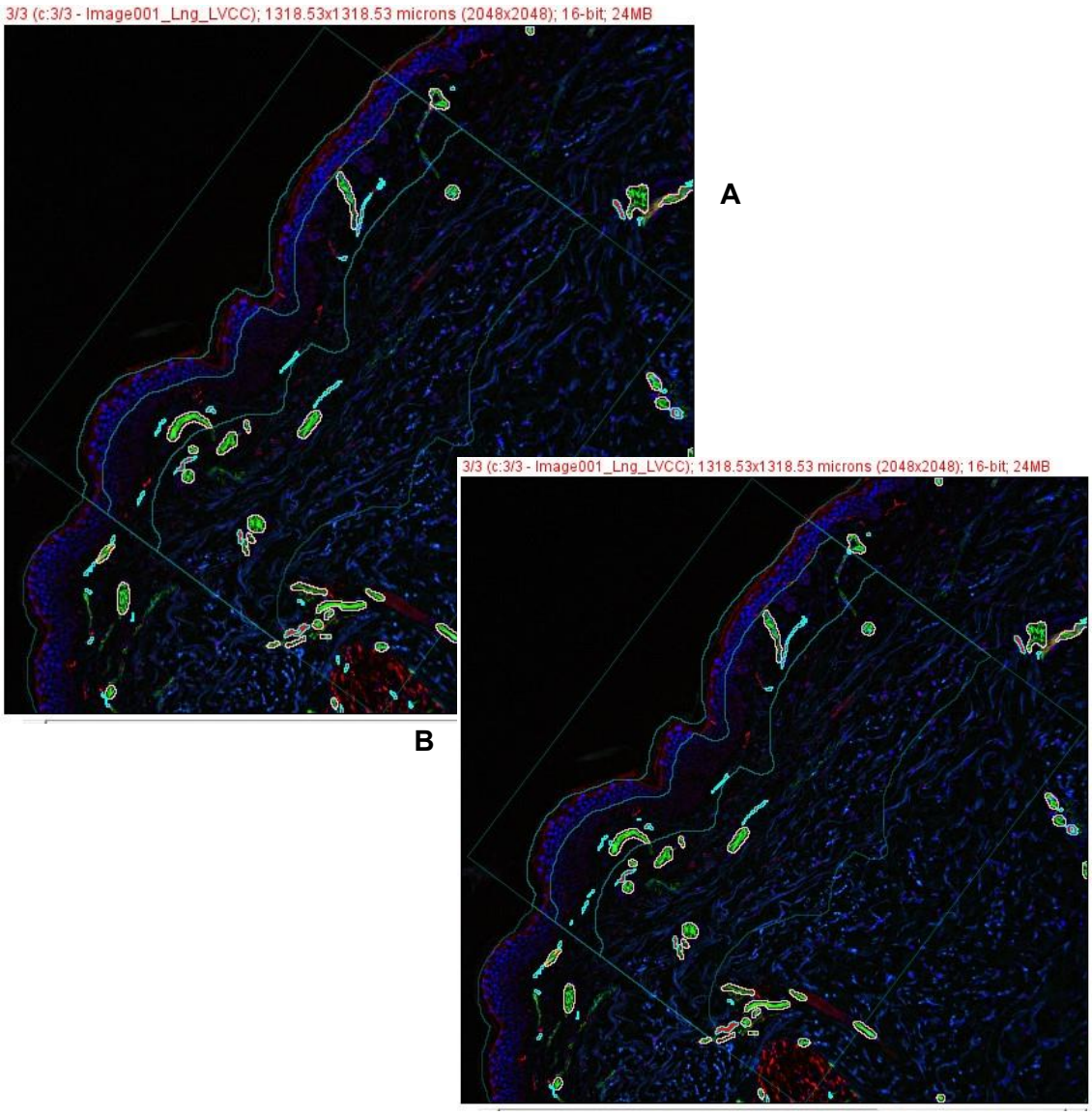


*Figure 26: Small nerve fibers*. A) Small fibers automatically identified by the software (red structures, delineated by blue line); B) Identification of all small fibers after manual correction.

6. The software then automatically provides a summary image of what was previously analyzed, with highlighted vessels, small fibers, and even neurovascular contacts (*Figure 27*). Furthermore, the program generates a table with all the data of the analyzed image, in a '.tsv' format file; this file can be opened using the 'Numbers' application, a step that allows subsequent conversion to an Excel file.

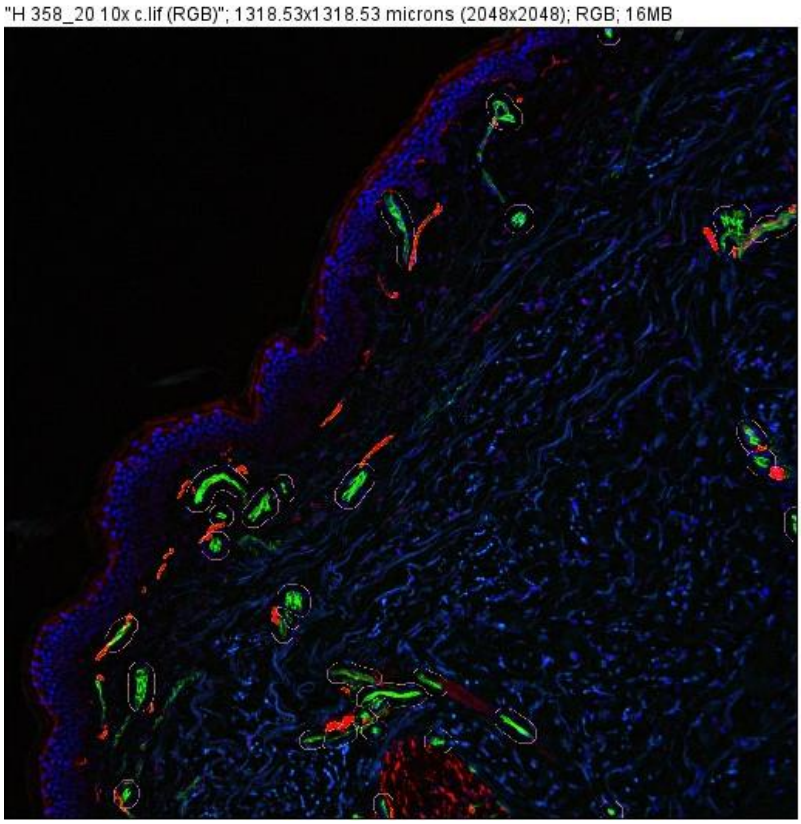


*Figure 27*: Vessels, small nerve fibers, and neurovascular contacts highlighted by Fiji software. In the image, various structures identified in the previous points can be appreciated, in addition to neurovascular contacts.

## *3.7 Data Collection and Organization of the Excel Worksheet*

Once the analysis of all the images of the collected sections was completed, the data provided by the Fiji software was gathered into a single Excel worksheet.

For each patient, images related to the three sections (M=medial, C=central, L=lateral) were analyzed. Specifically, the numerical data, obtained after the images analyses conducted with the Fiji software, were recorded in the worksheet:

- "Epidermis/ Subepidermis/ Dermis Vessel/ Small fiber number" = number of vessels/small fibers at the various layers within the ROI (epidermis, sub-epidermis, dermis).

- "Epidermis/ Subepidermis/ Dermis Vessel/ Small fiber Area in µm and in %" = sum of all vessel/small fiber areas within the various layers within the ROI, expressed in absolute value (µm) and %.

- "Epidermis/ Subepidermis/ Dermis Connection number" = number of neurovascular contacts in the various layers within the ROI.

- "Epidermis/ Subepidermis/ Dermis Connection Area in µm and in %" = sum of all neurovascular contact areas within the various layers within the ROI, expressed in absolute value (µm) and %.

It is important to remember that the neurovascular contact area is defined by the area of the small fibers located within the "onion shape" drawn around the vessel, as shown in *Figure 28.*

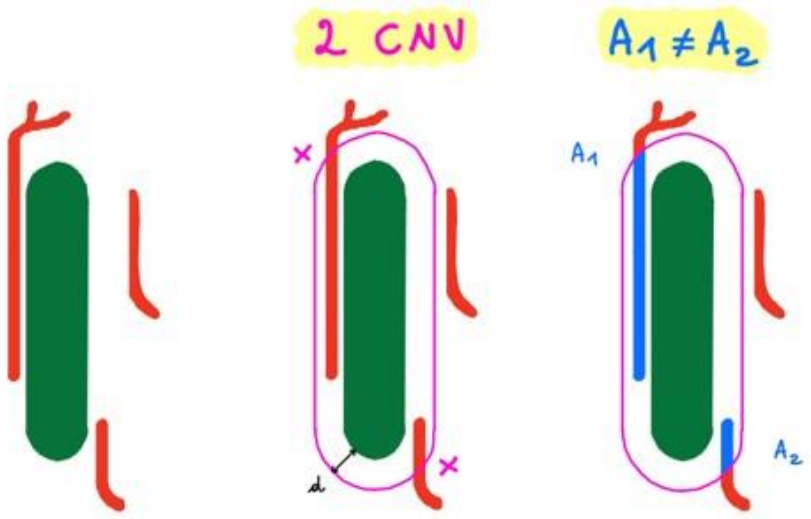


*Figure 28: Neurovascular contacts and contact area. In green, vascular structures are shown, while nerve fibers are depicted in red. In the central image, two neurovascular contacts (CNV) are highlighted with an X, as two nerve fibers cross the onion-shaped delineation line (colored pink) and therefore come into close contact with the vascular structure. In the figure on the right, it is emphasized how the contact area between the vessel and nerve fiber on the left (A1) is greater than the contact area between the vessel and nerve fiber on the right (A2). The contact parts between the vessels and fibers are colored blue.*

For each patient, the arithmetic means of the values obtained from the analysis of the three sections M, C, and L were then calculated.

As shown in *Figure 29*, from three columns of data for each patient, a single average value of the data for each patient was obtained.

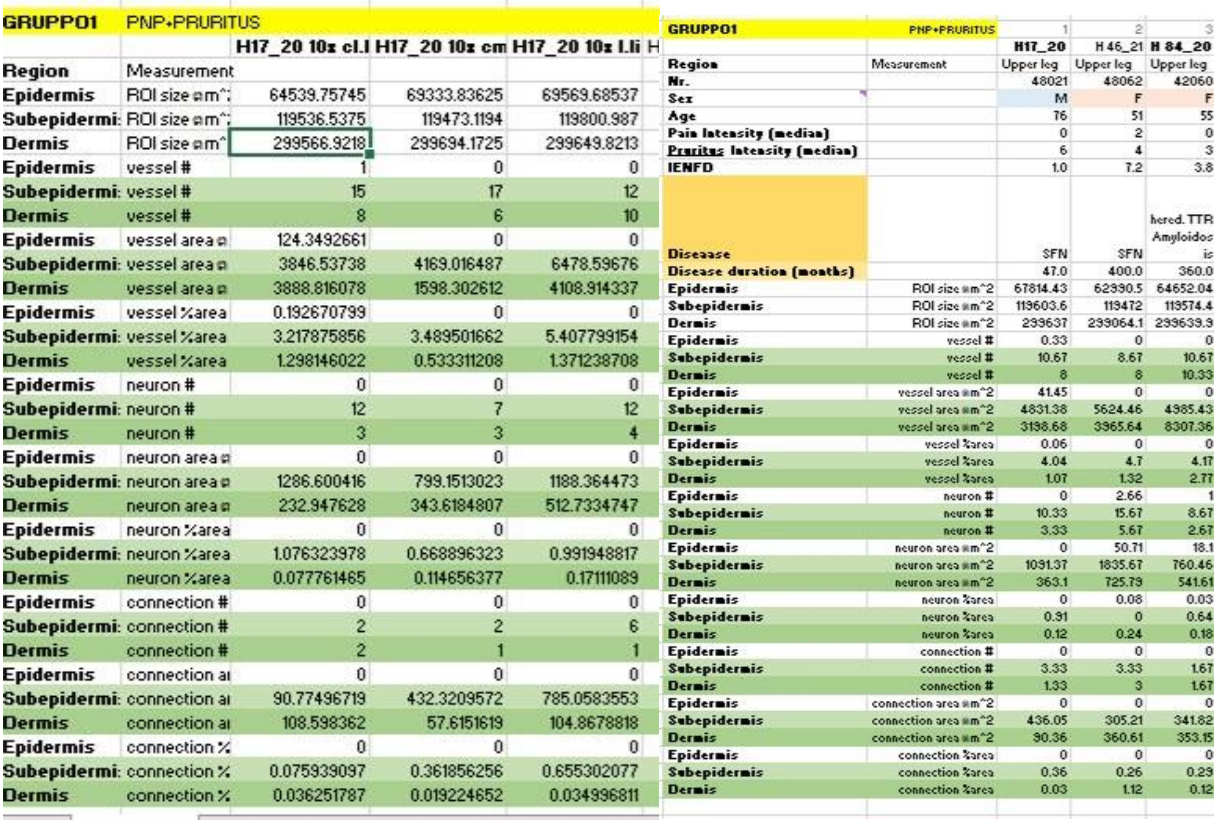

| GRUPPO1 | PNP+PRURITUS | | | |
|---|---|---|---|---|
| | | H17_20 10x cl.l | H17_20 10x cm | H17_20 10x l.li |
| Region | Measurement | | | |
| Epidermis | ROI size µm^2 | 64539.75745 | 69333.83625 | 69569.68537 |
| Subepidermi | ROI size µm^2 | 119536.5375 | 119473.1194 | 119800.987 |
| Dermis | ROI size µm^2 | 299566.9218 | 299694.1725 | 299649.8213 |
| Epidermis | vessel # | 1 | 0 | 0 |
| Subepidermi | vessel # | 15 | 17 | 12 |
| Dermis | vessel # | 8 | 6 | 10 |
| Epidermis | vessel area µ | 124.3492661 | 0 | 0 |
| Subepidermi | vessel area µ | 3846.53738 | 4169.016487 | 6478.59676 |
| Dermis | vessel area µ | 3888.816078 | 1598.302612 | 4108.914337 |
| Epidermis | vessel %area | 0.192670799 | 0 | 0 |
| Subepidermi | vessel %area | 3.217875856 | 3.489501662 | 5.407799154 |
| Dermis | vessel %area | 1.298146022 | 0.533311208 | 1.371238708 |
| Epidermis | neuron # | 0 | 0 | 0 |
| Subepidermi | neuron # | 12 | 7 | 12 |
| Dermis | neuron # | 3 | 3 | 4 |
| Epidermis | neuron area µ | 0 | 0 | 0 |
| Subepidermi | neuron area µ | 1286.600416 | 799.1513023 | 1188.364473 |
| Dermis | neuron area µ | 232.947628 | 343.6184807 | 512.7334747 |
| Epidermis | neuron %area | 0 | 0 | 0 |
| Subepidermi | neuron %area | 1.076323978 | 0.668896323 | 0.991948817 |
| Dermis | neuron %area | 0.077761465 | 0.114656377 | 0.17111089 |
| Epidermis | connection # | 0 | 0 | 0 |
| Subepidermi | connection # | 2 | 2 | 6 |
| Dermis | connection # | 2 | 1 | 1 |
| Epidermis | connection ar | 0 | 0 | 0 |
| Subepidermi | connection ar | 90.77496719 | 432.3209572 | 785.0583553 |
| Dermis | connection ar | 108.598362 | 57.6151619 | 104.8678818 |
| Epidermis | connection % | 0 | 0 | 0 |
| Subepidermi | connection % | 0.075939097 | 0.361856256 | 0.655302077 |
| Dermis | connection % | 0.036251787 | 0.019224652 | 0.034996811 |

| GRUPPO1 | PNP+PRURITUS | 1 | 2 | 3 |
|---|---|---|---|---|
| | | H17_20 | H 46_21 | H 84_20 |
| Region | Measurement | Upper leg | Upper leg | Upper leg |
| Nr. | | 48021 | 48062 | 42060 |
| Sex | | M | F | F |
| Age | | 76 | 51 | 55 |
| Pain Intensity (median) | | 0 | 2 | 0 |
| Pruritus Intensity (median) | | 6 | 4 | 3 |
| IENFD | | 1.0 | 7.2 | 3.8 |
| Diseaase | | SFN | SFN | hered. TTR Amyloidos is |
| Disease duration (months) | | 47.0 | 400.0 | 360.0 |
| Epidermis | ROI size µm^2 | 67814.43 | 62330.5 | 64652.04 |
| Subepidermis | ROI size µm^2 | 119603.6 | 119472 | 119574.4 |
| Dermis | ROI size µm^2 | 239637 | 239064.1 | 239639.9 |
| Epidermis | vessel # | 0.33 | 0 | 0 |
| Subepidermis | vessel # | 10.67 | 8.67 | 10.67 |
| Dermis | vessel # | 8 | 8 | 10.33 |
| Epidermis | vessel area µm^2 | 41.45 | 0 | 0 |
| Subepidermis | vessel area µm^2 | 4831.38 | 5624.46 | 4985.43 |
| Dermis | vessel area µm^2 | 3198.68 | 3965.64 | 8307.36 |
| Epidermis | vessel %area | 0.06 | 0 | 0 |
| Subepidermis | vessel %area | 4.04 | 4.7 | 4.17 |
| Dermis | vessel %area | 1.07 | 1.32 | 2.77 |
| Epidermis | neuron # | 0 | 2.66 | 1 |
| Subepidermis | neuron # | 10.33 | 15.67 | 8.67 |
| Dermis | neuron # | 3.33 | 5.67 | 2.67 |
| Epidermis | neuron area µm^2 | 0 | 50.71 | 18.1 |
| Subepidermis | neuron area µm^2 | 1091.37 | 1835.67 | 760.46 |
| Dermis | neuron area µm^2 | 363.1 | 725.79 | 541.61 |
| Epidermis | neuron %area | 0 | 0.08 | 0.03 |
| Subepidermis | neuron %area | 0.31 | 0 | 0.64 |
| Dermis | neuron %area | 0.12 | 0.24 | 0.18 |
| Epidermis | connection # | 0 | 0 | 0 |
| Subepidermis | connection # | 3.33 | 3.33 | 1.67 |
| Dermis | connection # | 1.33 | 3 | 1.67 |
| Epidermis | connection area µm^2 | 0 | 0 | 0 |
| Subepidermis | connection area µm^2 | 436.05 | 305.21 | 341.82 |
| Dermis | connection area µm^2 | 90.36 | 360.61 | 353.15 |
| Epidermis | connection %area | 0 | 0 | 0 |
| Subepidermis | connection %area | 0.36 | 0.26 | 0.29 |
| Dermis | connection %area | 0.03 | 1.12 | 0.12 |

Figure 29: Example of an Excel worksheet. In the images, the transition from 3 columns for each skin sample (3 sections: C, M, L) to a single column reporting the arithmetic mean values of the 3 sections can be appreciated

## *3.8 Statistical Analysis*

Statistical analysis was performed using the open-source software “Jamovi” (*Figure 30*).

To assess the normal distribution of the data, the Shapiro-Wilk test was used. Specifically, the null hypothesis, which assumes the normality of the distribution of the values, was considered true if $p > 0.05$. To evaluate the variance homogeneity, Levine’s test was used, and the null hypothesis, which assumes the homogeneity of the variance, was considered true if $p > 0.05$.

Data of patients and control subjects were compared with the Student’s T test or Mann-Whitney U test as appropriate. Notably, in the presence of data with normal distribution and homogeneous variance, Student’s T test was applied, otherwise, the Mann-Whitney U test was used.

First, the various patient groups (group 1, 2, 3, and 4) were compared with the control group (group 5), and the analysis was based on the following hypothesis: Group of patients < Group of controls.

Moreover, Age of patients/ Pruritus or Pain intensity/ ODSS* values/ mTCNs** values were correlated to values of vessel/ small fiber/ neurovascular contact in the different layers of the skin samples, with Pearson r correlation coefficient or Spearman rho correlation coefficient, as appropriate.

Spearman test was considered significative when p≤ 0.05. According to the Rho Sperman direction, the has the same way if r di Rho is positive, instead the correlation is inverse if r di Rho is negative.

[*ODSS= Overall disability sum score]
[**mTCNs= modified Toronto Clinical Neuropathy Score]


Figure 30: Logo of Jamovi

# *4. RESULTS*

The total number of skin samples analyzed was 104. First, we separated subjects affected by NP from those without NP, defined as controls (group 5). Then, a further differentiation among patients affected by NP was performed according to the presence of pain and/or pruritus symptoms and their intensity, measured with the numerical rating scale (NRS) ranging from 0 to 10 (0=absence of the symptom, and 10=maximum intensity of the symptom). Notably, for the pain/pruritus intensity a cut-off of ≥ 3 was assumed to categorize patients into various groups. At last, 5 groups were obtained: Group 1 (11 patients with PN + pruritus), Group 2 (25 patients with NP + pain), Group 3 (31 patients with PN + pain and pruritus), Group 4 (12 patients with NP, but no pain or pruritus), and Group 5 (25 healthy control individuals).

## 4.1 Population descriptive analysis

### *4.1.1 Group 1*

The *population* of group 1 (11 patients) consists of 5 females and 6 males with a mean age of 61.5 ± 17.6 years (median: 67, range 31-81), and with a mean disease duration of 103 months (range 11-400).
Pruritus intensity ranges from 3 to 10/10, with a median value of 5.
Six patients are affected by pure SFN (small fiber neuropathy), 3 by PNP (peripheral polyneuropathy), and 2 by a PNP with predominant impairment of small fibers. The etiology is idiopathic in 8 patients, while 2 subjects suffer from diabetic neuropathy, and one patient is affected by hereditary transthyretin-related amyloidosis.

### *4.1.2 Group 2*

The *population* of group 2 (25 patients) consists of 14 females and 11 males with a mean age of 49.8 ± 10.3 years (median: 52, range 24-71), and with a mean disease duration of 63 months (range 9-216).
Pain intensity ranges from 3 to 8/10, with a median value of 4.92.

Twenty-three patients are affected by pure SFN (small fiber neuropathy), 1 by PNP (peripheral polyneuropathy), and 1 by a PNP with predominant impairment of small fibers. The etiology is idiopathic in 23 patients, while 1 subject suffers from diabetic neuropathy, and one patient is affected by hereditary transthyretin-related amyloidosis.

### *4.1.3 Group 3*

The *population* of group 3 (31 patients) consists of 15 females and 16 males with a mean age of 48.4 ± 12.2 years (median: 50, range 29-72), and with a mean disease duration of 89.59 months (range 5-400).
Pain intensity ranges from 3 to 8/10, with a median of 5. Instead, pruritus intensity ranges from 3 to 6/10, with a median of 4.
Twenty-three patients are affected by pure SFN (small fiber neuropathy), 1 by PNP (peripheral polyneuropathy), and 7 by a PNP with predominant impairment of small fibers. The etiology is idiopathic in 24 patients, 2 subjects suffer from diabetic neuropathy, one patient is affected by hereditary transthyretin-related amyloidosis, three patients suffer from vitamin deficiency (B12, B6), and one patient is affected by an autoimmune disease.

### *4.1.4 Group 4*

The *population* of group 4 (12 patients) consists of 6 females and 6 males with a mean age of 59.5 ± 11.6 years (median: 59.5, range 42-77), and with a mean disease duration of 53.58 months (range 8-240).
Five patients are affected by pure SFN (small fiber neuropathy), 5 by PNP (peripheral polyneuropathy), and 2 by PNP with predominant impairment of small fibers. The etiology is idiopathic in 7 patients, one patient is affected by hereditary transthyretin-related amyloidosis, one suffers from critical illness, one is affected by an autoimmune disease, and in two patients a toxic cause was recognized.

### *4.1.5 Group 5*

Group 5 (25 patients) consists of 11 females and 14 males with a mean age of 49.6 ± 10.0 years (median: 52, range 23-67).

## 4.2 Comparison Analysis

### *4.2.1 Differences between the different groups of patients and the group of controls*

#### *4.2.1.1 Differences between Group 1 (NP + pruritus) and Group 5 (controls)*

Group 1 had a significant reduction in the following parameters compared with controls:

-Subepidermal layer:

- Vessel Area µm$^2$: p=0.046 (assessed with Mann-Whitney U test, *Diagram 1*)
- Vessel Area %: p=0.051 (assessed with Mann-Whitney U test, *Diagram 2*)

- Small fiber number: p=0.011 (assessed with Student t test (Shapiro-Wilk test: p=0.241; Levene's test: p=0.127), *Diagram 3*)
- Small fiber Area µm$^2$: p=0.007 (assessed with Mann-Whitney U test, *Diagram 4*)
- Small fiber Area %: p= 0.002 (assessed with Student t test (Shapiro-Wilk test: p=0.689.; Levene's test: p=0.656), *Diagram 5*)

- Contact number: p= 0.015 (assessed with Mann-Whitney U test, *Diagram 6*)
- Contact Area µm$^2$: p= 0.002 (assessed with Mann-Whitney U test, *Diagram 7*)
- Contact Area %: p= 0.002 (assessed with Mann-Whitney U test, *Diagram 8*)

-Dermal layer:

- Small fiber number: p= 0.021 (assessed with Mann-Whitney U test, *Diagram 9*)
- Small fiber Area µm$^2$: p= 0.018 (assessed with Student T test (Shapiro-Wilk test: p=0.554.; Levene's test: p=0.051), *Diagram 10*)
- Small fiber Area %: p= 0.008 (assessed with Mann-Whitney U test, Diagram *11*)

- Contact number: p= 0.012 (assessed with Mann-Whitney U test, *Diagram 12*)
- Contact Area µm$^2$: p= 0.023 (assessed with Mann-Whitney U test, *Diagram 13*)

Below, the charts related to the significant values are reported:

*<u>Diagram 1:</u>*
*Subepidermal vessel Area µm$^2$ in group 1 and in group 5.*

Mann-Whitney U test p= 0.046. In group 1 patients affected by NP and complaining only pruritus are included.

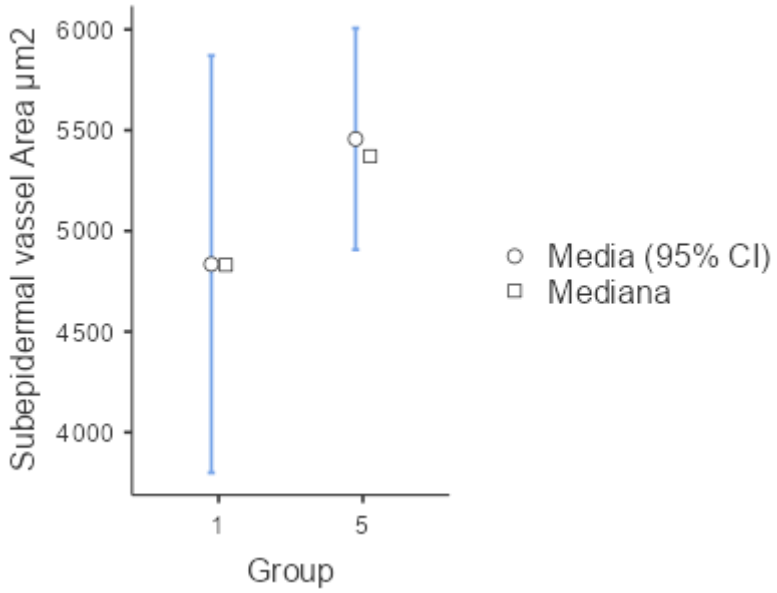


*<u>Diagram 2:</u> Subepidermal vessel Area % in group 1 and in group 5.*

Mann-Whitney U test p= 0.051. In group 1 patients affected by NP and complaining only pruritus are included.

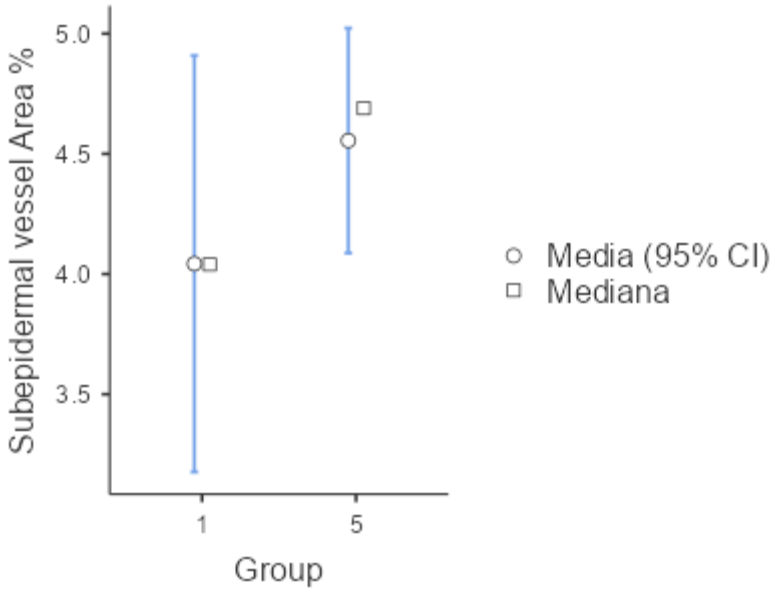

*<u>Diagram 3:</u> Subepidermal Small fiber number in group 1 and in group 5.*

Student t test p= 0.011. In group 1 patients affected by NP and complaining only pruritus are included.

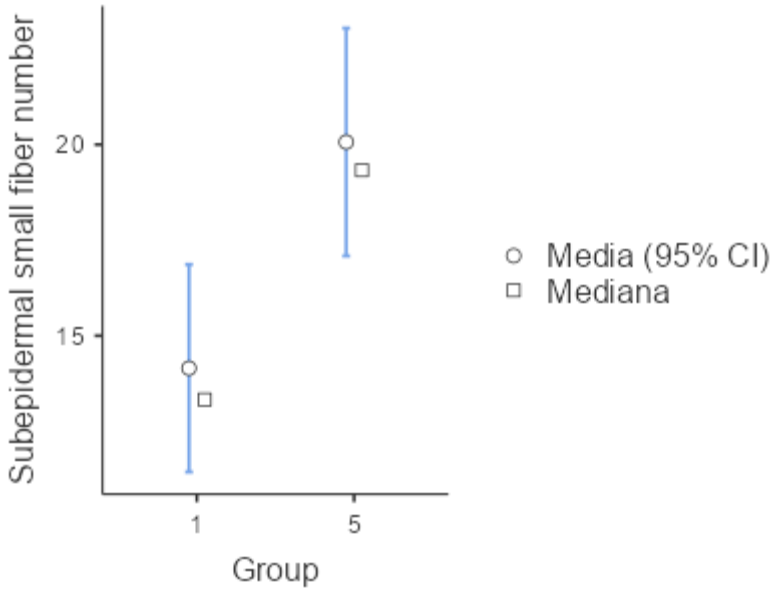


*<u>Diagram 4:</u> Subepidermal Small fiber Area µm² in group 1 and in group 5.*

Mann-Whitney U test p= 0.007. In group 1 patients affected by NP and complaining only pruritus are included.

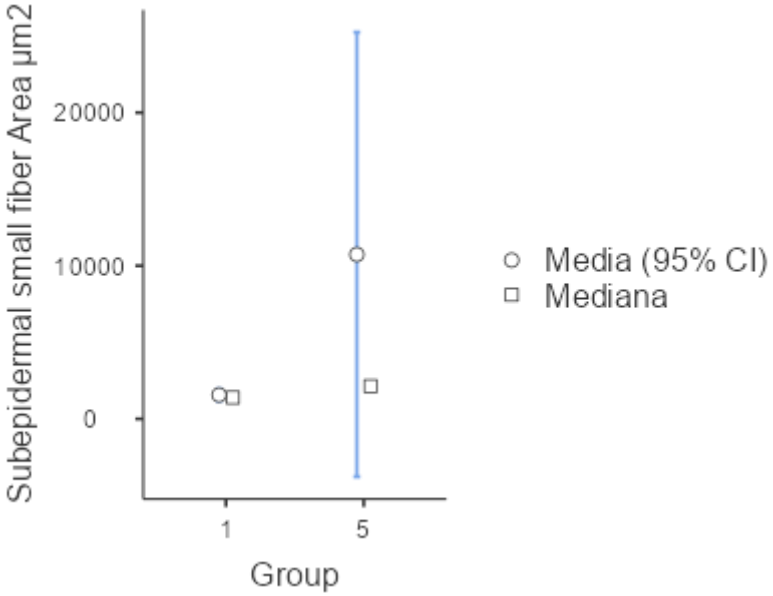


*<u>Diagram 5</u>: Subepidermal Small fiber Area % in group 1 and in group 5.*

Student T test p= 0.002. In group 1 patients affected by NP and complaining only pruritus are included.

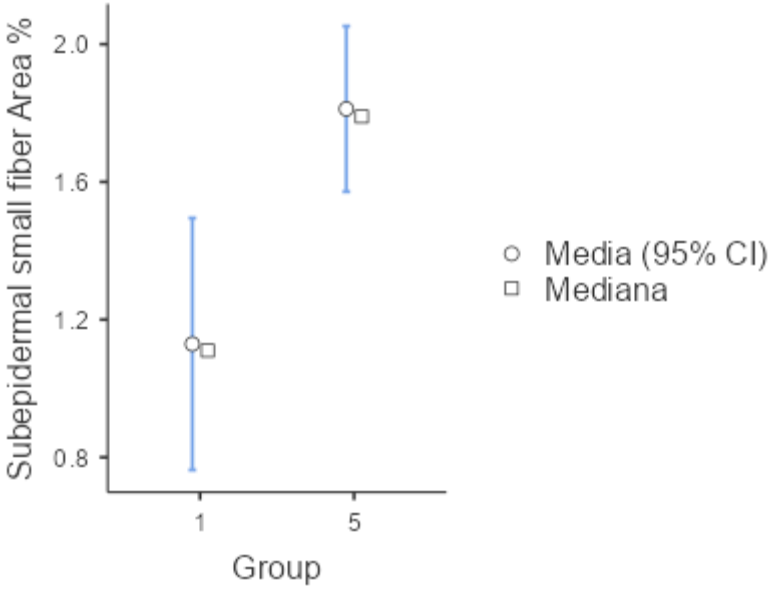

*<u>Diagram 6</u>: Subepidermal Contact number in group 1 and in group 5.*

Mann-Whitney U test p= 0.015. In group 1 patients affected by NP and complaining only pruritus are included.

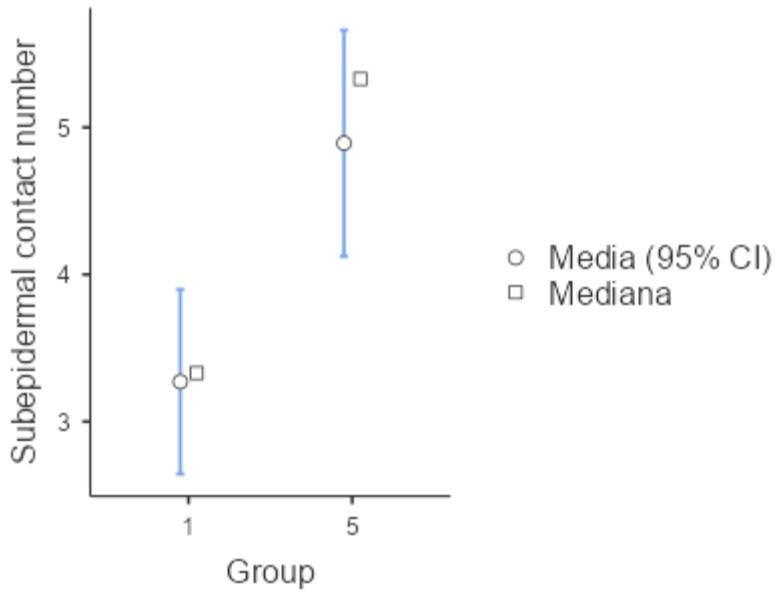


*<u>Diagram 7:</u> Subepidermal Contact Area µm² in group 1 and in group 5.*

Mann-Whitney U test p= 0.002. In group 1 patients affected by NP and complaining only pruritus are included.

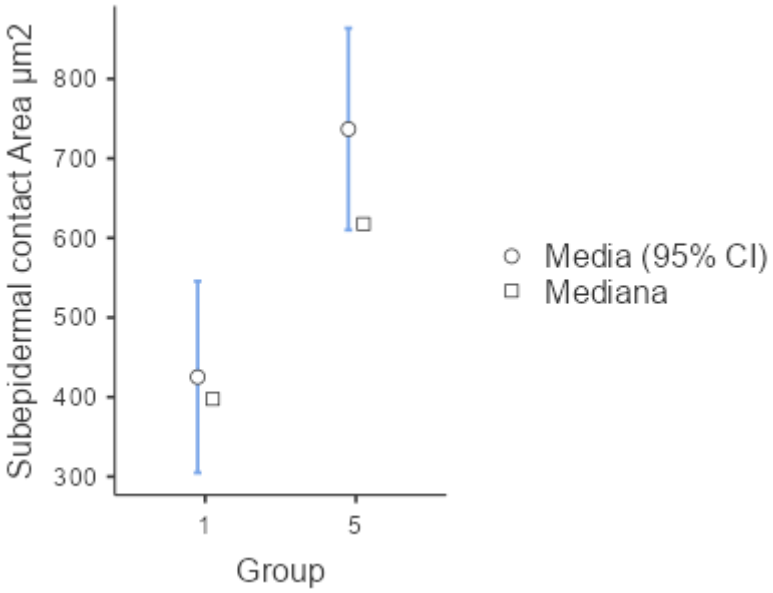


*<u>Diagram 8</u> Subepidermal Contact Area % in group 1 and in group 5.*

Mann-Whitney U test p= 0.002. In group 1 patients affected by NP and complaining only pruritus are included.

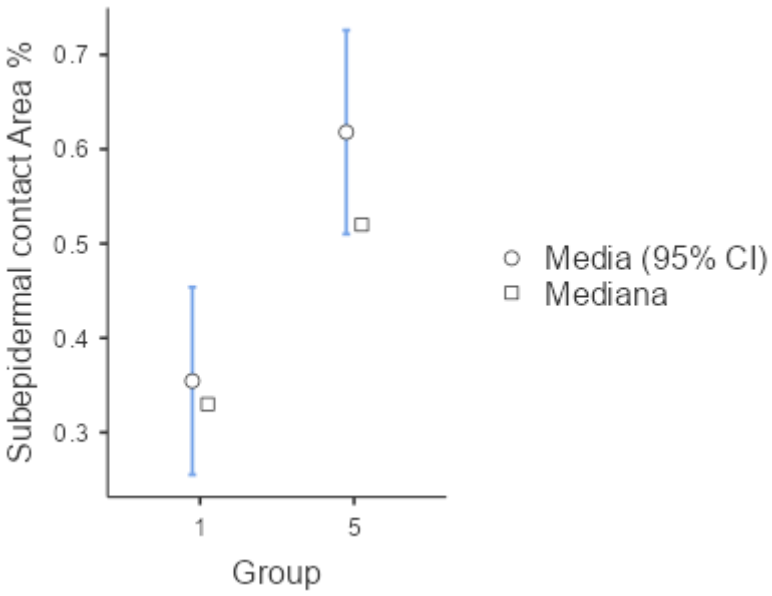

*<u>Diagram 9:</u> Dermal Small fiber number in group 1 and in group 5.*

Mann-Whitney U test p= 0.021. In group 1 patients affected by NP and complaining only pruritus are included.

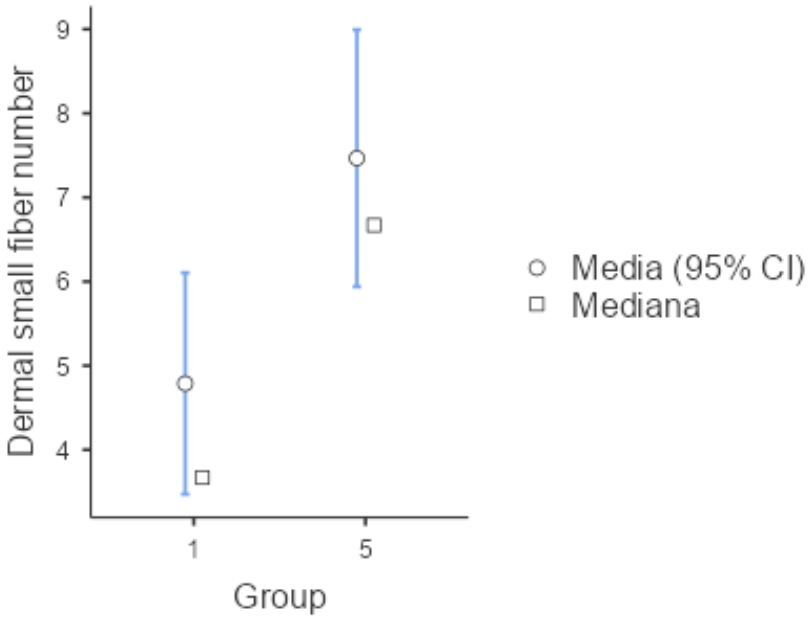


*<u>Diagram 10:</u> Dermal Small fiber Area µm² in group 1 and in group 5.*

Student T test p= 0.018. In group 1 patients affected by NP and complaining only pruritus are included.

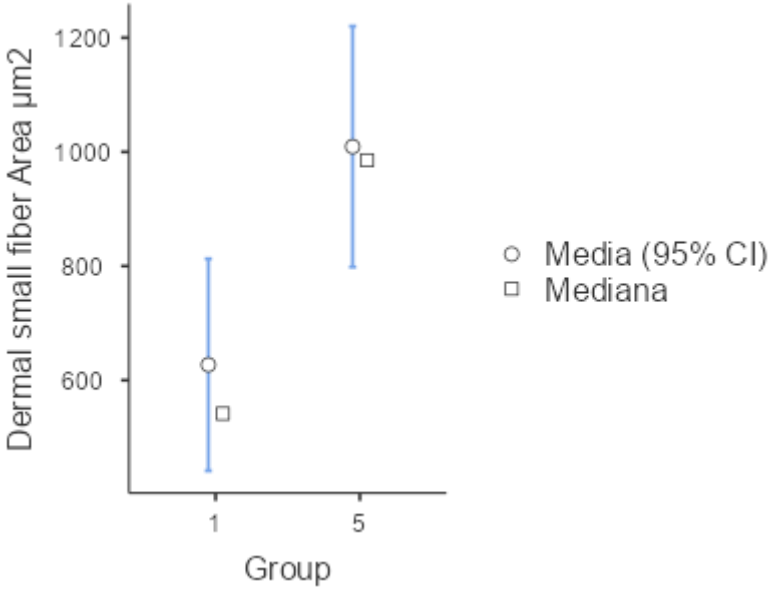


*<u>Diagram 11:</u> Dermal Small fiber Area % in group 1 and in group 5.*

Mann-Whitney U test p= 0.008. In group 1 patients affected by NP and complaining only pruritus are included.

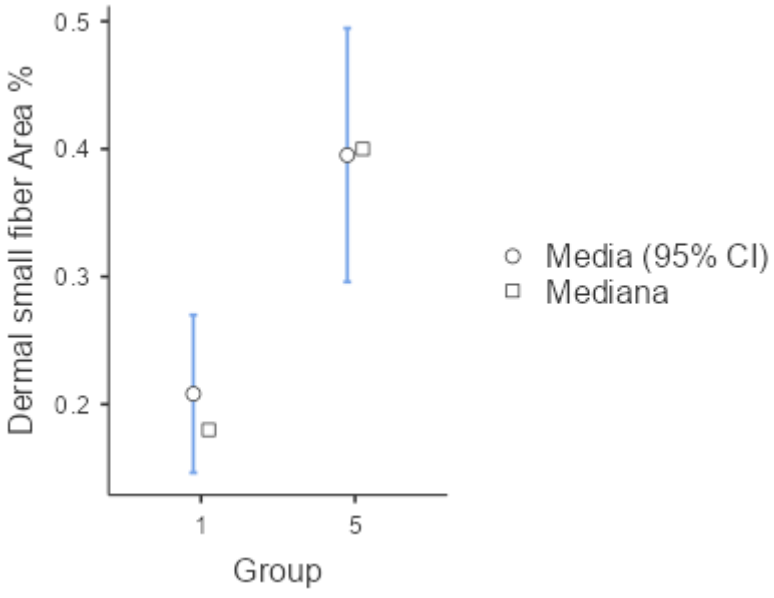

*<u>Diagram 12:</u> Dermal Contact number in group 1 and in group 5.*

Mann-Whitney U test p= 0.012. In group 1 patients affected by NP and complaining only pruritus are included.

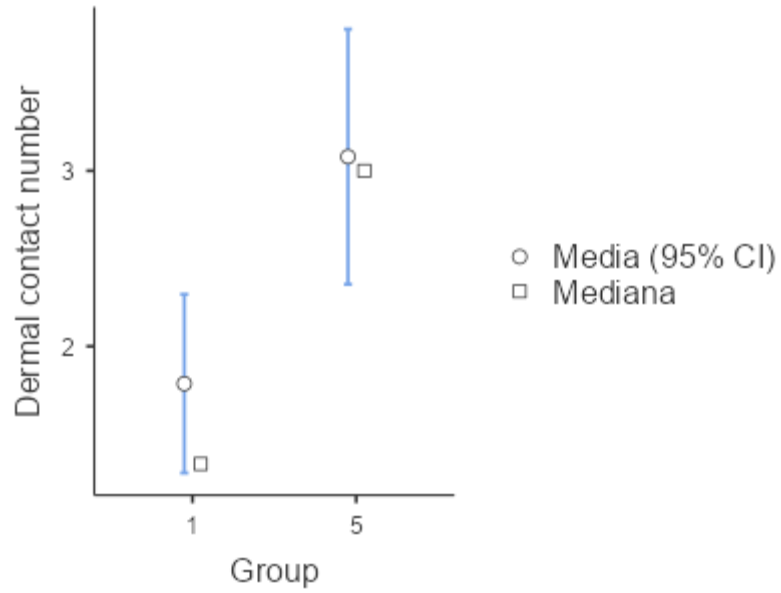


*<u>Diagram 13:</u> Dermal Contact Area µm² in group 1 and in group 5.*

Mann-Whitney U test p= 0.023. In group 1 patients affected by NP and complaining only pruritus are included.

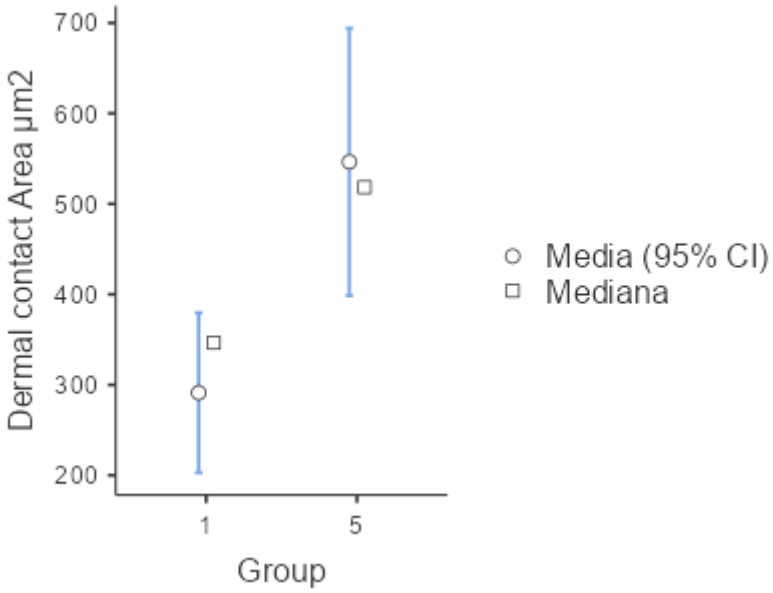


*4.2.1.2 Comparison between Group 2 (NP + pain) and Group 5 (controls)*

No significant differences were detected in either subepidermal or dermal layers for the following parameters:

- Vassel number, Area µm², and Area %
- Small fiber number, Area µm², and Area %
- Neurovascular contact number, Area µm², and Area %

*4.2.1.3 Comparison between Group 3 (NP + pruritus and pain) and Group 5 (controls)*

Group 3 had significantly smaller values compared to Group 5 in the following parameters:

- Subepidermal layer:
  - Small fiber number: p= 0.018 (assessed with Student T test (Shapiro-Wilk test: p=0.139.; Levene's test: p=0.651) *Diagram 14*)
  - Small fiber Area μm$^2$: p= 0.011 (assessed with Mann-Whitney U test, *Diagram 15)*
  - Small fiber Area %: p= 0.014 (assessed with Student T test (Shapiro-Wilk test: p=0.964.; Levene's test: p=0.623) *Diagram 16*)

- Dermal layer:
  - Contact number: p= 0.035 (assessed with Student T test (Shapiro-Wilk test: p=0.090.; Levene's test: p=0.421) *Diagram 17*)
  - Contact Area μm$^2$: p= 0.038 (assessed with Mann-Whitney U test *Diagram 18*)

Below, the charts related to the significant values are reported:

*Diagram 14: Subepidermal Small fiber number in group 3 and in group 5.*

Student T U test p= 0.018. In group 3 patients affected by NP and complaining pruritus and pain are included.

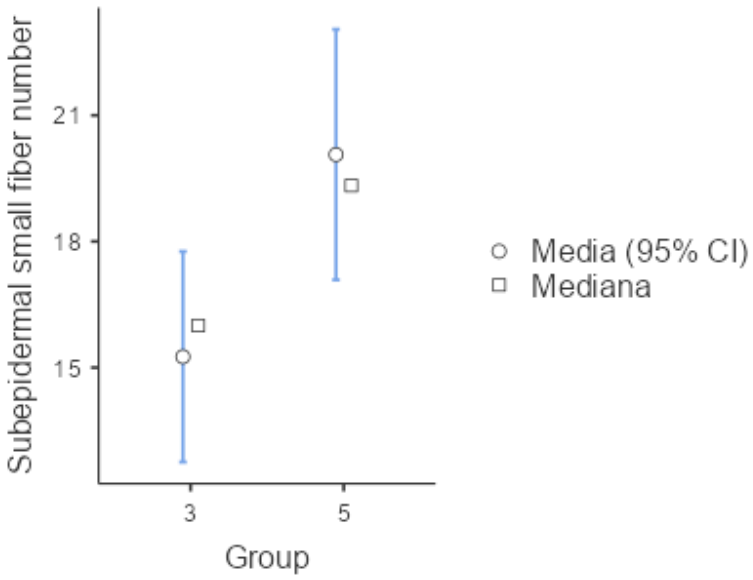

*<u>Diagram 15</u>: Subepidermal Small fiber Area µm² in group 3 and in group 5.*

Mann-Whitney U test p= 0.011. In group 3 patients affected by NP and complaining pruritus and pain are included.

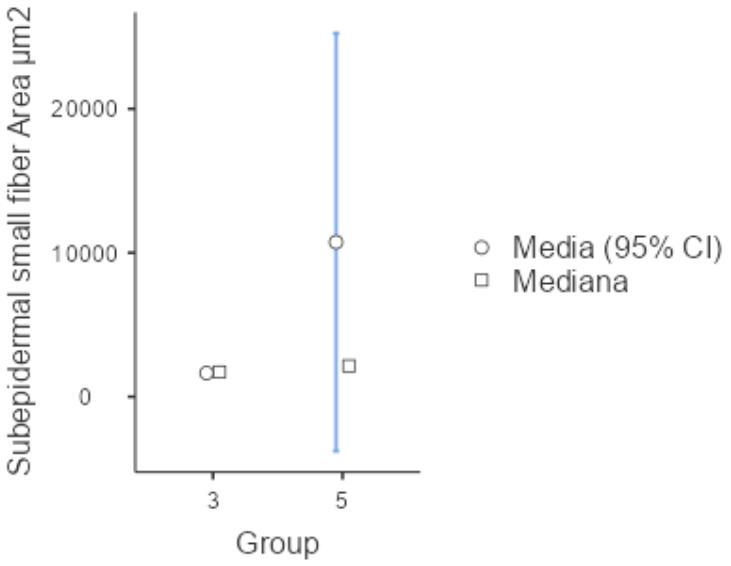


*<u>Diagram 16</u>: Subepidermal Small fiber Area % in group 3 and in group 5.*

Student T test p= 0.014. In group 3 patients affected by NP and complaining pruritus and pain are included.

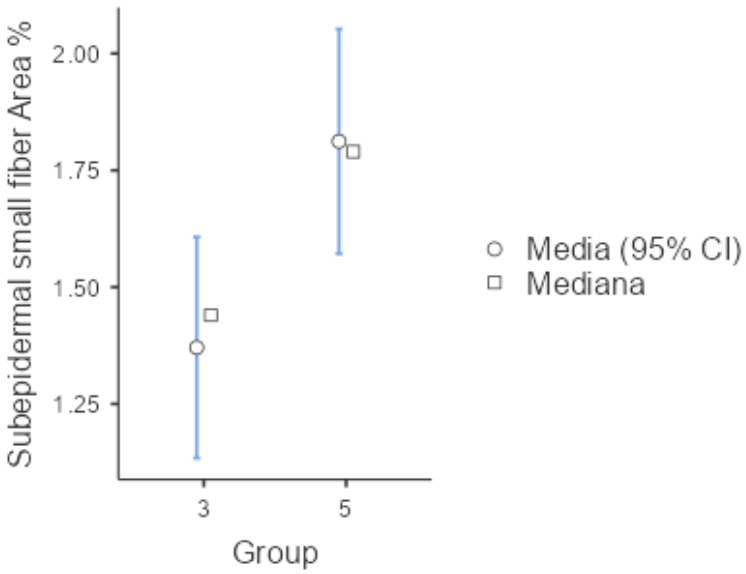


*<u>Diagram 17</u>: Dermal Contact number in group 3 and in group 5.*

Student T test p= 0.018. In group 3 patients affected by NP and complaining pruritus and pain are included.

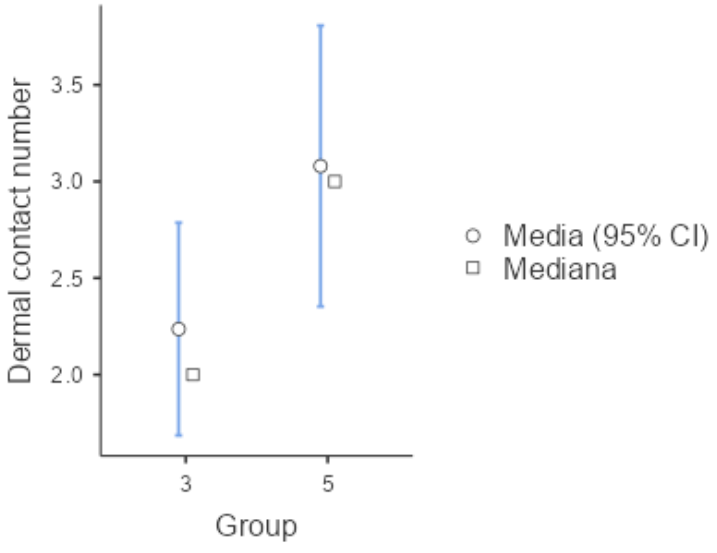

*<u>Diagram 18</u>: Dermal Contact Area µm² in group 3 and in group 5.*

Mann-Whitney U test p= 0.018. In group 3 patients affected by NP and complaining pruritus and pain are included.

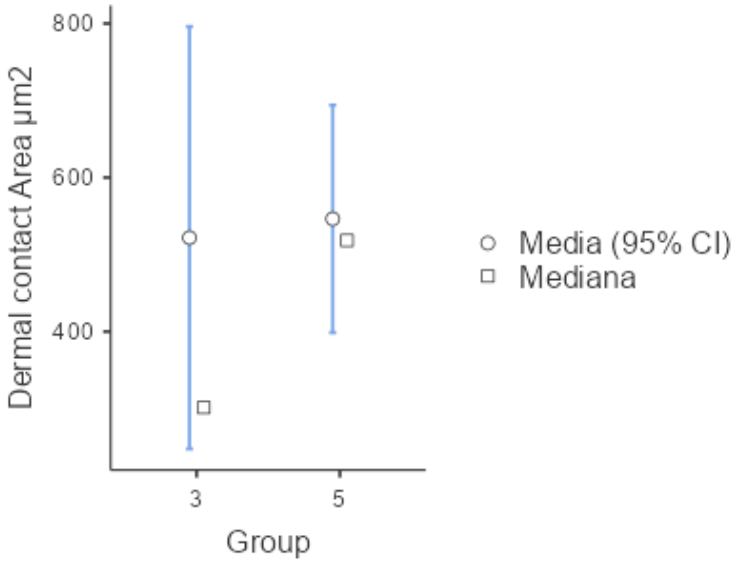


#### *4.2.1.4 Comparison between Group 4 (NP without pruritus or pain) and Group 5 (controls)*

Group 4 had decreased values in the following parameters:

- Subepidermal layer:
    - Small fiber number: p= 0.14 (assessed with Student T test (Shapiro-Wilk test: p=0.576.; Levene's test: p=0.275) *Diagram 19*)
    - Small fiber Area µm²: p=0.033 (assessed with Mann-Whitney U test, *Diagram 20*)

    - Contact Area µm²: p=0.044 (assessed with Student T test (Shapiro-Wilk test: p=0.144.; Levene's test: p=0.851) *Diagram 21*)
    - Contact Area %: p=0.044 (assessed with Student T test (Shapiro-Wilk test: p=0.109.; Levene's test: p=0.776) *Diagram 22*)

Below, the charts related to the significant values are reported:

*<u>Diagram 19</u> Subepidermal Small fiber number in group 4 and in group 5.*

Student T test p= 0.014. In group 3 patients affected by NP and not complaining any symptoms.

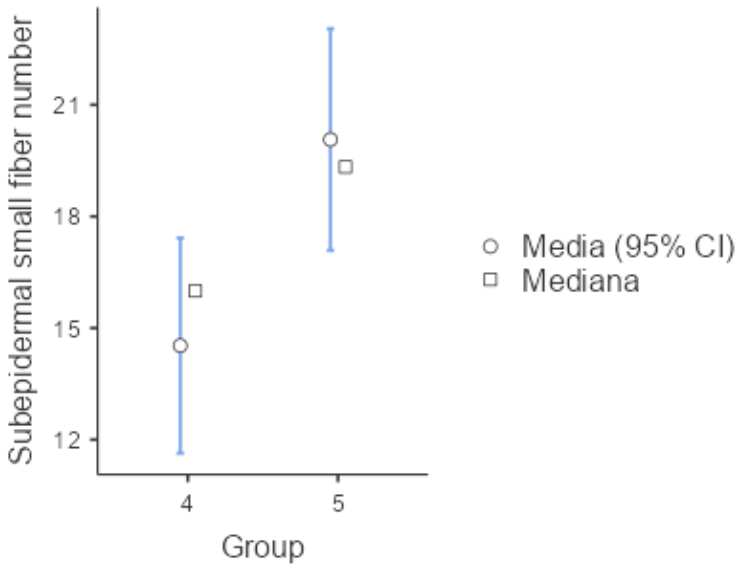


*<u>Diagram 20</u>: Subepidermal Small fiber Area µm² in group 4 and in group 5.*

Mann- Whitney U test p= 0.033. In group 3 patients affected by NP and not complaining any symptoms.

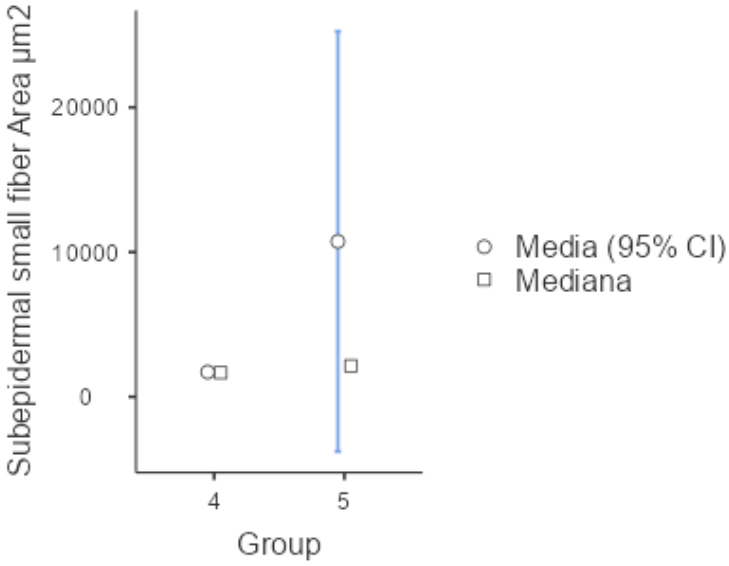


*<u>Diagram 21</u>: Subepidermal Contact Area µm² in group 4 and in group 5.*

Student T test p= 0.044. In group 3 patients affected by NP and not complaining any symptoms.

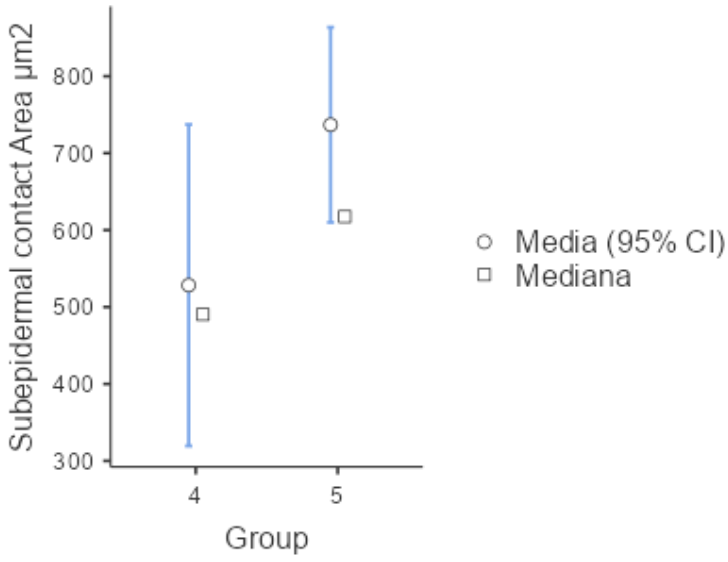

*<u>Diagram 22</u>: Subepidermal Contact Area % in group 4 and in group 5.*

Student T test p= 0.044. In group 3 patients affected by NP and not complaining any symptoms.

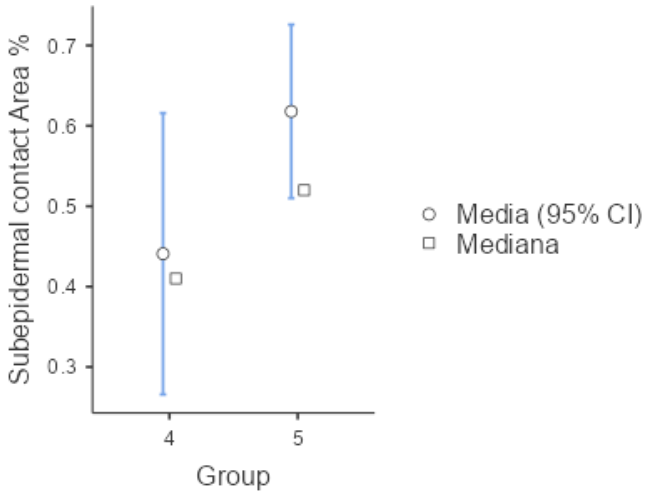


### *4.2.2 Comparison between the Group of patients complaining symptoms versus the Group of patients with only NP*

No significant differences ($p<0.05$) were detected in either subepidermal or dermal layers between the groups of patients complaining of symptoms, pain and/or pruritus (groups 1,2, and 3) and those affected by NP, but not complaining of any symptoms (group 4) for the following parameters:

- Vassel number, Area $\mu m^2$, and Area %
- Small fiber number, Area $\mu m^2$, and Area %
- Neurovascular contact number, Area $\mu m^2$, and Area %

### *4.2.3 Comparison between the Group of patients complaining of only pruritus versus the Group of patients complaining of only pain*

Patients complaining of only pruritus (group 1) compared with those complaining of only pain (group 2) showed a significant reduction in the following parameters:

- Subepidermal layer:
    - Small fibers Area %: p= 0.017 (assessed with Student T test (Shapiro-Wilk test: p=0.090.; Levene's test: p=0.381) Diagram 23)

    - Contact number: p= 0.035 (assessed with Student T test (Shapiro-Wilk test: p=0.345.; Levene's test: p=0.105, Diagram 24)

- Contact Area µm$^2$: p= 0.035 (assessed with Mann-Whitney U test, Diagram 25)
- Contact Area %: p= 0.044 (assessed with Mann-Whitney U test, Diagram 26)

- Dermal layer:
  - Small fiber number: p= 0.023 (assessed with Student T test(Shapiro-Wilk test: p=0.642.; Levene's test: p=0.690) Diagram 27)
  - Small fiber Area µm$^2$: p= 0.034 (assessed with Student T test(Shapiro-Wilk test: p=0.245.; Levene's test: p=0.173), Diagram 28)
  - Small fiber Area %: p= 0.021 (assessed with Mann-Whitney U test, Diagram 29)

Below, the charts related to the significant values are reported:

*Diagram 23*: *Subepidermal small fiber Area % in group 1 and in group 2.*

Student T test p= 0.017. In group 1 patients affected by NP, complaining only pruritus are included, instead in group 2 patients affected by NP, complaining only pain are included.

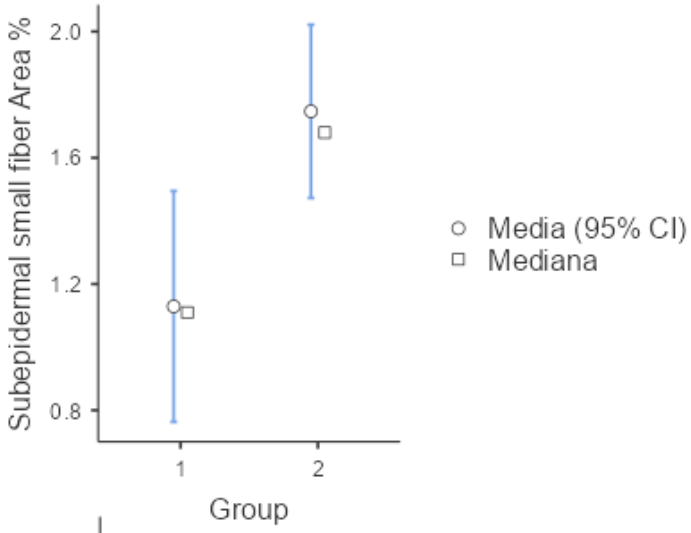


*Diagram 24*: Subepidermal contact number *in group 1 and in group 2.*

Student T test p= 0.035. In group 1 patients affected by NP, complaining only pruritus are included, instead in group 2 patients affected by NP, complaining only pain are included.

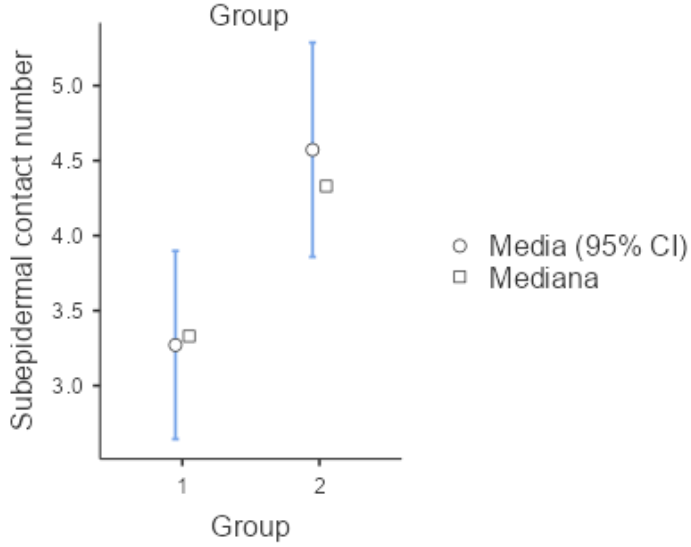

*Diagram 25*: *Subepidermal contact Area μm² in group 1 and in group 2.*

Mann-Whitney U test p= 0.035. In group 1 patients affected by NP, complaining only pruritus are included, instead in group 2 patients affected by NP, complaining only pain are included.

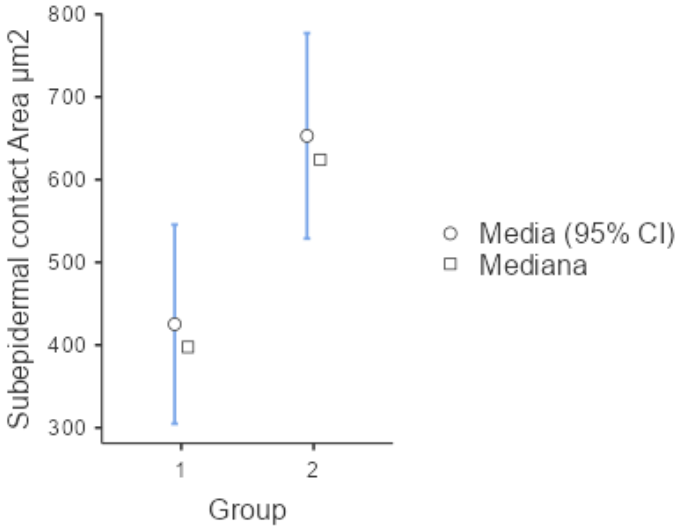


*Diagram 26*: Subepidermal contact Area % *in group 1 and in group 2.*

Mann Whitney U test p= 0.044. In group 1 patients affected by NP, complaining only pruritus are included, instead in group 2 patients affected by NP, complaining only pain are included.

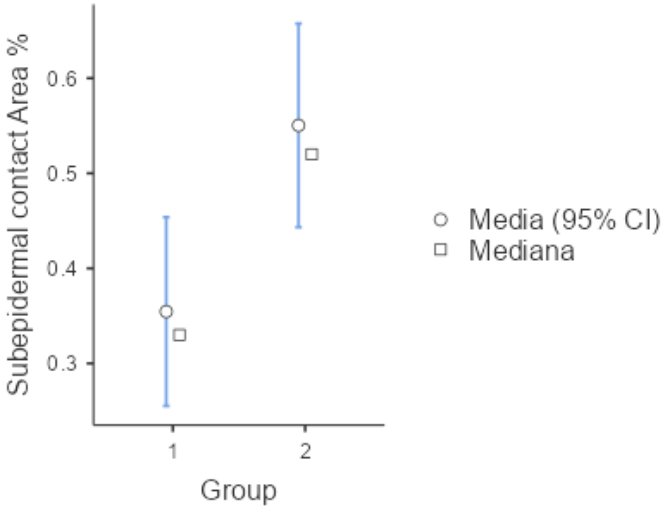


*Diagram 27: Dermal small fiber number in group 1 and in group 2.*

Student T test p= 0.023. In group 1 patients affected by NP, complaining only pruritus are included, instead in group 2 patients affected by NP, complaining only pain are included.

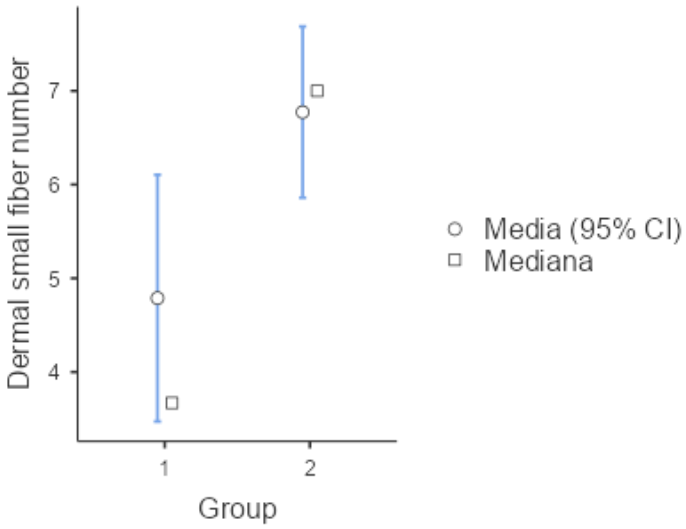

*<u>Diagram 28</u>: Dermal small fiber Area μm² in group 1 and in group 2.*

Student T test p= 0.034. In group 1 patients affected by NP, complaining only pruritus are included, instead in group 2 patients affected by NP, complaining only pain are included.

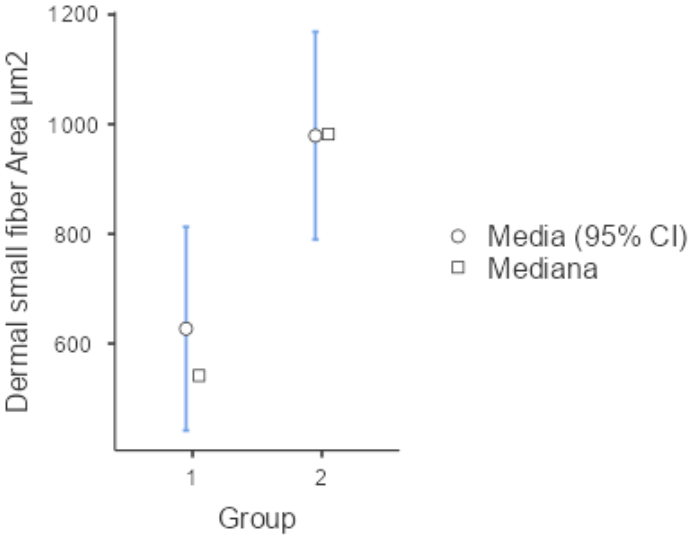


*<u>Diagram 29</u>: Dermal small fiber Area % in group 1 and in group 2.*

Mann Whitney U test p= 0.021. In group 1 patients affected by NP, complaining only pruritus are included, instead in group 2 patients affected by NP, complaining only pain are included.

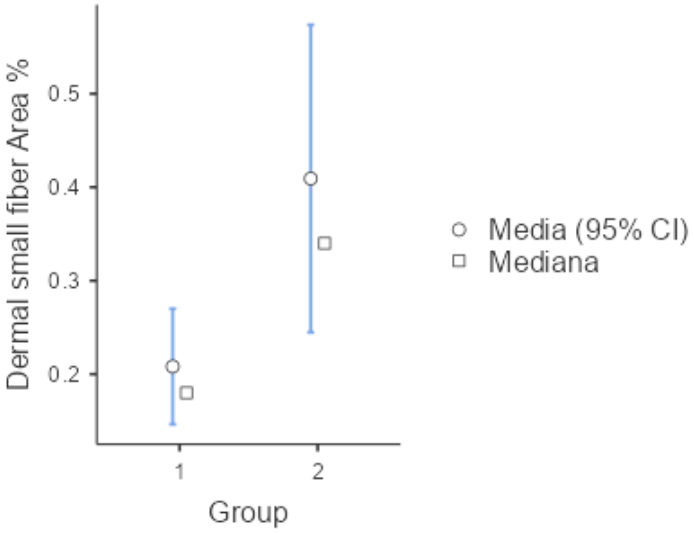


## 4.3 Correlation Matrix

### *4.3.1 Group 1*

A significant correlation was observed between *pruritus intensity* and subepidermal contact number (rho = +0.766, p=0.010), subepidermal contact area μm² (rho = +0.796, p=0.006), and subepidermal contact area % (rho = +0.777, p=0.008).

Instead, no significances were detected in the correlation with *Age, ODSS*, and *mTCNs.*

### *4.3.2 Group 2*

A significant correlation emerged between *age* and dermal vessel number (rho= +0.048, p=0.037), dermal vessel area μm$^2$ (rho +0.492; p=0.015), and dermal vessel area % (rho= +0.488; p=0.016).

Instead, no significances were observed in the correlation with *Pain intensity, ODSS*, and *mTCNs.*

### *4.3.3 Group 3*

*Age* significantly correlated with dermal vessel Area μm$^2$ (rho = -0.380, p = 0.035), dermal vessel Area % (rho = -0.365, p = 0.044), and dermal contact number (r di Rho = -0.450, p = 0.011).

*Pain intensity* significantly correlated with dermal small fiber number (rho=+ 0.47, p=0.012 0) and dermal small fiber Area μm$^2$ (rho=+ 0.365, p=0.044).

Lastly, *ODSS* was significantly correlated with the dermal contact number (rho= -0.431, p = 0.022).

Instead, *Pruritus intensity* did not correlate with *mTCNs*

### *4.3.4 Group 4*

No significant correlations emerged between the parameters assessed with skin biopsy and *Pruritus intensity, Pain intensity, ODSS,* or *mTCNs*

### *4.3.5 Group 5*

Dermal Small fiber number significantly correlated with age in healthy individuals (rho= -0.466, p=0.019).

.

## *5. DISCUSSION*

Keeping in mind the hypotheses established in this study, the critical analysis of the results aims to identify any significant differences in terms of the number and area of vascular structures, small nerve fibers, and neurovascular contacts at different layers of the skin (dermis, sub-epidermis, and epidermis) between groups of patients affected by peripheral neuropathy and controls.

Remarkable outcomes came to light mainly in the comparison between group 1 (patients affected by NP complaining of pruritus) and group 5 (controls).

In both layers of the skin, sub-epidermis and dermis, a decreased number and area of small fibers and neurovascular contacts was detected; moreover, a reduction in vessel area was detected in the sub-epidermidis.

Studies on interactions between the peripheral nervous system and blood vessels have been conducted since the early 2000s. Among the first studies on this topic, the work by Ruocco I, published in 2002, is certainly one of the most important. This was the first comprehensive study demonstrating that both sensory and autonomic fibers (sympathetic and parasympathetic fibers) innervate the same skin blood vessels. An initial description of the innervation of vessels by sensory, sympathetic, and parasympathetic fibers was accomplished in cerebral blood vessels. In this study, the role of C fibers and parasympathetic autonomic fibers in the vasodilation of the capillaries is described. Notably, vasodilation occurs through the release of substance P by sensory fibers and acetylcholine by parasympathetic fibers. On the other hand, sympathetic fibers are involved in vasoconstriction through to the release of noradrenaline.[75]

Moreover, several studies demonstrated that the peripheral nervous system, in particular the sympathetic fibers, has a trophic effect on the vascular wall. To demonstrate this, when levels of SNS activity are diminished, the arterial wall undergoes changes similar to those usually seen in the aging process. In particular, when the aortic wall is deprived of adrenergic nerve stimuli, there is an increase in connective tissue content, and this phenomenon resembles the trend seen in the natural aging of the aorta.[76]

Despite the knowledge of a correlation between the peripheral nervous system and vascular structures has been known for many years, few studies have examined the innervation of the cutaneous vasculature and no broadly reliable standardized methods for quantification exist.

The publication of Sohn E.'s work in 2019 represented a significant advancement in this context, providing a reliable and reproducible method for quantifying the density of nerves, blood vessels, and neurovascular contacts. In this case-control study patients affected by diabetes were compared with a group of healthy controls. For each subject, a skin sample was taken both from the thigh (proximal site) and the leg (distal site), and double IF (PGP 9.5 and CD31) was used for the staining. Various parameters were compared between the two groups, assuming the hypothesis that the density of vessels, small fibers, and neurovascular contacts in the two skin regions, sub-epidermis and dermis, might be reduced in the patient group. A reduction in the density of vessels, small fibers, and neurovascular contacts was observed only in the subepidermal layer of the patients, while not in the dermis. [70]

Comparing the results of the work from Sohn E. to the ones obtained in our study from the comparison between group 1 and group 5, the outcomes partially overlap, in particular regarding the reduction of vessel, small fiber, and neurovascular contact density in the sub-epidermis. Therefore, our results confirm the hypothesis that in subjects affected by peripheral neuropathy, either a SFN or a polyneuropathy of different type, there is a concurrent reduction in the density of small fibers and vessels, leading to a decrease in the density of neurovascular contacts. This supports the existence of a close association between the PNS and vascular structures.

In our study, unlike Sohn E.'s, not only patients with peripheral neuropathy caused by diabetes were enrolled, but also patients with NP of different etiologies. The two main criteria for study enrollment were the presence of pain and/or pruritus along with the presence of a PN diagnosis. The second goal of the study was to correlate the biopsy findings with the different types and intensities of symptoms to better understand the underlying pathogenetic mechanism.

No significance emerged in group 2, patients with NP reporting pain when compared to group 5, controls. However, group 3, which consisted of patients with NP reporting both pain and itching, differed from group 5 in terms of the number and area of small fibers in the subepidermal layer, and the number and area of neurovascular contacts in the dermal region.

A critical analysis of these results shows that group 1 is the most compromised, followed by group 3, both of which include patients reporting itching. This leads to the hypothesis that itching, compared to pain, has a greater impact on the condition of vessels and small fibers in the skin layers, particularly in the subepidermal space.

Some studies have reported neurocutaneous morphological alterations in neuropathic pruritic conditions, focusing more on the IENFD. In this study, IENFD was non taken into account because the focus has been primarily on the interaction between vessels and small fibers. Thus, the examination of the epidermal neural architecture may provide important hints for the diagnosis of a neuropathic pruritic condition. Clinically, the entity of the decrease in IENFD seems to influence the perception of dysesthesias. Importantly, scratch lesions, scars or other skin conditions (e.g., eczema, skin infections) should be avoided when choosing the biopsy site, since such alterations may lead to false pathological findings. [77]

These results seem to demonstrate a significant difference between group 1, patients experiencing itching, and group 2, patients experiencing pain, in terms of number, area, and density of vessels, small fibers, and neurovascular contacts in different skin layers. This could suggest that the two symptoms do not share the same pathogenic mechanism.

Itch and pain are different sensations, among which complex interactions exist. Several studies have been showed that their commonalities, in terms of molecules, cells, and circuits, are undeniable. Pain and itch-detecting neurons are anatomically indistinguishable; both are sensed by small-diameter, unmyelinated C-fibers in fact participants often report coexisting pain and itch sensations (“stinging itch” and “itching burn”) in response to itchy and painful exogenous

stimuli, and moreover even similar therapeutic strategies have been tried successfully (e.g., carbamazepine, gabapentin…) [19,78]

Itch was believed to perceive when the fiber was activated by a “milder” stimulus, while a more severe stimulus of the sensory nociceptors would indicate pain. However, this has been proven to be incorrect. Studies have found a subset of C fibers that only convey the sensation of pruritus to the spinal cord. Possible explanation of the unique pruritic-associated C fibers was proposed in a study by Liu and Ji, which entailed irritative chemicals selectively activating different intracellular pathways and distant receptors in the same neuron to differentiate the sensation of itch or pain. Moreover, this study also proposed that pruritus may depend on completely different intracellular signaling pathways in sensory neurons than pain stimuli. [14]

Moreover, it is interesting to note that these results were obtained despite group 1 is smaller (11 patients) compared to group 2 (25 patients) and group 5 (25 healthy subjects).

The fact that group 1 is the smallest among all the groups should not be surprising, as neuropathic itch occurs in a limited percentage of patients with small-fiber neuropathy (SFN), and in most cases it is associated with a burning pain sensation[17], explaining the high numerosity of group 3 (31 patients).

From the comparison between group 1 and group 4, which includes patients with NP who do not report either itching or pain, no differences emerged. Since Group 4 patients have NP without pruritus or pain, smaller histologic alterations were expected compared to those of patients with symptoms. Thus, our results are likely due to the small sample size analyzed.

Therefore, the first major limitation of this study is the small sample size. For this reason, it is hoped that in the future, the study can be expanded by enrolling more subjects to obtain larger and more uniform groups, allowing to bring to light new significances.

A strength of the study is the use of the new image analysis software “dermal layer analysis”, a tool provided by Fiji program. Before the introduction of the new software, the counting was performed manually following conventional rules

reported in the literature. As it is explained in the study by Sohn E., a circular grid mask of 48.3 μm in diameter and space in the orthogonal direction was applied above the area of interest (AOI). Nerve fibers and blood vessels located within the circle or touching it were counted individually. The percentage of circles with nerve or vessel contacts was defined respectively as nerve density and vessel density; instead, the neurovascular contact was defined as the percentage of circles with both nerve and vessel contacts *(Figure 31).*[70] Therefore, the limitations of the manual counting proposed in the 2019 study include the high operator-dependent subjectivity in counting the structures, resulting in a high error rate, the fact that the grid drawn on the Area of Interest (AOI) considers only half of the actual AOI, and the high time spent performing the counting. These issues are essentially erased in the technique proposed in this study, as the program autonomously identifies the specific structures to consider based on the criteria indicated by the operator in the initial window. However, it should be noted that manual correction of what the software identifies is often necessary. The introduction of this software has certainly represented a significant step forward in image analysis, precise rules need to be established to minimize operator-dependent variability that still exists during the manual correction process.

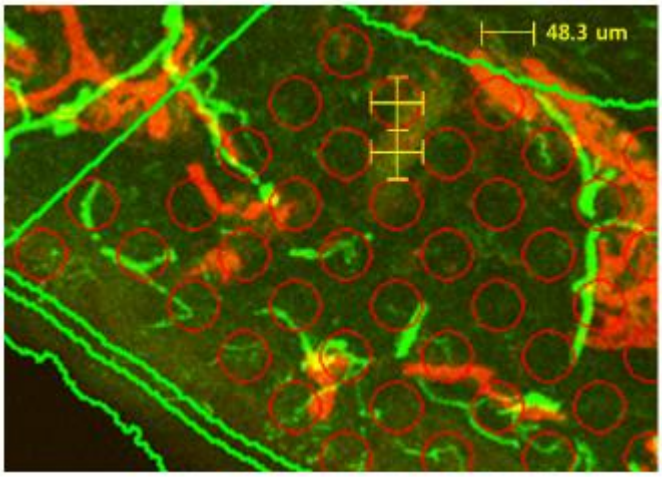


*Figure 31: conventional manual counting representation.* Size and distribution of the circular grid mask for stereological analysis. The circles, 48.3μm in diameter, were distributed in an orthogonal pattern at a distance of 48.3 μm.

Image taken from the paper “A novel method to quantify cutaneous vascular innervation” by Sohn E.

In the future, it will be interesting to compare the data obtained from the analysis of skin samples taken from the thigh with those taken from the leg, to understand whether the trend of the observed results is consistent or if there are differences. This comparison can help determine whether the pattern of NP distribution is length-dependent or length-independent concerning symptoms such as itching or pain.

Another potential avenue for future research could be, with a larger number of enrolled subjects, a further subdivision of the groups into subgroups based on the etiology of NP. This could help to determine if there is a correlation between symptoms and etiology.

## *6. CONCLUSION*

We evaluated the alterations in small fibers, vessels, and neurovascular contacts at the subepidermal and dermal layers, in patients affected by SFN, neuropathies of different type with or without itch and /or pain, correlating the changes with these symptoms, in order to identify any symptom-related differences in the biopsy findings.

Additionally, we assessed whether SFNs are associated not only with a reduction in the number and density of small fibers, but also if there is a correlation with an impairment, in terms of the number and density, of the vascular structures in sub-epidermis and dermis. This was intended to support the hypothesis that the impairment of neurovascular contacts at the subepidermal and dermal areas may contribute to supporting the disease.

A significant reduction in the number, area, and density of small fibers, vessels, and neurovascular contacts was observed in the sub-epidermis of patients with peripheral neuropathy, particularly those experiencing pruritus. Instead, the reduction in these structures was less pronounced or absent in the dermis. These findings seem to support the hypothesis that the impairment of neurovascular contacts in the sub-epidermis may contribute to disease progression at least in the group of patients with neuropathy complaining of pruritus. Moreover, according to our results, the impairment of neurovascular contacts seems more closely associated with itching rather than pain We can then speculate that these two symptoms do not share the same pathomechanisms.

Finally, we consider that the image analysis software used in this study could be helpful, since it significantly improved the accuracy and efficiency of the analysis, minimizing operator-dependent subjectivity and errors.

A larger sample size and further research are needed to validate these results and explore the relationship between symptomatology and the etiology of PN.

## 7. REFERENCES


(1) Finsterer, J.; Scorza, F. A. Small Fiber Neuropathy. *Acta Neurol. Scand.* **2022**, *145* (5), 493–503. https://doi.org/10.1111/ane.13591.

(2) Devigili, G.; Cazzato, D.; Lauria, G. Clinical Diagnosis and Management of Small Fiber Neuropathy: An Update on Best Practice. *Expert Rev. Neurother.* **2020**, *20* (9), 967–980. https://doi.org/10.1080/14737175.2020.1794825.

(3) Peters, M. J. H.; Bakkers, M.; Merkies, I. S. J.; Hoeijmakers, J. G. J.; van Raak, E. P. M.; Faber, C. G. Incidence and Prevalence of Small-Fiber Neuropathy: A Survey in the Netherlands. *Neurology* **2013**, *81* (15), 1356–1360. https://doi.org/10.1212/WNL.0b013e3182a8236e.

(4) Johnson, S. A.; Shouman, K.; Shelly, S.; Sandroni, P.; Berini, S. E.; Dyck, P. J. B.; Hoffman, E. M.; Mandrekar, J.; Niu, Z.; Lamb, C. J.; Low, P. A.; Singer, W.; Mauermann, M. L.; Mills, J.; Dubey, D.; Staff, N. P.; Klein, C. J. Small Fiber Neuropathy Incidence, Prevalence, Longitudinal Impairments, and Disability. *Neurology* **2021**, *97* (22), e2236–e2247. https://doi.org/10.1212/WNL.0000000000012894.

(5) Cazzato, D.; Lauria, G. Small Fibre Neuropathy. *Curr. Opin. Neurol.* **2017**, *30* (5), 490. https://doi.org/10.1097/WCO.0000000000000472.

(6) Masingue, M.; Fernández-Eulate, G.; Debs, R.; Tard, C.; Labeyrie, C.; Leonard-Louis, S.; Dhaenens, C.-M.; Masson, M. A.; Latour, P.; Stojkovic, T. Strategy for Genetic Analysis in Hereditary Neuropathy. *Rev. Neurol. (Paris)* **2023**, *179* (1–2), 10–29. https://doi.org/10.1016/j.neurol.2022.11.007.

(7) Gross, F.; Üçeyler, N. Mechanisms of Small Nerve Fiber Pathology. *Neurosci. Lett.* **2020**, *737*, 135316. https://doi.org/10.1016/j.neulet.2020.135316.

(8) Sopacua, M.; Hoeijmakers, J. G. J.; Merkies, I. S. J.; Lauria, G.; Waxman, S. G.; Faber, C. G. Small-fiber Neuropathy: Expanding the Clinical Pain Universe. *J. Peripher. Nerv. Syst.* **2019**, *24* (1), 19–33. https://doi.org/10.1111/jns.12298.

(9) Martinelli-Boneschi, F.; Colombi, M.; Castori, M.; Devigili, G.; Eleopra, R.; Malik, R. A.; Ritelli, M.; Zoppi, N.; Dordoni, C.; Sorosina, M.; Grammatico, P.; Fadavi, H.; Gerrits, M. M.; Almomani, R.; Faber, C. G.; Merkies, I. S. J.; Toniolo, D.; INGI Network; Cocca, M.; Doglioni, C.; Waxman, S. G.; Dib-Hajj, S. D.; Taiana, M. M.; Sassone, J.; Lombardi, R.; Cazzato, D.; Zauli, A.; Santoro, S.; Marchi, M.; Lauria, G. COL6A5 Variants in Familial Neuropathic Chronic Itch. *Brain J. Neurol.* **2017**, *140* (3), 555–567. https://doi.org/10.1093/brain/aww343.

(10) Azcue, N.; Del Pino, R.; Acera, M.; Fernández-Valle, T.; Ayo-Mentxakatorre, N.; Pérez-Concha, T.; Murueta-Goyena, A.; Lafuente, J. V.; Prada, A.; López De Munain, A.; Ruiz Irastorza, G.; Martín-Iglesias, D.; Ribacoba, L.; Gabilondo, I.; Gómez-Esteban, J. C.; Tijero-Merino, B. Dysautonomia and Small Fiber Neuropathy in Post-COVID Condition and Chronic Fatigue Syndrome. *J. Transl. Med.* **2023**, *21* (1), 814. https://doi.org/10.1186/s12967-023-04678-3.

(11) Terkelsen, A. J.; Karlsson, P.; Lauria, G.; Freeman, R.; Finnerup, N. B.; Jensen, T. S. The Diagnostic Challenge of Small Fibre Neuropathy: Clinical Presentations, Evaluations, and Causes. *Lancet Neurol.* **2017**, *16* (11), 934–944. https://doi.org/10.1016/S1474-4422(17)30329-0.

(12) Tavee, J.; Zhou, L. Small Fiber Neuropathy: A Burning Problem. *Cleve. Clin. J. Med.* **2009**, *76* (5), 297–305. https://doi.org/10.3949/ccjm.76a.08070.

(13) Pereira, M. P.; Derichs, L.; Meyer Zu Hörste, G.; Agelopoulos, K.; Ständer, S. Generalized Chronic Itch Induced by Small-fibre Neuropathy: Clinical Profile and Proposed Diagnostic Criteria. *J. Eur. Acad. Dermatol. Venereol.* **2020**, *34* (8), 1795–1802. https://doi.org/10.1111/jdv.16151.

(14) Anzelc, M.; Burkhart, C. G. Pain and Pruritus: A Study of Their Similarities and Differences. *Int. J. Dermatol.* **2020**, *59* (2), 159–164. https://doi.org/10.1111/ijd.14678.
(15) Sène, D. Small Fiber Neuropathy: Diagnosis, Causes, and Treatment. *Joint Bone Spine* **2018**, *85* (5), 553–559. https://doi.org/10.1016/j.jbspin.2017.11.002.
(16) Gemignani, F.; Bellanova, M. F.; Saccani, E.; Pavesi, G. Non-length-dependent Small Fiber Neuropathy: Not a Matter of Stockings and Gloves. *Muscle Nerve* **2022**, *65* (1), 10–28. https://doi.org/10.1002/mus.27379.
(17) Devigili, G.; Eleopra, R.; Pierro, T.; Lombardi, R.; Rinaldo, S.; Lettieri, C.; Faber, C. G.; Merkies, I. S. J.; Waxman, S. G.; Lauria, G. Paroxysmal Itch Caused by Gain-of-Function Nav1.7 Mutation. *Pain* **2014**, *155* (9), 1702–1707. https://doi.org/10.1016/j.pain.2014.05.006.
(18) Kwatra, S. G.; Kambala, A.; Dong, X. Neuropathic Pruritus. *J. Allergy Clin. Immunol.* **2023**, *152* (1), 36–38. https://doi.org/10.1016/j.jaci.2023.04.006.
(19) Meixiong, J.; Dong, X.; Weng, H.-J. Neuropathic Itch. *Cells* **2020**, *9* (10), 2263. https://doi.org/10.3390/cells9102263.
(20) Brouwer, B. A.; van Kuijk, S. M. J.; Bouwhuis, A.; Faber, C. G.; van Kleef, M.; Merkies, I. S. J.; Hoeijmakers, J. G. J. The Pain Dynamics of Small Fiber Neuropathy. *J. Pain* **2019**, *20* (6), 655–663. https://doi.org/10.1016/j.jpain.2018.11.009.
(21) Albrecht, P. J.; Rice, F. L. Role of Small-Fiber Afferents in Pain Mechanisms with Implications on Diagnosis and Treatment. *Curr. Pain Headache Rep.* **2010**, *14* (3), 179–188. https://doi.org/10.1007/s11916-010-0105-y.
(22) Lauria, G.; Ziegler, D.; Malik, R.; Merkies, I. S. J.; Waxman, S. G.; Faber, C. G.; PROPANE Study group. The Role of Sodium Channels in Painful Diabetic and Idiopathic Neuropathy. *Curr. Diab. Rep.* **2014**, *14* (10), 538. https://doi.org/10.1007/s11892-014-0538-5.
(23) Tesfaye, S.; Boulton, A. J. M.; Dyck, P. J.; Freeman, R.; Horowitz, M.; Kempler, P.; Lauria, G.; Malik, R. A.; Spallone, V.; Vinik, A.; Bernardi, L.; Valensi, P.; on behalf of the Toronto Diabetic Neuropathy Expert Group. Diabetic Neuropathies: Update on Definitions, Diagnostic Criteria, Estimation of Severity, and Treatments. *Diabetes Care* **2010**, *33* (10), 2285–2293. https://doi.org/10.2337/dc10-1303.
(24) Blackmore, D.; Siddiqi, Z. A. Diagnostic Criteria for Small Fiber Neuropathy. *J. Clin. Neuromuscul. Dis.* **2017**, *18* (3), 125–131. https://doi.org/10.1097/CND.0000000000000154.
(25) Devigili, G.; Tugnoli, V.; Penza, P.; Camozzi, F.; Lombardi, R.; Melli, G.; Broglio, L.; Granieri, E.; Lauria, G. The Diagnostic Criteria for Small Fibre Neuropathy: From Symptoms to Neuropathology. *Brain* **2008**, *131* (7), 1912–1925. https://doi.org/10.1093/brain/awn093.
(26) Jensen, T. S.; Finnerup, N. B. Allodynia and Hyperalgesia in Neuropathic Pain: Clinical Manifestations and Mechanisms. *Lancet Neurol.* **2014**, *13* (9), 924–935. https://doi.org/10.1016/S1474-4422(14)70102-4.
(27) Mücke, M.; Cuhls, H.; Radbruch, L.; Baron, R.; Maier, C.; Tölle, T.; Treede, R.-D.; Rolke, R. Quantitative Sensory Testing (QST). English Version. *Schmerz* **2021**, *35* (S3), 153–160. https://doi.org/10.1007/s00482-015-0093-2.
(28) Chiang, J. C. B.; Roy, M.; Kim, J.; Markoulli, M.; Krishnan, A. V. In-Vivo Corneal Confocal Microscopy: Imaging Analysis, Biological Insights and Future Directions. *Commun. Biol.* **2023**, *6* (1), 652. https://doi.org/10.1038/s42003-023-05005-8.
(29) Im, S.; Kim, S.-R.; Park, J. H.; Kim, Y. S.; Park, G.-Y. Assessment of the Medial Dorsal Cutaneous, Dorsal Sural, and Medial Plantar Nerves in Impaired Glucose Tolerance and Diabetic Patients with Normal Sural and Superficial Peroneal Nerve Responses. *Diabetes Care* **2012**, *35* (4), 834–839. https://doi.org/10.2337/dc11-1001.
(30) Serra, J.; Solà, R.; Quiles, C.; Casanova-Molla, J.; Pascual, V.; Bostock, H.; Valls-Solé, J. C-Nociceptors Sensitized to Cold in a Patient with Small-Fiber Neuropathy and Cold Allodynia. *Pain* **2009**, *147* (1–3), 46–53. https://doi.org/10.1016/j.pain.2009.07.028.

(31) De Keyser, R.; van den Broeke, E. N.; Courtin, A.; Dufour, A.; Mouraux, A. Event-Related Brain Potentials Elicited by High-Speed Cooling of the Skin: A Robust and Non-Painful Method to Assess the Spinothalamic System in Humans. *Clin. Neurophysiol. Off. J. Int. Fed. Clin. Neurophysiol.* **2018**, *129* (5), 1011–1019. https://doi.org/10.1016/j.clinph.2018.02.123.
(32) Siedler, G.; Sommer, C.; Üçeyler, N. Pain-Related Evoked Potentials in Patients with Large, Mixed, and Small Fiber Neuropathy. *Clin. Neurophysiol.* **2020**, *131* (3), 635–641. https://doi.org/10.1016/j.clinph.2019.12.006.
(33) Treede, R. D.; Meyer, R. A.; Raja, S. N.; Campbell, J. N. Evidence for Two Different Heat Transduction Mechanisms in Nociceptive Primary Afferents Innervating Monkey Skin. *J. Physiol.* **1995**, *483 ( Pt 3)* (Pt 3), 747–758. https://doi.org/10.1113/jphysiol.1995.sp020619.
(34) Arendt-Nielsen, L.; Chen, A. C. N. Lasers and Other Thermal Stimulators for Activation of Skin Nociceptors in Humans. *Neurophysiol. Clin. Clin. Neurophysiol.* **2003**, *33* (6), 259–268. https://doi.org/10.1016/j.neucli.2003.10.005.
(35) Truini, A.; Galeotti, F.; Romaniello, A.; Virtuoso, M.; Iannetti, G. D.; Cruccu, G. Laser-Evoked Potentials: Normative Values. *Clin. Neurophysiol.* **2005**, *116* (4), 821–826. https://doi.org/10.1016/j.clinph.2004.10.004.
(36) Wu, S.-W.; Wang, Y.-C.; Hsieh, P.-C.; Tseng, M.-T.; Chiang, M.-C.; Chu, C.-P.; Feng, F.-P.; Lin, Y.-H.; Hsieh, S.-T.; Chao, C.-C. Biomarkers of Neuropathic Pain in Skin Nerve Degeneration Neuropathy: Contact Heat-Evoked Potentials as a Physiological Signature. *Pain* **2017**, *158* (3), 516–525. https://doi.org/10.1097/j.pain.0000000000000791.
(37) Lagerburg, V.; Bakkers, M.; Bouwhuis, A.; Hoeijmakers, J. G. J.; Smit, A. M.; Van Den Berg, S. J. M.; Hordijk-De Boer, I.; Brouwer-Van Der Lee, M. D. G.; Kranendonk, D.; Reulen, J. P. H.; Faber, C. G.; Merkies, I. S. J. Contact Heat Evoked Potentials: Normal Values and Use in Small-Fiber Neuropathy. *Muscle Nerve* **2015**, *51* (5), 743–749. https://doi.org/10.1002/mus.24465.
(38) Novak, V.; Freimer, M. L.; Kissel, J. T.; Sahenk, Z.; Periquet, I. M.; Nash, S. M.; Collins, M. P.; Mendell, J. R. Autonomic Impairment in Painful Neuropathy. *Neurology* **2001**, *56* (7), 861–868. https://doi.org/10.1212/wnl.56.7.861.
(39) Donadio, V.; Incensi, A.; Vacchiano, V.; Infante, R.; Magnani, M.; Liguori, R. The Autonomic Innervation of Hairy Skin in Humans: An in Vivo Confocal Study. *Sci. Rep.* **2019**, *9* (1), 16982. https://doi.org/10.1038/s41598-019-53684-3.
(40) Donadio, V.; Nolano, M.; Provitera, V.; Stancanelli, A.; Lullo, F.; Liguori, R.; Santoro, L. Skin Sympathetic Adrenergic Innervation: An Immunofluorescence Confocal Study. *Ann. Neurol.* **2006**, *59* (2), 376–381. https://doi.org/10.1002/ana.20769.
(41) Illigens, B. M. W.; Gibbons, C. H. Sweat Testing to Evaluate Autonomic Function. *Clin. Auton. Res. Off. J. Clin. Auton. Res. Soc.* **2009**, *19* (2), 79–87. https://doi.org/10.1007/s10286-008-0506-8.
(42) Low, P. A.; Caskey, P. E.; Tuck, R. R.; Fealey, R. D.; Dyck, P. J. Quantitative Sudomotor Axon Reflex Test in Normal and Neuropathic Subjects. *Ann. Neurol.* **1983**, *14* (5), 573–580. https://doi.org/10.1002/ana.410140513.
(43) Gibbons, C. H.; Illigens, B. M. W.; Centi, J.; Freeman, R. QDIRT: Quantitative Direct and Indirect Test of Sudomotor Function. *Neurology* **2008**, *70* (24), 2299–2304. https://doi.org/10.1212/01.wnl.0000314646.49565.c0.
(44) Stewart, J. D.; Nguyen, D. M.; Abrahamowicz, M. Quantitative Sweat Testing Using Acetylcholine for Direct and Axon Reflex Mediated Stimulation with Silicone Mold Recording; Controls versus Neuropathic Diabetics. *Muscle Nerve* **1994**, *17* (12), 1370–1377. https://doi.org/10.1002/mus.880171205.
(45) Ponirakis, G.; Petropoulos, I. N.; Fadavi, H.; Alam, U.; Asghar, O.; Marshall, A.; Tavakoli, M.; Malik, R. A. The Diagnostic Accuracy of Neuropad for Assessing Large and Small Fibre

Diabetic Neuropathy. *Diabet. Med. J. Br. Diabet. Assoc.* **2014**, *31* (12), 1673–1680. https://doi.org/10.1111/dme.12536.
(46) Casellini, C. M.; Parson, H. K.; Richardson, M. S.; Nevoret, M. L.; Vinik, A. I. Sudoscan, a Noninvasive Tool for Detecting Diabetic Small Fiber Neuropathy and Autonomic Dysfunction. *Diabetes Technol. Ther.* **2013**, *15* (11), 948–953. https://doi.org/10.1089/dia.2013.0129.
(47) Teoh, H. L.; Chow, A.; Wilder-Smith, E. P. Skin Wrinkling for Diagnosing Small Fibre Neuropathy: Comparison with Epidermal Nerve Density and Sympathetic Skin Response. *J. Neurol. Neurosurg. Psychiatry* **2008**, *79* (7), 835–837. https://doi.org/10.1136/jnnp.2007.140947.
(48) Wilder-Smith, E. P.; Guo, Y.; Chow, A. Stimulated Skin Wrinkling for Predicting Intraepidermal Nerve Fibre Density. *Clin. Neurophysiol. Off. J. Int. Fed. Clin. Neurophysiol.* **2009**, *120* (5), 953–958. https://doi.org/10.1016/j.clinph.2009.03.011.
(49) Siepmann, T.; Pintér, A.; Buchmann, S. J.; Stibal, L.; Arndt, M.; Kubasch, A. S.; Kubasch, M. L.; Penzlin, A. I.; Frenz, E.; Zago, W.; Horváth, T.; Szatmári, S.; Bereczki, D.; Takáts, A.; Ziemssen, T.; Lipp, A.; Freeman, R.; Reichmann, H.; Barlinn, K.; Illigens, B. M.-W. Cutaneous Autonomic Pilomotor Testing to Unveil the Role of Neuropathy Progression in Early Parkinson's Disease (CAPTURE PD): Protocol for a Multicenter Study. *Front. Neurol.* **2017**, *8*, 212. https://doi.org/10.3389/fneur.2017.00212.
(50) Siepmann, T.; Gibbons, C. H.; Illigens, B. M.; Lafo, J. A.; Brown, C. M.; Freeman, R. Quantitative Pilomotor Axon Reflex Test: A Novel Test of Pilomotor Function. *Arch. Neurol.* **2012**, *69* (11), 1488–1492. https://doi.org/10.1001/archneurol.2012.1092.
(51) Raasing, L. R. M.; Vogels, O. J. M.; Veltkamp, M.; Van Swol, C. F. P.; Grutters, J. C. Current View of Diagnosing Small Fiber Neuropathy. *J. Neuromuscul. Dis.* **2021**, *8* (2), 185–207. https://doi.org/10.3233/JND-200490.
(52) Freeman, R. Assessment of Cardiovascular Autonomic Function. *Clin. Neurophysiol.* **2006**, *117* (4), 716–730. https://doi.org/10.1016/j.clinph.2005.09.027.
(53) Sirois, S.; Brisson, J. Pupillometry. *Wiley Interdiscip. Rev. Cogn. Sci.* **2014**, *5* (6), 679–692. https://doi.org/10.1002/wcs.1323.
(54) Clemens, J. Q. Basic Bladder Neurophysiology. *Urol. Clin. North Am.* **2010**, *37* (4), 487–494. https://doi.org/10.1016/j.ucl.2010.06.006.
(55) Fall, M.; Lindström, S.; Mazières, L. A Bladder-to-Bladder Cooling Reflex in the Cat. *J. Physiol.* **1990**, *427*, 281–300. https://doi.org/10.1113/jphysiol.1990.sp018172.
(56) Häbler, H. J.; Jänig, W.; Koltzenburg, M. Activation of Unmyelinated Afferent Fibres by Mechanical Stimuli and Inflammation of the Urinary Bladder in the Cat. *J. Physiol.* **1990**, *425*, 545–562. https://doi.org/10.1113/jphysiol.1990.sp018117.
(57) Dmochowski, R. Cystometry. *Urol. Clin. North Am.* **1996**, *23* (2), 243–252. https://doi.org/10.1016/s0094-0143(05)70308-6.
(58) Gammie, A.; Drake, M. J. The Fundamentals of Uroflowmetry Practice, Based on International Continence Society Good Urodynamic Practices Recommendations. *Neurourol. Urodyn.* **2018**, *37* (S6), S44–S49. https://doi.org/10.1002/nau.23777.
(59) Sharrack, B.; Hughes, R. A. Scale Development and Guy's Neurological Disability Scale. *J. Neurol.* **1999**, *246* (3), 226. https://doi.org/10.1007/s004150050340.
(60) Merkies, I. S.; Schmitz, P. I.; van der Meché, F. G.; van Doorn, P. A. Psychometric Evaluation of a New Sensory Scale in Immune-Mediated Polyneuropathies. Inflammatory Neuropathy Cause and Treatment (INCAT) Group. *Neurology* **2000**, *54* (4), 943–949. https://doi.org/10.1212/wnl.54.4.943.
(61) Merkies, I. S. J.; Schmitz, P. I. M.; van der Meché, F. G. A.; Samijn, J. P. A.; van Doorn, P. A.; Inflammatory Neuropathy Cause and Treatment (INCAT) group. Clinimetric Evaluation of a New Overall Disability Scale in Immune Mediated Polyneuropathies. *J. Neurol. Neurosurg. Psychiatry* **2002**, *72* (5), 596–601. https://doi.org/10.1136/jnnp.72.5.596.

(62) Idiaquez, J. F.; Alcantara, M.; Bril, V. Optimal Cut-off Value of the Modified Toronto Clinical Neuropathy Score in the Diagnosis of Polyneuropathy. *Eur. J. Neurol.* **2023**, *30* (8), 2481–2487. https://doi.org/10.1111/ene.15870.
(63) Bril, V.; Perkins, B. A. Validation of the Toronto Clinical Scoring System for Diabetic Polyneuropathy. *Diabetes Care* **2002**, *25* (11), 2048–2052. https://doi.org/10.2337/diacare.25.11.2048.
(64) Bril, V.; Tomioka, S.; Buchanan, R. A.; Perkins, B. A.; mTCNS Study Group. Reliability and Validity of the Modified Toronto Clinical Neuropathy Score in Diabetic Sensorimotor Polyneuropathy. *Diabet. Med. J. Br. Diabet. Assoc.* **2009**, *26* (3), 240–246. https://doi.org/10.1111/j.1464-5491.2009.02667.x.
(65) Hsieh, P.-C.; Tseng, M.-T.; Chao, C.-C.; Lin, Y.-H.; Tseng, W.-Y. I.; Liu, K.-H.; Chiang, M.-C.; Hsieh, S.-T. Imaging Signatures of Altered Brain Responses in Small-Fiber Neuropathy: Reduced Functional Connectivity of the Limbic System after Peripheral Nerve Degeneration. *Pain* **2015**, *156* (5), 904–916. https://doi.org/10.1097/j.pain.0000000000000128.
(66) Ebadi, H.; Siddiqui, H.; Ebadi, S.; Ngo, M.; Breiner, A.; Bril, V. Peripheral Nerve Ultrasound in Small Fiber Polyneuropathy. *Ultrasound Med. Biol.* **2015**, *41* (11), 2820–2826. https://doi.org/10.1016/j.ultrasmedbio.2015.06.011.
(67) Sommer, C.; Lauria, G. Skin Biopsy in the Management of Peripheral Neuropathy. *Lancet Neurol.* **2007**, *6* (7), 632–642. https://doi.org/10.1016/S1474-4422(07)70172-2.
(68) Sommer, C. Pathology of Small Fiber Neuropathy: Skin Biopsy for the Analysis of Nociceptive Nerve Fibers. In *Small Fiber Neuropathy and Related Syndromes: Pain and Neurodegeneration*; Hsieh, S.-T., Anand, P., Gibbons, C. H., Sommer, C., Eds.; Springer: Singapore, 2019; pp 11–24. https://doi.org/10.1007/978-981-13-3546-4_2.
(69) Lauria, G.; Hsieh, S. T.; Johansson, O.; Kennedy, W. R.; Leger, J. M.; Mellgren, S. I.; Nolano, M.; Merkies, I. S. J.; Polydefkis, M.; Smith, A. G.; Sommer, C.; Valls-Solé, J. European Federation of Neurological Societies/Peripheral Nerve Society Guideline on the Use of Skin Biopsy in the Diagnosis of Small Fiber Neuropathy. Report of a Joint Task Force of the European Fe-deration of Neurological Societies and the Peripheral Nerve Society. *Eur. J. Neurol.* **2010**, *17* (7), 903. https://doi.org/10.1111/j.1468-1331.2010.03023.x.
(70) Sohn, E.; Suh, B. C.; Wang, N.; Freeman, R.; Gibbons, C. H. A Novel Method to Quantify Cutaneous Vascular Innervation. *Muscle Nerve* **2020**, *62* (4), 492–501. https://doi.org/10.1002/mus.26889.
(71) Moretti, G. The Blood Vessels of the Skin. In *Normale und Pathologische Anatomie der Haut I*; Achten, G., Brody, I., Braun-Falco, O., Cramer, H. J., Dotzauer, G., Eberhartinger, Chr., Ebner, H., Ehlers, G., Ellis, R. A., Hagen, E., Koecke, H. U., Moretti, G., Niebauer, G., Pinkus, H., Pochi, P. E., Rupec, M., Schmidt, W., Strauss, J. S., Tamaska, L., Tanay, A., Zaun, H., Gans, O., Steigleder, G. K., Eds.; Springer: Berlin, Heidelberg, 1968; pp 491–623. https://doi.org/10.1007/978-3-662-30268-2_9.
(72) Johnson, J. M.; Minson, C. T.; Kellogg, D. L. Cutaneous Vasodilator and Vasoconstrictor Mechanisms in Temperature Regulation. *Compr. Physiol.* **2014**, *4* (1), 33–89. https://doi.org/10.1002/cphy.c130015.
(73) Low, D. A.; Jones, H.; Cable, N. T.; Alexander, L. M.; Kenney, W. L. Historical Reviews of the Assessment of Human Cardiovascular Function: Interrogation and Understanding of the Control of Skin Blood Flow. *Eur. J. Appl. Physiol.* **2020**, *120* (1), 1–16. https://doi.org/10.1007/s00421-019-04246-y.
(74) Pappano, A. J.; Gil Wier, W. Special Circulations. In *Cardiovascular Physiology*; Elsevier, 2013; pp 237–262. https://doi.org/10.1016/B978-0-323-08697-4.00012-5.
(75) Ruocco, I.; Cuello, A. C.; Parent, A.; Ribeiro-da-Silva, A. Skin Blood Vessels Are Simultaneously Innervated by Sensory, Sympathetic, and Parasympathetic Fibers. *J. Comp. Neurol.* **2002**, *448* (4), 323–336. https://doi.org/10.1002/cne.10241.

(76) Fronek, K. Trophic Effect of the Sympathetic Nervous System on Vascular Smooth Muscle. *Ann. Biomed. Eng.* **1983**, *11* (6), 607–615. https://doi.org/10.1007/BF02364090.
(77) *Neuropathic Itch: Routes to Clinical Diagnosis - PubMed*. https://pubmed.ncbi.nlm.nih.gov/33732722/ (accessed 2024-06-19).
(78) Ikoma, A.; Steinhoff, M.; Ständer, S.; Yosipovitch, G.; Schmelz, M. The Neurobiology of Itch. *Nat. Rev. Neurosci.* **2006**, *7* (7), 535–547. https://doi.org/10.1038/nrn1950.

## 8. ACKNOWLEDGMENTS

Vorrei in questo piccolo spazio, poter ringraziare tutti coloro che hanno partecipato alla stesura ed alla realizzazione della mia tesi.

Prima di tutto vorrei ringraziare il *Professor Angelo Schenone*, per la grande opportunità datami e per l'infinita disponibilità e professionalità con cui mi ha seguita; è stato un piacere aver avuto l'occasione di lavorare con Lei per la realizzazione di questo lavoro di cui sono molto orgogliosa.

I would like to thank *Professor Claudia Sommer* for her trust, immense availability, and kindness. I want to thank her for welcoming me into her work group, allowing me to interact with brilliant people who shared their knowledge with me, helping me grow both professionally and personally. I am extremely grateful to have participated in and contributed, even in a small part, to this important project.

I would also like to thank *Dr. Katharina Papagianni*, who has patiently and readily guided me remotely over these past few months, providing me with all the necessary information to complete the study.

A *Sara*, mia correlatrice. Grazie per la pazienza, i preziosi consigli e tutto il tempo dedicatomi nonostante i tuoi mille impegni lavorativi e nonostante il progetto non ti avesse interessato direttamente. Grazie per avermi permesso di frequentare l'ambulatorio e per avermi coinvolto nelle visite, è stato molto stimolante e mi ha dato conferma di quanto mi piaccia questo ambito della medicina. Spero in futuro di aver la possibilità di lavorare insieme e come una spugna assorbire quanto più possibile tutte le conoscenze che condividerai come me.

A *Sabrina e Alessandro*. È stato molto stimolante lavorare con voi. Grazie Alessandro per avermi suggerito di fare quest'esperienza meravigliosa e soprattutto per il tuo contributo iniziale risultato fondamentale per la progressione

di questo studio. Grazie Sabrina per tutte le conoscenze e i consigli trasmessi, grazie per tutto il lavoro condiviso insieme finora e che ci aspetterà ancora in futuro per terminare il progetto. Sono grata di aver condiviso il mio primo progetto di ricerca con due splendidi e volenterosi colleghi come voi.

A *Viola*. Mi ha fatto molto piacere condividere con te questa esperienza fantastica che è la tesi, fatta di tante soddisfazioni, ma altrettanti momenti di panico e smarrimento. Grazie per avermi sempre tranquillizzata rispondendo alle mie mille domande, per aver condiviso i tuoi consigli preziosi e dubbi che alla fine erano anche i miei. Chi lo avrebbe mai detto che da biotec saremo arrivate fin qui e chi lo sa magari un domani future colleghe (ce lo auguro con tutto il cuore)!